Distributed Power Control in Ad Hoc Networks

Neil Robert Pate

Submitted in fulfillment of the academic requirements for the degree
Master of Science in Engineering
in the School of Electrical, Electronic and Computer Engineering
at the University of Natal, Durban, South Africa

March 24, 2003

As the candidate's supervisor I have approved this dissertation for submission.

Signed: _____

Name: Prof. Fambirai Takawira

Date: March 24, 2003

Abstract

Wireless communication is currently enjoying unprecedented popularity, and the present trend indicates an exponential growth rate. Both GSM, the traditional and now mature cellular architecture, and UMTS, the international 3G standard, are hampered by their need for the installation of expensive and unsightly base-stations, which have to be hard-wired to a central switching station.

A new network concept, the *ad hoc network*, does away with the need for these base-stations, and all local communication is done on a multi-hop, peer-to-peer basis. This does of course present a significant engineering problem, as the removal of the centralized controllers (base stations) necessitates that all decisions related to, for example: routing, MAC and power control need to be done at the node.

This dissertation discusses the concept of an ad hoc network, and specifically focuses on *power control* in a system with a CDMA air interface. Power control is a technique whereby the transmission power of a node is constantly adjusted, normally with the aim of minimizing the interference to other nodes while still maintaining a signal level that will achieve successful communication. Benefits of this include increased network capacity and throughput, usually coupled with an increase in battery lifetime. Due to the lack of any centralized radio network controller, a fully distributed scheme needs to be developed, whereby each node adjusts its power based only on information locally available.

Due to the relative infancy of the topic, very little literature exists on power control in ad hoc networks using a distributed non-clustering based approach, and new methods are presented based on a scheme developed for cellular networks. In order to conserve the limited available bandwidth, a single-bit adaptive signalling scheme is implemented whereby a node will attempt to control the power of a subset of its surrounding nodes. Methods for determining which nodes belong in this subset are introduced, and the entire system simulated in a custom designed environment. Techniques for determining the controlling connectivity for a node are also presented, and their effect on the system performance are investigated. Some of the metrics used to classify the performance of the network include system outage and convergence speed, as well as overall network connectivity.

A model for an ad hoc network with predefined connectivity is presented, and an optimum transmit power vector derived. A *standard interference function* power control algorithm is deduced, and tested in sample networks. It was shown that when the system is feasible, in the absence of shadow fading and mobility, the proposed power control algorithm is able to exactly converge to the calculated ideal power vector, and when mobility and slow fading are introduced the algorithm is able to track the channel changes.

Preface

The contents of this dissertation are the culmination of the research work done by Mr Neil Robert Pate in fulfilment of the MScEng degree. The work was done in the Centre for Radio Access Technologies at The University of Natal, School of Electrical, Electronic and Computer Engineering. The research was funded partially by Telkom SA Ltd and Alcatel Altech Telecoms.

The author has presented parts of this dissertation at the following conferences:

- SATNAC 2001 Conference, Wild Coast Sun, South Africa
- SATNAC 2002 Conference, Champagne Sports, Drakensberg, South Africa

The entire dissertation, unless otherwise indicated, is the author's own work and has not been submitted in part, or in whole to any other University for degree purposes.

Acknowledgements

I extend my sincere appreciation to my parents for their wisdom in allowing me to set and pursue my own unique goals. Without their sacrifices my tertiary education would have never happened. Thanks Mom and Dad.

A special mention needs to be made of my supervisor Prof. Fambirai Takawira, who's valuable insight and dedication kept things running smoothly, particularly during the darker hours.

Many thanks go out to Telkom SA Ltd and Alcatel Altech Telecoms for their financial support, without which my post-graduate study would not have been possible.

I wish to thank all the staff, too numerous to mention individually, at the School of Electrical, Electronic and Computer Engineering, for all their valuable support.

Thanks go also to Tamren for the tedious task of proof reading this dissertation.

Lastly, thanks are extended to my post-grad colleagues for making the work bearable, and sometimes even fun.

Dedicated to Pooh Bear, for understanding how my mind works.

Contents

List of Figures

List of Tables

List of acronyms

2G	Second Generation
3G	Third Generation
ACK	ACKnowledge
AMPS	Advanced Mobile Phone System
AOA	Angle Of Arrival
AWGN	Additive White Gaussian Noise
BECA	Basic Energy Conserving Algorithm
BER	Bit Error Rate
BPSK	Binary Phase Shift Keying
BS	Base Station
CCK	Complementary Code Keying
CDMA	Code Division Multiple Access
CH	Cluster Head
COMPOW	COMmon POWer
CTS	Clear-To-Send
DCPC	Distributed Constrained Power Control
DPC	Distributed Power Control
DPC/ALP	Distributed Power Control with Active Link Protection
DSSS	Direct-Sequence Spread Spectrum
ETSI	European Telecommunications Standards Institute
EWA	Exponentially Weighted Average

FDMA	Frequency Division Multiple Access
FER	Frame Error Rate
FHSS	Frequency-Hopping Spread Spectrum
FM	Frequency Modulation
GPRS	General Packet Radio Service
GPS	Global Positioning System
GSM	Global System for Mobile communication
GW	Gateway
HSCSD	High Speed Circuit Switched Data
IEEE	Institute of Electrical and Electronics Engineers
IMT-2000	International Mobile Telecommunications for the 21st Century
IRP	Ideal Received Power
ISM	Industrial, Scientific and Medical
ITU	International Telecommunications Union
LAN	Local Area Network
LEO	Low Earth Orbital
LINT	Local Information No Topology
LILT	Local Information Link-State Topology
MAC	Medium Access Control
MPA	Minimum Power Assignment
MS	Mobile Station
MST	Minimum Spanning Tree
MTP	Minimum Transmitted Power
MUD	Multiuser Detection
NAP	Neighbour Addition Protocol
NTC	Novel Topology Control
OFDM	Orthogonal Frequency Division Multiplexing
PAN	Personal Area Network
PDF	Probability Density Function

PI	Proportional-Integral
PN	Pseudonoise
PDA	Personal Digital Assistant
PCC	Power Control Command
PCSP	Power Control Sampling Period
POTS	Plain Old Telephone System
PUP	Periodic Update Protocol
QAM	Quadrature Amplitude Modulation
QoS	Quality of Service
QPUP	Quasi-Periodic Update Protocol
QPSK	Quadrature Phase Shift Keying
RTS	Request-To-Send
SEEDEX	SEED EXchange
SIR	Signal-to-Interference Ratio
SMS	Short Message Services
TDC	Time Delay Compensation
TDD	Time Division Duplex
TDMA	Time Division Multiple Access
UMTS	Universal Mobile Telecommunications System
UNII	Unlicensed National Information Infrastructure
VLSI	Very Large Scale Integration
WLAN	Wireless Local Area Network
W-CDMA	Wideband-CDMA

List of symbols

χ	Average node true connectivity
δ	QoS maximum outage specifications
γ	Signal-to-interference ratio
$\tilde{\gamma}$	Simulation SIR cap
γ^*	Target SIR
$\bar{\gamma}_j$	K^{th} greatest SIR received at node j
$\boldsymbol{\gamma}_j$	Received SIR vector at node j
Γ	Target (despread) SIR
η_i	Thermal noise power at node i
$\boldsymbol{\eta}$	Normalized noise vector
φ	Power control step-size
μ	Mean node journey duration
$\boldsymbol{\mu}$	System duration countdown vector
ρ	Channel correlation coefficient
ρ_A	Spectral radius of A matrix
θ	System direction vector
τ	Power control period
ω_k	Probability node k is transmitting
ξ_{ji}	Binary signal quality indicator
$\mathbf{A}$	Connectivity matrix
B	Spread-spectrum bandwidth

C_j	Set of nodes controlled by node j
d_{max}	Maximum distance to control node
d_{ij}	Distance between node i and node j
D_0	Correlation distance
g_{ij}	Total path gain to node i from node j
H	Normalized gain matrix
$\bar{I}_j$	Mean interference at node j
I(p)	Interference function
K	Number of controlled nodes
l_{ij}	Path loss between nodes node i and node j
L	Inter-node distance attenuation matrix
L	Sliding interference window length
N	Number of nodes in network
N_0	Single-sided noise spectral density
$\mathcal{N}$	Set of all possible target nodes
p_{min}	Minimum node transmit power
$\hat{p}_i$	Maximum node transmission power
p_i	Transmit power of node i
$p(0)$	Initial transmit power
p	System transmit power vector
$\mathbf{p}^*$	Optimum system transmit power vector
r_{ji}	Received power at node j from node i
r_j^*	Ideal received power at node j
$\mathbf{r}_j$	Received power vector at node j
r_{min}	Minimum receive power threshold
R_j	Total received power at node j
S_{ij}	Shadow-fading to node i from node j
v	Mean node velocity
V_j	Variance of interference at node j

$\mathbf{S}$	Inter-node shadow fading matrix
$\mathbf{S}^t$	Inter-node shadow fading duration matrix
$\mathbf{T}$	System activity switch countdown vector
$\mathbf{v}$	System velocity vector
W	CDMA processing gain
X_k	Boolean activity factor for node k

Chapter 1

Introduction

1.1 Wireless networks

Demand for untethered, global communication is rising exponentially. Wireless communication growth is outpacing wireline installations by at least an order of magnitude, and cellular technology in the form of 3G is currently being rolled out world-wide. The freedom of mobility associated with wireless radio communication is a convenience that has very rapidly become integral in a large percentage of the planet's developed, and increasingly so, developing nations. Civilization has become progressively more reliant on real-time communication and information retrieval, and the cellular telephone, for example, is now no longer considered a luxury item, rather it has become a necessity.

Traditional cellular systems are into their third evolution, and have matured as a technology since the first inception of analogue wireless communication in the 1980's. Most new and developing standards are designed from the beginning to be inter-operable, and research into making cellular systems more efficient (and thus more cost effective) is at a peak. Digital communication offers many improvements over older analogue based schemes; compression and coding enhancements allow much greater data rates over unreliable fading channels [1].

However, cellular systems are hampered by several major limitations. One of the key components of the cellular system is the base-station. These large physical structures are not only very expensive to install, but also are extremely unsightly and generally are not a welcome addition to a neighbourhood. Disguising them as palm-trees only very slightly detracts from their ugliness. Unfortunately, the cellular system by its very nature relies totally on these base stations which also have to be hard-wired to local switching stations; removal of the base stations is not an option with current technology and development.

1.2 Types of wireless networks

Since the discovery and subsequent *taming* of radio technology, increasingly more sophisticated methods have been used to provide the human species with the communication that is so desired. In the last two decades, the focus has been on a highly structured cellular-type architecture, with user mobility supported through the introduction of wireless capabilities on the *last-link*. More recently though, research has branched out into more diverse network types, and a few of these are presented.

1.2.1 Cellular networks

The basic goal of the cellular wireless network is to enable point-to-point wireless telephony (and now data services). If a common radio carrier frequency was used for all the mobiles, then signal levels would need to be very high to overcome all the interference generated. Instead the geographical distribution is divided up into smaller areas, referred to as *cells*. By breaking the total coverage area into cells, and assigning different carrier frequencies to each cell, the interference experienced at a base station is only due to the mobiles in that cell. Neighbouring cells operate on slightly different frequencies, and due to the signal level attenuating exponentially with distance, the same frequency can be re-used in another cell that is located far enough away from

cells with the same carrier frequency. Fig. 1.1 indicates a typical cellular system with a frequency re-use factor of 7.

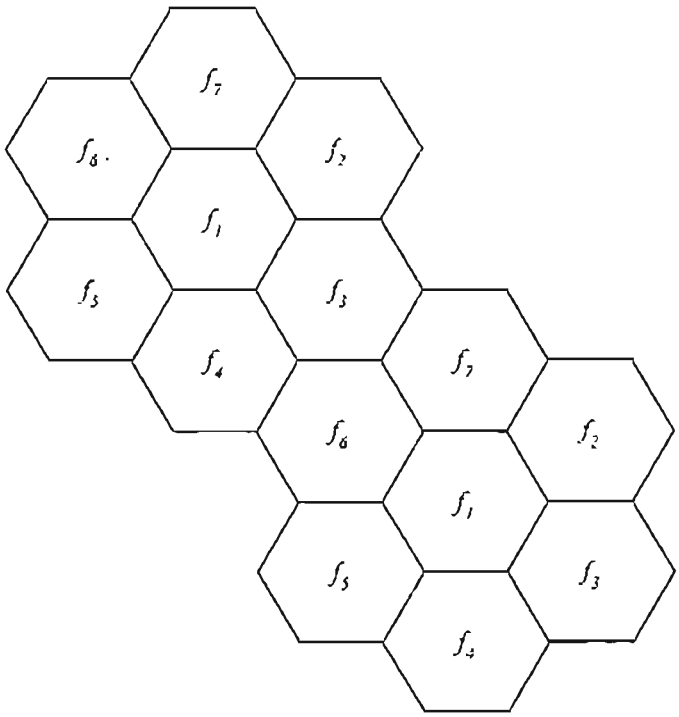

Figure 1.1: Idealized cellular architecture with frequency reuse of 1/7 as used, for example, in GSM

A detailed description of the functioning of a cellular network is complicated, and is not within the scope of this dissertation. Without going into unnecessary particulars, the fundamental operation of the cellular network is as follows: typically, a mobile will establish a connection with the local base-station and the call data will then be forwarded through the local switching stations via a dedicated hard-wired link to the base station of the recipient mobile. User mobility is supported due to the wireless nature of the last-link.

First generation

One of the more successful of the first wireless communication systems, AMPS, the Advanced Mobile Phone System developed by Bell Telephone System, used analogue frequency modulation (FM) techniques for voice communication, and also incorporated digital control signals. It was characterized by analogue voice only transmission, using frequency division multiple access (FDMA) with 30 kHz separation per channel and a re-use factor of 1/7. This leads to a spectrum allocation of $7 \times 30\,\text{kHz} = 210\,\text{kHz}$. The required signal-to-interference ratio (SIR) was 18 dB, and this resulted in an operator only being able to service 60 calls per cell in a 12.5 MHz allocated band.

Second generation

The low capacity associated with the first generation schemes, coupled with the rapid increase in the number of wireless subscribers and the different standards' inherent technological incompatibilities necessitated development of more efficient, digital, communication systems. One of the advantages offered by digital communication is increased network capacity through the use of data compression algorithms and sophisticated coding techniques [2]. The dominant standard for second generation (2G) cellular communication is the Global System for Mobile communication (GSM), [3]. The North American TDMA (time division multiple access) digital standard IS-136 uses digital control channels and allows value added services such as short message service (SMS) etc. [4]. IS-136 increases the capacity by multiplexing more users onto the 30 kHz AMPS channels.

A third 2G standard, IS-95 (also known as cdmaOne), was introduced in the United States of America. Unlike GSM and IS-136 which use TDMA as their core multiple access method, IS-95 uses code division multiple access (CDMA). This is a technique whereby a user's transmitted bit stream is multiplied by a pseudo-random code signal with a significantly greater rate. The effect of this is to *smear* the signal in the

frequency domain, hence the term *spread-spectrum*. Some of the benefits of CDMA include increased capacity due to voice activity detection and a common frequency for all cells, leading to a frequency reuse factor of unity [5, 6].

Although cdmaOne is in theory a more promising technology choice than TDMA [7], its implementation is significantly more difficult and has failed to capture world-wide attention and market penetration like GSM has.

Third generation (3G)

The goal of 3G is to provide a wide variety of multimedia services; voice, video and data all on the same network, seamlessly. Even though CDMA was not particularly successful in its IS-95 incarnation, its theoretical benefits could not be overlooked, and the International Telecommunications Union (ITU) decided on CDMA as the multiple access mechanism of choice for the 3G standard, IMT-2000. Once again Europe and the United States have slightly different views on the particular CDMA implementation, with America choosing cdma2000 which is backwards compatible with their legacy IS-95 cellular network. Wideband CDMA (W-CDMA) is the CDMA variant chosen by the European Telecommunications Standards Institute (ETSI) for their 3G standard, the Universal Mobile Telecommunications System (UMTS), and is able to support the entrenched GSM market.

1.2.2 WLAN

Cellular networks operate in (increasingly more expensive) licensed spectrum, and they are useful for communicating across large distances. In South Africa, GSM, the 2G choice for all the cellular operators, was initially designed with voice traffic in mind. Although the technology has since been extended to data transmission the data rates are relatively low, reaching a theoretical peak (though practically unattainable) rate of 171.2 kbps using GPRS (general packet radio service). Other 2.5G technologies such as

HSCSD (high speed circuit switched data) also allow greater data rates.

Third generation systems are designed from the ground up to support high speed data, and the standard specifies rates of up to 2 Mbps. While these data rates may be high enough for the transferring of small amounts of data, large files would still take too long to be conveniently downloaded using any of the cellular technologies.

Cellular systems were designed for communication on a large scale, ranging from users in the same cell, possibly less that 1 km away, to mobiles on different continents. Often a wireless link is needed to connect to a network only a few metres away. The 802.11x standards were developed by the institute of electrical and electronics engineers (IEEE) for wireless access on a much smaller scale than a cellular network. By installing a radio access point onto the existing local area network (LAN) infrastructure a user with a wireless LAN (WLAN) card attached to their PC or hand-held device can seamlessly access all the network resources such as servers or printers. a simple depiction of this is given in Fig. 1.2.

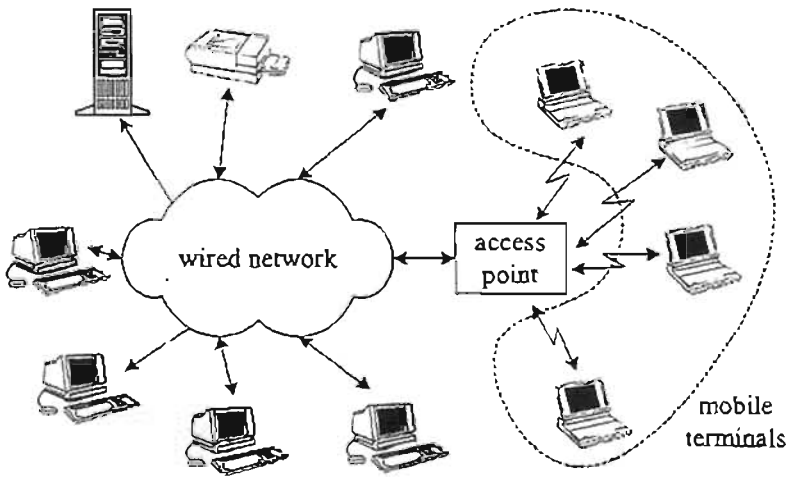

Figure 1.2: Wireless LAN application

The earliest incarnation of WLAN, IEEE 802.11, operates in the unlicensed 2.4 GHz ISM (industrial, scientific and medical) band. Depending on the channel quality, the

radio modulation mechanism can be either BPSK (binary phase shift keying) or QPSK (quadrature phase shift keying). The latter provides the maximum transmission rate of 2 Mbps, but due to the more complex signal constellation, can only be used when the wireless link quality is good. A spread spectrum air interface is used with the standard dictating either frequency-hopping spread spectrum (FHSS) or direct-sequence spread spectrum (DSSS).

The introduction of a new coding technique called complementary code keying (CCK), lead to the evolution of the 802.11 standard into 802.11b, or Wi-Fi™. Operating in the 2.4 GHz ISM band Wi-Fi™can achieve a theoretical maximum transmission rate of 11 Mbps using DSSS. Due to early equipment inter-operability issues, the Wi-Fi™ accreditation is used to ensure that devices from different manufacturers operate harmoniously.

The 2.4 GHz ISM band is fairly noisy (sharing spectrum with microwave ovens and wireless telephones), and 802.11a was designed to operate in the 5 GHz UNII (unlicensed national information infrastructure) band which was more recently allocated. The 802.11a standard uses OFDM (orthogonal frequency division multiplexing). This transmission technique has the advantage that due to its transmitted symbols being longer than the maximum delay spread a flat fading channel results, which is more easily equalized. OFDM has the disadvantage of having a high peak-to-average power, but this is not too crucial for short range applications [8] and thus OFDM is ideal for indoor office use where it would typically be deployed in a WLAN scenario. A maximum transmission rate of 54 Mbps is supported using by 64 QAM (quadrature amplitude modulation).

Transmission power in current WLAN devices are limited to a set of between four and eight discrete levels and changing this level is typically only possible through a firmware reset of the wireless LAN card [9], which currently takes too long to make any form of dynamic power control feasible.

WLAN systems can also operate in *ad hoc* mode where each terminal is able to forward data as necessary, but no standard method for multihop communication has been proposed by for 802.11 by the IEEE.

1.2.3 Bluetooth

Initially developed by a group of mobile telephone vendors, Bluetooth is a totally wireless network solution designed to serve as a personal area network (PAN), consequently the range of a Bluetooth network is much smaller than that of WLAN or cellular systems. The goal of Bluetooth was a standardized protocol allowing seamless information flow between a variety of personal devices, for example from a PDA (personal digital assistant) to a notebook. A piconet is formed when two or more Bluetooth units share the same channel. One of the devices becomes the master, and up to seven slave units are allowed per piconet. All communication in the piconet is done via the master unit, very similar to a cellular network structure. Two or more piconets can overlap, forming a scatternet where the connection or gateway node is a member of both piconets. Fig. 1.3 shows the interconnection of three piconets to form a larger scatternet. Bluetooth is also known as IEEE 802.15 standard, and operates in the 2.4 GHz ISM

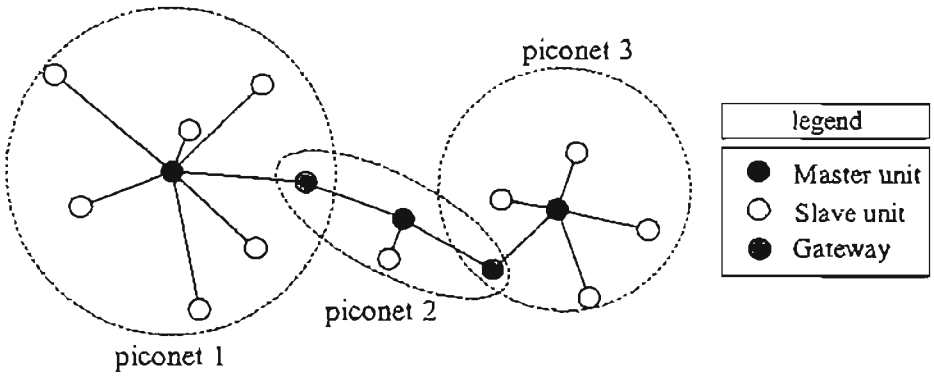

Figure 1.3: Three overlapping piconets forming a scatternet

band using frequency-hopping spread spectrum techniques. Full-duplex transmission is possible due to the slotted time-division duplex (TDD) mechanism, with a slot duration

of 0.0625 ms. A slave unit in a piconet is only able to transmit after it has been polled by its master unit. Bluetooth equipment is divided into three categories depending on the maximum output transmission power (20 dBm, 4 dBm and 0 dBm). Some rudimentary power control mechanisms are defined in the Bluetooth specifications [10], but no actual power control algorithms are suggested.

1.2.4 Ad hoc networks

Due to the necessity to operate at peak efficiency and extract value from the system, a cellular network needs to be very carefully planned (Chapter 8 of [11]). Once the locations of the base stations has been decided upon they need to be constructed and hard wired together through dedicated high speed land lines. In a cellular system, this need for a wired, permanent and expensive infrastructure, coupled with extensive planning is prohibitive when rapid deployment of a network is required. Ad hoc networks attempt to overcome this reliance on existing infrastructure, and operate in a totally wireless domain; thus allowing, amongst other things, fast deployment.

An ad hoc network is an impromptu collection of wireless nodes where every terminal also acts as a router, forwarding other nodes' data packets. Peer-to-peer communication is done on a multi-hop basis and all network *intelligence* and *control* needs to be embedded in each node.

It is the distributed nature of an ad hoc network which is one of its desirable properties in a military sense. The terrorist attack of the World Trade Center in New York on September 11, 2001 highlighted the risk that exists in centralized communication. The destruction of the cellular base stations atop the Twin Towers, along with the loss of the vast amount of wired data network lines and equipment, coupled with the obvious increase in teletraffic immediately following the incident lead to a major decrease in the ability of the service providers to cope with the communication demand.

Other disaster scenarios, for example a large earthquake, will also lead to the severing

of vital communication infrastructure and more than likely a serious loss of communication. In order for any large disaster relief (or military) operation to be effectively carried out the need will exist for robust, real-time voice and data communication. In such an event an ad hoc network could be rapidly deployed. Needing only an energy source to power the electronic devices and transmission antennae, wireless terminals could be set up to form a relay network which, although diminished in transmission capacity compared to a fixed land-line, would enable point-to-point communication to continue as necessary.

Other scenarios where the use of ad hoc networks would be favourable include military operations in foreign territories. The time delay inherent in geostationary satellites makes full-duplex voice communication barely tolerable, and the larger transmission distances require greater transmission powers which in turn leads to increased battery size and thus bulkier handsets. Since ease of mobility is a desired attribute in an infantry unit, equipment sizes and mass should be kept to a bare minimum. A low-Earth orbital (LEO) satellite communication link suffers from decreased transmission foot-print, and so to have total coverage of a large area, multiple satellites are needed. This dramatically increases the coordination necessary and also leads to a similar cost increase. Several global satellite based communication systems were launched in the 1990's, most notable the failed Iridium project [12].

A multi-hop ad hoc network could be implemented in a military scenario with each unit carrying a transceiver which would enable point-to-point communication. A CDMA spread-spectrum air interface would also help in decreasing the likelihood of an enemy detecting, and possibly jamming the communication system [13].

An example of where an ad hoc network could be used is the situation depicted by Fig. 1.4. Military units situated as shown would need to remain in contact with each other, and this can be done by forming a relay network where communication is achieved through a multi-hop path. If any of the nodes are removed from the network (possibly destroyed in battle or lose operational ability due to equipment failure) the nodes will

adjust to the topology change and route data accordingly. Some of the nodes may have to then increase their transmission power so that the network remains connected.

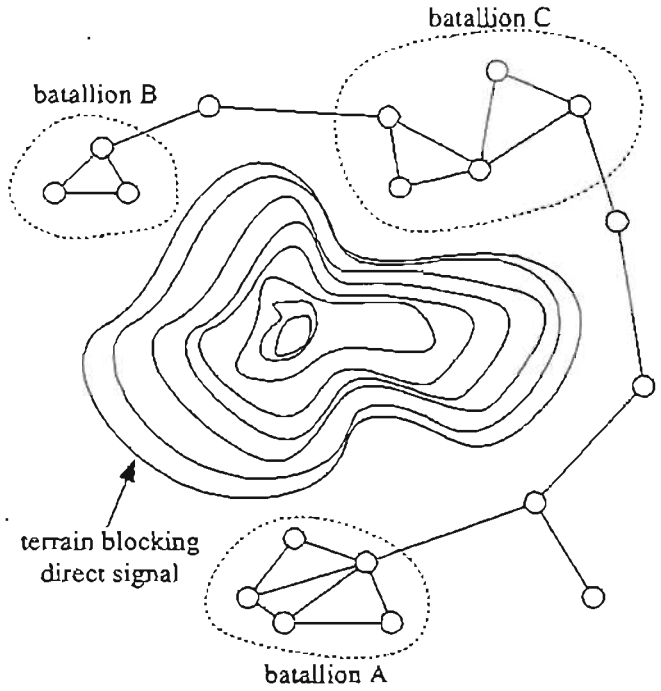

Figure 1.4: Typical military use of an ad hoc network.

However, it is the distributed nature of the ad hoc network which leads to some of the greatest engineering challenges. The removal of all centralized control structure means that decision related to, for example, routing, medium access control (MAC) and power control all need to be done at each node, using only (possible outdated) information available to each node. The vast majority of research in ad hoc networks has been devoted to solving the issues surrounding real-time communication and the need for robust routing [14, 15, 16, 17], and MAC layer problems [18, 19, 20].

Somewhat less research has been devoted to solving issues related to transmission power and network connectivity. Power constraints of the mobile terminals limit the maximum transmission distance, and the greater the output power the more interference

is caused to neighbouring nodes, this in turn reduces the effectiveness of the network which decreases the throughput. By transmitting with just enough power to reach a certain subset of its neighbours, a node is able to conserve energy and also present less interference to the rest of the network. This is beneficial in two ways: firstly the battery lifetime of the node is increased, and secondly the network capacity is increased due to reduced interference. A tradeoff to lower transmission power is that there is a cost associated with using more relay nodes to transmit a message, as the delay a packet experiences increases, and the network routing problem becomes greater. Multi-hop routing can actually increase transmission throughput if spatial and temporal advantages exist (i.e. nodes are well distributed in space) [21].

1.3 Power Control

One of the greatest concerns in engineering work is to strive for maximum efficiency. It is in the field of problem optimization that some of the greatest challenges lie. In the case of multi-billion Rand wireless communication networks, cost effectiveness is the number one optimization goal. This is generally achieved by maximizing the number of subscribers sharing the constrained bandwidth[1]. It is a well accepted fact that networks with a CDMA interface are interference limited and suffer from the near far effect [22, 23]. If the levels of the transmitted signals are not carefully controlled then a nearby terminal can smother the fainter signal received from a distant node, unless sophisticated signal processing techniques such as multiuser detection (MUD) are employed [24]. Ideally, the signals from all the terminals should be received at the target base-station with the same power [25]. In Fig. 1.5 node j is a base-station controlling nodes n, o and p. Ideally the product of the transmitted power and the path gain to j for all surrounding nodes should be equal. A rough estimate for maximum network capacity is often derived using this assumption [26]. By ensuring that a mobile

[1] In all likelihood, licensing the spectrum off the local government was probably one of the operators' largest expenses.

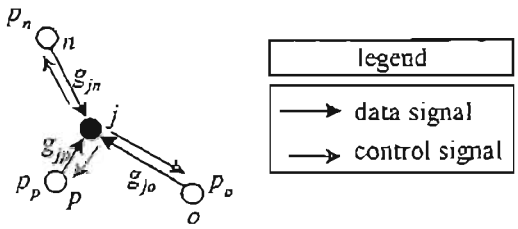

ideally: $p_n \cdot g_{jn} = p_o \cdot g_{jo} = p_p \cdot g_{jp}$

Figure 1.5: Perfect power control in a cellular CDMA system

transmits with the minimum possible power that will ensure the QoS (quality of service) guarantee is not violated then the network capacity is increased, and thus it is able to sustain more users concurrently. If a mobile is able to transmit with a lower power and still maintain an acceptable SIR with its receiver, then less interference is presented to the rest of the network, and the system as a whole will benefit. This is the essence of *power control*.

Resource conservation is one of the pleasant side effects/goals of power control. Generally, a mobile terminal is limited in terms of its battery capacity, and by lowering the transmission power an increase in battery lifetime is achieved. Techniques, of which power control is just one of many, for preserving mobile resources fall under the category of *power management* [27].

1.4 Motivation for research

Ad hoc networks should not be seen as competition for cellular networks. Issues arising from the decentralized nature, such as the need for robust and dynamic routing, MAC and power control techniques, will likely result in ad hoc networks providing a much more specialized role.

Cellular systems need to be carefully planned beforehand to ensure optimum network efficiency due mainly to the large cost associated with the permanent base stations, and

spectrum licensing payment. The need for rapid deployment in certain circumstances, for example a military operation into foreign territory, prohibits the use of cellular technology. A towering, expensive, base station erected near an enemy camp would surely present an enjoyable target for aiming practice.

An ad hoc network is capable of filling the role that a cellular network is unable to provide. However with all new technologies come significant problems. The fully distributed nature of the ad hoc network presents new engineering challenges. In order to extract the most from a network employing CDMA, power control is a fundamental and absolutely necessary component. Unlike cellular systems where power control has been widely studied ([28] and the references therein), its effect and implementation details in an ad hoc network are still the subject of some research. Due to the lack of any fixed infrastructure in an ad hoc network, power control is necessary to help maintain connectivity under varying channel conditions [29], this coupled with limited battery capacity, places constraints on maximum transmit power and an effective power control algorithm is crucial to overcoming these problems.

1.5 Dissertation overview

This dissertation is separated into 6 chapters. Chapter 1 provides an introduction into the topic of wireless networks, describing some current ad hoc network developments. The subject of power control is introduced and its necessity in a wireless network explained.

Chapter 2 provides a more in depth discussion of power control, explaining some of the pertinent concepts. A literature survey of selected power control techniques used in cellular and ad hoc networks is also presented.

A distributed power control algorithm is described in chapter 3. There are two main parts to the algorithm: connectivity criteria and transmit power adaptation. Due to

the lack of any predefined connectivity as well as the fully distributed nature of the algorithm, a means of determining which nodes a particular node should attempt to control is presented in the connectivity criteria section 3.3. A node may receive conflicting power control command signals, and various methods are proposed in section 3.4 which control the transmit power adaptation based upon these commands. The decision as to issue an increase or decrease control signal is based upon an ideal received power, as defined by Mitra [30].

The system model for the ad hoc network is presented in chapter 4. Mathematical models for the total path loss, including distance attenuation and shadow fading are formulated. A method of calculating the ideal received power factor, as described in section 3.4.2, is presented and a general description of the simulation environment is given. Due to the large number of simulation parameters it is not possible to present an exhaustive output of all the different combinations, and select results are presented.

The mathematical analysis of the convergence conditions for an ad hoc network are presented in chapter 5. The *standard interference function* approach introduced by Yates [23] and applied later [31, 32, 33] is used to give the conditions under which a feasible power vector exists. A predefined network with strong connectivity is used as an input to the transmit power adaptation algorithm, and the convergence properties of the algorithm tested in a simulation environment.

Chapter 6 presents a summary of some of the conclusion drawn throughout the dissertation and discusses some possible extensions to the work done.

1.6 Original contributions in the dissertation

The original contributions made by the author in this dissertation include:

- Proposition of new node controlling connectivity criteria

- Various new transmit power adaptation algorithms
- Convergence analysis of an ad hoc network with a defined connectivity matrix

Parts of this research have been presented by the author at two local conferences:

- N. R. Pate and F. Takawira, "Power control in ad hoc networks," in *Proc. South African Telecommunications, Networks and Applications Conference (SATNAC) 2001*, (Wild Coast Sun, Kwa-Zulu Natal, South Africa), September 2001. [34]
- N. R. Pate and F. Takawira, "Adaptive distributed power control in ad hoc networks with different controlling node connectivity criteria," in *Proc. South African Telecommunications, Networks and Applications Conference (SATNAC) 2002*, (Champagne Sports, Drakensberg, Kwa-Zulu Natal, South Africa), September 2002. [35]

Chapter 2

Power Control in Ad Hoc Networks

2.1 Introduction

This chapter serves as an introduction to the general concepts behind power control. As the topic of power control in ad hoc network is a relatively new one, not much literature exists on the subject, however the subject of power control in other environments (e.g. cellular systems) is well understood and comprehensively documented. A brief description of some general power control techniques used in wireless communication networks is given, and this is followed by a literature survey of some of the power control methods proposed for use in an ad hoc network.

Careful control of a nodes' transmission power is a crucial aspect for the efficient functioning of all wireless radio communication systems. By transmitting with the lowest possible power that will enable reliable communication, the network as a whole benefits, and the use of vital mobile resources, for example battery lifetime, can be maximized.

The controlling of co-channel interference is paramount in a TDMA/FDMA multicellular networks, where frequency reuse in close-by cells degrades system performance. Systems which employ direct-sequence CDMA need to compensate for the near-far

effect arising from the non-zero cross correlation of the users pseudonoise (PN) codes inherent in this multiple access scheme. Without proper power control a CDMA system will have less capacity than other multiple access schemes utilizing the same bandwidth.

2.2 Power control concepts

Some concepts the are common to all power controlled networks are presented in this section. Power control in cellular networks is now a very well understood subject, and a brief overview of some of the more pertinent concepts follows.

2.2.1 Centralized power control

In a cellular system, it is the job of the base station to control the received power from all the nodes in that cell, as well as the nodes in soft-handoff. Centralized control uses all the information available about the system, and is able to determine an optimum power vector through some predetermined formula. Convergence to the optimum vector generally occurs rapidly, assuming a feasible formulation exists. This type of control requires coordination throughout the network, and usually knowledge of all link gains. This information is generally not available due to excessive signaling and overhead delays, however a centralized algorithm is useful in that it gives an upper bound for the performance of any power control algorithm.

2.2.2 Distributed power control

Unlike centralized power control, a distributed algorithm generally functions in an iterative manner, converging to the optimum region slower than a fully centralized implementation would. Less knowledge about the system is required (for example all inter-node path gains, etc.) and thus little or no coordination between nodes is needed. However, the outage probability when using distributed control is greater than if a

centralized controller was used [36]. A distributed power control system only controls the transmit power of a single terminal, as opposed to a centralized scheme which has control over all the nodes' transmit powers.

2.2.3 Open loop power control

Systems not employing any decision feedback are referred to as open loop. Open loop control is generally used as a coarse estimate which is fed into a closed loop system to provide a slowly changing estimate of the system. In a cellular environment open loop control is used to obtain an estimate of the total link gain due to distance attenuation and shadow fading; it is used to compensate for *large* changes in the channel.

In open loop power control the channel gain (distance attenuation and shadow fading) is estimated by measuring the strength of a received pilot signal. The larger the pilot signal attenuation, the greater the propagation loss, and thus the greater the mobile transmit power needs to be to overcome this loss. The inverse of the measured gain (loss) is used, together with a correction factor to obtain the new transmit power. This value for the reverse link transmit power is only an estimate as there is generally a frequency separation between forward and reverse channels.

2.2.4 Closed loop power control

Open loop control is used as an initial estimate of the link gain, but it is not able to counter the effects of multipath fading on the downlink (base station to mobile). As a frequency separation between the forward and reverse channels exists, the multipath fading on these two links are independent processes and not strongly correlated. Although the average power needed to overcome the slow fading processes is the same, short term power needs are different, and thus open loop control is not able to counteract this. In the IS-95 CDMA standard, 20 MHz separates the two channels, and this

greatly exceeds the coherence bandwidth[1] of the channel, thus closed loop control is used. The outer loop control provides a target for the inner loop to try and maintain. In a cellular CDMA system the outer loop target is a signal-to-interference ratio which is adjusted over time depending on the bit error rate (BER), or sometimes frame error rate (FER) of the system. Typically a single-bit increase or decrease signal is sent to the mobile terminal instructing it to raise or lower its transmission power by the fixed (pre-specified) amount e.g. 1 dB. These signals are sent at a rate which is fast enough to counter the effect of fast-fading when the terminal is moving at slow to moderate speeds (less than $50\,\mathrm{kmh}^{-1}$). In the UMTS 3G specification fast power control updates happen at a frequency of 1.5 kHz.

2.2.5 Quality Measures

In a cellular radio communication system the majority of the digital data being transmitted is dedicated to voice conversations. Unfortunately, as speech quality is very subjective, the performance based purely on audible statistics of two different systems is difficult to accurately quantify, measure and compare. A more accurate measure of the quality of a link is the SIR. It is generally accepted that if the SIR of a link is above some target, γ^*, then the communication is assumed successful. The best quality measure is actually the bit error rate, but this requires delving deeper into the workings of the communication system as it is a function of many things including modulation and coding schemes. In a data communication system the QoS is more likely to be specified as a maximum tolerable BER, not SIR. It has been argued that SIR is as good as BER when considering the performance of a system, as the two are often considered equivalent, but this is only true when the signal and interference levels do not change over the course of the measurement. Even though the *average* SIR may satisfy the requirements, the instantaneous SIR may drop below the target causing the

[1] In a frequency selective fading channel, spectral components are subject to different attenuations, and if the transmitted signal occupies a bandwidth greater than the coherence bandwidth the received signal will be distorted [26]

BER to increase. The frame error rate is sometimes used in place of BER, where the measurement is taken after interleaving and temporal diversity (convolutional coding) have been accounted for.

2.2.6 Available measurements

Any resource management algorithm is only practically implementable if the correct functioning of the scheme depends on quantities readily available i.e. easily measured/obtained. In reality, a power control system must be distributed, with the decision logic needing only locally available information for correct functioning. The speed at which the measurements can be taken and the non-zero time for the control signals to be propagated to the intended user affects the minimum time duration between power control iterations. Using outdated information will lead to a degradation in system performance. Some of the available measurements include: attenuation a channel will experience, interference power received, signal received, SIR received, BER experienced and transmitted power. Often these quantities have to be estimated, and the less accurate the estimation the greater the performance degradation of the system will be.

2.2.7 Constraints

All physical devices have constraints in terms of maximum transmission power. Usually government law regulates the maximum output power of a device to ensure the safety of users, and also to ensure interference is kept to manageable levels. Mobile terminals are also limited in their battery capacity, and this too places a constraint on transmit power as a device may not be able to sustain transmitting at maximum power for long periods.

2.2.8 Power control techniques

In a cellular environment, different techniques are applied to the uplink and downlink, and different measurements can be used. Power control decisions can be based on received signal strengths, SIR, bit error rate or frame error rate and the control loop can be open or closed or some combination of both. Strength based control is the easiest to implement, but does not provide an adequate measure of system performance. Older power control algorithms use a fixed step-size for adjusting the transmission power, but some newer concepts involve an adaptive step-size which generally leads to quicker convergence and better performance. Analysis has shown that adaptive step-size algorithms perform better, but single-bit signaling inherent in fixed-step size control requires less information overhead [28].

Although many power control algorithms are derived assuming that a device can transmit at any power level with a certain range, in reality the power is often quantized and this leads to a decrease in the performance of the algorithm. When quantization is taken into account, an ideal power vector optimal solution often worsens into an ideal region of convergence which is suboptimal. The outage of the system is greater, and oscillation may occur when quantization is used. Fig. 2.1 depicts the relationship of power control techniques.

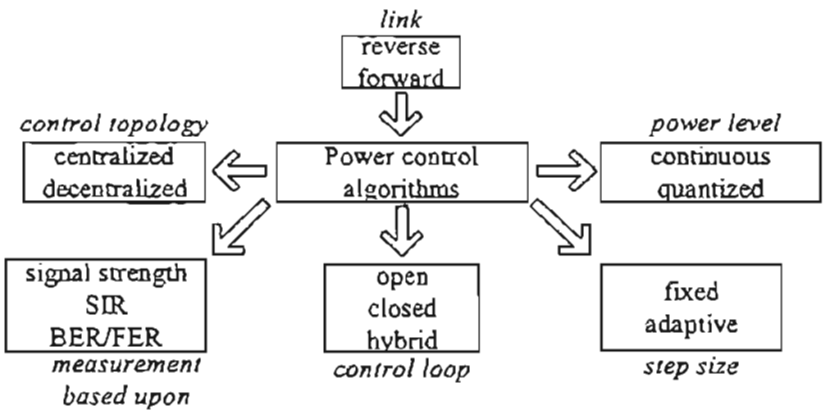

Figure 2.1: Classification of power control techniques

2.3 Power control in cellular systems

Some of the earliest work on power control was done by Aein [37], where a satellite system was considered. The algorithm attempted to balance the uplink power of the terrestrial transmitters so that the minimum SIR was maximized. This algorithm has the benefit of fast convergence, however it needs a centralized controller to compute a global normalization factor. Also, as the SIR is the same on every link (equalization), the algorithm is not suitable when different services are used over the same channel, as the QoS requirements may need different SIR's on various links [38].

The problem of assigning a unique transmission power to each mobile in a cellular system has been studied in depth, with a typical implementation given by Grandhi [39] or Bambos [40].

Considering a cellular radio system with N mobiles, mobile i transmitting with power p_i, and the link gain from terminal j to the base station to which i is communicating denoted g_{ij}. The SIR of i at its corresponding base station, γ_i is given by:

$$\gamma_i = \frac{p_i \cdot g_{ii}}{\sum_{j \neq i}^{N} p_j \cdot g_{ij} + \eta_i}, \quad 1 \leqslant i \leqslant N \tag{2.1}$$

where $\eta_i > 0$ is the thermal noise power at the receiver. For the communication to be suitable on each defined link, the actual SIR, γ_i, must be greater than the target SIR, γ_i^*, defined by the QoS:,

$$\gamma_i \geqslant \gamma_i^*, \text{ for all } i \in \{1 \ldots N\} \tag{2.2}$$

This relationship between QoS and SIR is valid under the assumption that the number of users sharing the common channel is large and the central limit theorem holds, thus the interference follows a Gaussian distribution. This assumption has been shown to be valid in reality [41]. Substituting the minimum SIR requirement into (2.1) and dividing

through by the g_{ii} normalization to isolate the p_i term leads to:

$$p_i \geq \gamma_i^* \cdot \left(\sum_{j \neq i}^{N} p_j \cdot \frac{g_{ij}}{g_{ii}} + \frac{\eta_i}{g_{ii}} \right) \tag{2.3}$$

Introducing the $N \times N$ matrix $\mathbf{A} = \{A_{ij}\}$ where

$$A_{ij} = \begin{cases} \left(\frac{\gamma_i^* \cdot g_{ij}}{g_{ii}} \right) & \text{if } i \neq j \\ 0 & \text{if } i = j \end{cases} \tag{2.4}$$

and the $N \times 1$ vector, η, with element $\eta_i = \gamma_i^* \cdot \eta_i / g_{ii}$ and substituting into (2.3) gives the matrix form of the system

$$\mathbf{p} \geq \mathbf{A}\mathbf{p} + \eta \tag{2.5}$$

where $\mathbf{p} = (p_1, p_2 \ldots p_N)^T$ is the column vector of each node's transmit power. A solution to the power assignment problem is then given by solving for p:

$$\mathbf{p}\,(\mathbf{I} - \mathbf{A}) \geq \eta \tag{2.6}$$

The minimum energy solution, $\mathbf{p}^*$, is when the transmit power exactly satisfies the SIR target, so the inequality in (2.6) becomes:

$$\mathbf{p}^* = (\mathbf{I} - \mathbf{A})^{-1} \eta \tag{2.7}$$

where I is an $N \times N$ identity matrix.

In order for the system defined by (2.5) to have a real, positive solution for every element of $\mathbf{p}^*$, it is clear from the RHS of (2.7) that $(\mathbf{I} - \mathbf{A})^{-1}$ must exist and have all non-negative entries.

From the theory of Perron and Frobenius in matrix theory [42], given a system of equations, $\mathbf{p} = \mathbf{A}\mathbf{p} + \eta$, and the fact that A is a square, nonnegative, irreducible matrix, a nonnegative solution for p exists only if $\rho_A < 1$. Known as the spectral radius, ρ_A is the maximum modulus eigenvalue of the A matrix. By Perron and Frobenius, ρ_A is positive and simple, and the eigenvector corresponding to this eigenvalue is component-wise positive. The normalized gain matrix, A, is nonnegative in that every element of

$\mathbf{A} \geqslant 0$, and it is also primitive as $\mathbf{A}^2 > 0$, and these two conditions imply that $\mathbf{A}$ is irreducible. The solution provided by (2.7) is *Pareto optimal* in that no other system power vector will satisfy the SIR target and have a component less than $\mathbf{p}^*$.

A central controller with access to all the inter-node path gains, thermal noise terms and the target SIR would be able to set the system power vector to its optimal value. This information is seldom available, and so a more practical, iterative implementation, first introduced by Foschini and Miljanic [43] is:

$$\mathbf{p}(n) = \mathbf{A}\mathbf{p}(n-1) + \eta \tag{2.8}$$

where n is the iteration number, and this converges to the optimal solution, as can be seen through recursion:

$$\begin{aligned}
\mathbf{p}(1) &= \mathbf{A}\mathbf{p}(0) + \eta \qquad (2.9)\\
\mathbf{p}(2) &= \mathbf{A}\mathbf{p}(1) + \eta \\
&= \mathbf{A}(\mathbf{A}\mathbf{p}(0) + \eta) + \eta \\
&= \mathbf{A}^2\mathbf{p}(0) + \mathbf{A}\eta + \eta \\
\mathbf{p}(3) &= \mathbf{A}\mathbf{p}(2) + \eta \\
&= \mathbf{A}\left(\mathbf{A}^2\mathbf{p}(0) + \mathbf{A}\eta + \eta\right) + \eta \\
&= \mathbf{A}^3\mathbf{p}(0) + \left(\mathbf{A}^2 + \mathbf{A} + 1\right)\eta \\
\mathbf{p}(n) &= \mathbf{A}^n\mathbf{p}(0) + \left(\sum_{k=0}^{n-1}\mathbf{A}^k\right)\eta
\end{aligned}$$

In the limit as $n \to \infty$

$$\lim_{n\to\infty}\mathbf{p}(n) = \lim_{n\to\infty}\left(\mathbf{A}^n\right)\mathbf{p}(0) + \lim_{n\to\infty}\left(\sum_{i=0}^{n-1}\mathbf{A}^i\right)\eta \tag{2.10}$$

assuming $\rho_A < 1$ then

$$\begin{aligned}
\lim_{n\to\infty}\mathbf{p}(n) &= 0 + \left(\sum_{i=0}^{\infty}\mathbf{A}^i\right)\eta \qquad (2.11)\\
&= (\mathbf{I} - \mathbf{A})^{-1}\eta \\
&= \mathbf{p}^*
\end{aligned}$$

The substitution $\sum_{k=0}^{\infty} \mathbf{A}^k = (\mathbf{I} - \mathbf{A})^{-1}$ arises from the Perron-Frobenius theorem and the assumption that $\rho_A < 1$. If the system is not feasible the algorithm will continuously ramp up the transmit power. The iteration defining equation, (2.8), can be written for node i as

$$p_i(n) = \frac{\gamma_i^*}{g_{ii}} \cdot \left(\sum_{j \neq i}^{N} p_j(n-1) \cdot g_{ij} + \eta_i \right) \tag{2.12}$$

and this may be reduced using (2.1) to

$$p_i(n) = \frac{\gamma_i^*}{\gamma_i(n-1)} \cdot p_i(n-1) \tag{2.13}$$

for all nodes $1 < i < N$ in the network. Equation (2.13) gives an iterative, distributed procedure for solving for the optimum power vector that does not require the knowledge of all the link gains and node transmit powers. Essentially the base station measures the received SIR and transmits it back to the mobile unit. Under the assumption that all other mobiles do not change their transmit power, and the link gains are constant, the mobile is able to calculate, via (2.13), the exact (minimum) transmit power required so that its SIR target at the base station will be perfectly satisfied. Of course all the other mobiles will also be running the same algorithm, and so the dynamic, generally known as the distributed power control (DPC) scheme, specified by (2.13) will continue indefinitely. The DPC is often used as a reference algorithm when comparing speed of convergence

A problem with the DPC algorithm as described is that it aims for exactly the required SIR target, assuming all the other nodes do not change their transmit power. Another cause for concern is the admission of new calls to the channel, which will cause even further interference and degradation of the SIR. In order to maintain the SIR above the required target throughout the duration of the algorithm a *protection margin* joint power control and admission control algorithm was introduced by Bambos *et al.* [44]. Essentially during normal operation, a link which has already powered up (those belonging to the set $\mathcal{A}_i$) strives for slightly greater than the target SIR, and any new calls to the system (in set $\mathcal{B}_i$) start off at a low power and are only allowed to

increase slightly during each power control iteration, to protect the established calls. The active link protection distributed power control (DPC/ALP) is summarized:

$$p_i(n) = \begin{cases} \delta \cdot \frac{\gamma_i^*}{\gamma_i(n-1)} \cdot p_i(n-1) & \text{if } i \in \mathcal{A}_i \\ \delta \cdot p_i(n-1) & \text{if } i \in \mathcal{B}_i \end{cases} \tag{2.14}$$

The safety margin introduced by the δ parameter helps the system adapt to random changes in state due to, for example, mobility. Clearly choosing a δ too high will lead to excessive transmission powers being used and thus actually limiting the system capacity and reducing node lifetime.

In reality, the mobile terminals are upper bounded by some maximum permissable transmission power. The DCPC introduced in [39] is a constrained version of the DPC, and it has a similar form to (2.13), but includes means for limiting the power of a node:

$$p_i(n) = \min\left\{\frac{\gamma_i^*}{\gamma_i(n-1)} \cdot p_i(n-1), \hat{p}_i\right\} \tag{2.15}$$

where $\hat{p}_i$ is the maximum transmission power for node i.

Due to the intrinsic feedback nature of power control in a cellular system, many algorithms based upon control theory have been proposed. A PI (proportional-integral) controller derived from the discretization of the continuous model of the DPC had been proposed and it was shown to significantly enhance the convergence speed compared to the traditional DPC model [45]. A second-order power control method which uses the previous power level as well as the current power level has been shown to have a high potential for increasing the wireless capacity [46]:

$$p_i(n) = \min\left\{\hat{p}_i, \max\left\{0, \omega(n-1) \cdot \frac{\gamma_i^*}{\gamma_i(n-1)} \cdot p_i(n-1) + (1-\omega(n-1)) \cdot p_i(n-1)\right\}\right\} \tag{2.16}$$

The $\omega(n)$ control parameter is a non-increasing sequence satisfying

$$\omega(1) = \omega(2) < \omega(3) = \omega(4) < \ldots < \omega(2n-1) = \omega(2n) < \ldots \tag{2.17}$$

The algorithm has a much faster convergence rate than the geometric rate exhibited by DPC, but as more information is used in the algorithm (requiring measurement), errors could result in less performance gain than obtained through the initial simulations.

As there is a delay between measurements being taken, transmitted and actually used in most power control algorithms the longer the delay the worse the performance of the algorithm. By including the time delay in the analysis, and compensating for it, the dynamic behaviour of an algorithm can be improved. The time delay compensation (TDC) algorithm presented in [47] can be adapted to most power control algorithms and the effects of time delay can be reduced. Some other research using a control theoretic approach is given in [48, 49].

The power control algorithms that have been presented were all based on the assumption that the base station assignment was fixed (and known). Adding another dimension to the problem is the challenge of selecting to which base station a mobile should transmit such that the total power of all the nodes is minimized. Termed the minimum transmitted power (MTP) algorithm [50], the problem can be formally stated:

$$\begin{aligned} &\text{minimize } \textstyle\sum_i p_i \\ &\text{subject to} \\ &g_{a_i i} \cdot p_i \geqslant \gamma_i^* \left(\textstyle\sum_{j \neq i} g_{a_i j} \cdot p_j + \eta_{a_i} \right) \quad 1 \leqslant i \leqslant N \\ &p_i \geqslant 0 \qquad\qquad 1 \leqslant i \leqslant N \\ &a_i \in (1, \ldots, M) \qquad\qquad 1 \leqslant i \leqslant N \end{aligned} \tag{2.18}$$

The base station assignment vector, $\mathrm{a} = [a_1, a_2, \ldots, a_N]$, has $a_i = k$ if mobile i is assigned to base station k. The constraints given in (2.18) state that: the SIR target needs to be achieved, the transmit power has to be non-negative, and the assignment vector has to consist of integer values. A minimum power assignment (MPA) algorithm is an iterative solution to the MTP problem, at each iteration a mobile terminal selects a base station which would need the minimum transmit power to achieve the necessary SIR target. This occurs under the assumption that the other mobiles do not change their transmit power:

$$p_i(n) = \min_k \frac{\gamma_i^* \left(R_k(n-1) - g_{ki} \cdot p_i(n-1) \right)}{g_{ki}} \tag{2.19}$$

and $R_k(n-1)$ is the total received power at base station k during the previous time instant (i.e. using the system transmit power vector $\mathrm{p}(n-1)$).

All similar forms of algorithms suffer from relying on the accuracy of the SIR measurement. It was proposed that the SIR target should be scaled up by 1 dB if the measurement error is between 1 % and 5 % [51].

Common to all the preceding power control schemes is the feedback of various information measures e.g. total received power at the target or SIR experienced. These measurements have to be transmitted back to the mobile terminal, and are used by the mobile to calculate a new transmit power. The obvious drawback to this method of power control is that as the number of nodes in the network increases, so to does the feedback overhead, especially if high-precision values are being transmitted every power control iteration. The solution is to use a much more coarse feedback signal, in the extreme case using only a single data bit to indicate the status. This single bit feedback is the basis for most modern schemes, and is used in all 3G specifications. Also known as *bang-bang* control, this method of feedback uses much less bandwidth to convey the required signalling. Clearly a trade-off exists between precision of feedback and performance of the algorithm. In order to adjust for the lack of signalling precision, the feedback is done at a much higher rate. This allows the algorithm to adjust to rapid changes in channel conditions [52, 53].

A typical single bit feedback algorithm would function as follows. The SIR received from a mobile unit would be compared to some reference value, and if it falls below this target an increase power command is sent to the mobile. Similarly if the received SIR is greater than the desired target a decrease command is transmitted. In most implementations the target SIR is set by some outer loop which will slowly adjust the target depending on, for example, the BER or FER experienced. The mobile terminal will receive either an increase or decrease signal, and will adjust its transmission power

by the predefined fixed step size[2] i.e.:

$$p_i(n) = \begin{cases} \delta \cdot p_i(n-1), & \text{if } \gamma_i < \gamma_i^* \\ \delta^{-1} \cdot p_i(n-1), & \text{if } \gamma_i \geq \gamma_i^* \end{cases} \tag{2.20}$$

Normally these fast power control feeback signals do not enjoy the error-correcting benefits of temporal interleaving.

2.4 Power control in ad hoc networks

Unlike a cellular network, where if a mobile maintains an acceptable connection with its associated base station, then it is able to reach any other mobile in the network, in an ad hoc network there is no such connectivity guarantee. This is because the cellular architecture has base stations permanently hard wired together maintaining network connectivity, whilst in an ad hoc network there are no fixed links. In an ad hoc network the mobiles are randomly distributed, and there is no guarantee that if a node maintains an acceptable connection with its neighbour that the network is connected. In order for the network to function, and point-to-point communication between any node pair to be possible, a route needs to exist between every node in the network. Through the use of power control the network topology can be adjusted so that this connectivity is maintained. Fig. 2.2 shows the same node distribution with poor connectivity resulting in network partitioning, and a more desirable topology which would result in proper functioning. It is one of the basic requirements of a power control algorithm in an ad hoc network to maintain network connectivity.

2.4.1 Power management

Efficient use of the resources available at a node are crucial in a wireless ad hoc network. Some techniques for energy management include: low power mode, energy efficient

[2] A mobile in soft-handover may be receiving more than one command. The situation is then slightly more complicated, for an overview of the procedure refer to [11], chapter 9.2

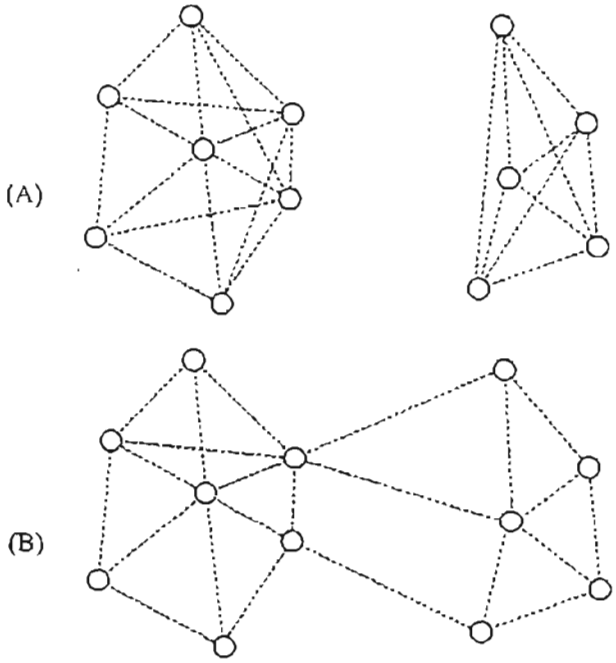

Figure 2.2: (A) Poor node connectivity, (B) Desirable node connectivity

routing and transmission power control. In low power mode the device goes into a power efficient sleep mode, and awakes periodically.Using the model for 802.11 WaveLAN radios [54] where the energy requirements for idle, send, and receive are 1:1.05:1.4 respectively, the energy consumption is dominated by the node idle time. By turning off the nodes and lengthening their sleep intervals, an energy saving of nearly 50 % can be achieved when using the Basic Energy Conserving Algorithm (BECA) proposed [55]. A trade-off does exist, in that turning off the radios leads to increased latency. More information on this and similar energy conservation methods can be found in [56] and the references therein. Energy efficient routing protocols in ad hoc networks have been the focus of significant research and are beyond the scope of this dissertation. A good starting point though would be [57].

2.4.2 MAC power control

The 802.11 MAC protocol for transmission of data involves the following signaling pattern: Request-To-Send (RTS)/Clear-To-Send (CTS)/data/acknowledge (ACK), shown in Fig. 2.3. Modifications to this proposed by Agarwal et al, [58], embed extra informa-

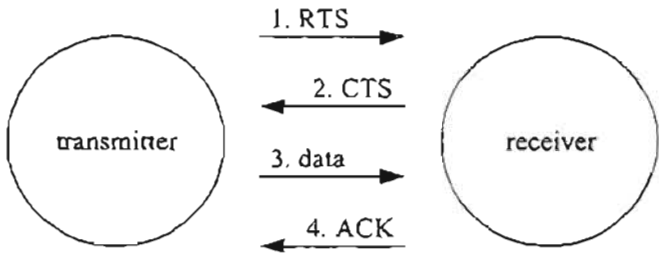

Figure 2.3: IEEE 802.11 signaling for addressed messages

tion in the CTS and DATA packets. After receiving an RTS signal from a nearby node, the received node measures the SIR experienced, and then encodes the CTS packet with the ratio of received SIR to minimum acceptable SIR. Then when the initial transmitter receives the CTS command it is able to determine the quality of the wireless link to the destination. Similarly, when transmitting the data to the receiver, the transmitter also includes an indication of the reverse link channel quality by embedding the ratio of the received SIR of the CTS command to its minimum allowable SIR. By exchanging messages like this the two nodes are aware of the channel quality in both directions. At each node, a small table of various parameters is kept. These relate to factors such as: current transmit power level for each node, an exponentially weighted average (EWA) of the received signal strength ratio history (*cf_pwr*), and the EWA history of the *cf_pwr* when the link experienced a packet loss (*dr_pwr*).

A count-down timer is used to reduce power level oscillations. When a node is sent a message it is able to extract the information on the quality of its previous transmission, and this information is added to the *cf_pwr* field. If the countdown timer has reached zero and the *cf_pwr* is greater than the *dr_pwr* value, then the transmission power

is decremented a step. A total of ten transmit power levels are defined (GSM uses between eight and fifteen), varying linearly between the maximum transmit power and one-tenth of this value. The node increases its transmission power one level when the MAC experiences a timeout, and the *dr_pwr* value is updated. The goal of this particular algorithm is to converge to the minimum power level that will ensure a successful transmission.

Simulation results show small improvements in energy savings and throughput, however when nodes are communicating at the maximum power level the overhead associated with including the extra information in the message headers degrades the performance of the algorithm. Typically, a 10 % energy saving and 5 % increase in throughput is noted compared with the traditional 802.11 MAC. These results were for random mobility and movement models. If group mobility and traffic patterns are incorporated into the simulation, then throughput is seen to improve approximately 15 %. As this method of power control only functions on a per-link basis, it does not attempt to guarantee network connectivity, and it is assumed that some higher level component will decide which links are necessary for connectivity.

2.4.3 Cluster based power control

Control of a node's transmission power within a cluster is used in [27]. The size of the individual clusters depends on the system parameter, N, which is the number of neighbouring nodes a single node will consider. Power adaptation takes place only within the cluster. The two algorithms proposed include:

- No power adjustment within a cluster
- Power adjustment within a cluster

In the first scheme a node will transmit with the same power regardless of which node in the cluster is the target of the communication. This fixed power level is equal to

the power required to reach the farthest node, i.e. the channel experiencing the most attenuation. The second method specifies that only the minimum power required to successfully communicate with the intended node is used. The first method will not lead to maximum efficiency because a node will transmit to all nodes, excluding the one with the worst channel quality, with a power greater than required for successful reception of data. It is generally accepted that little is gained from a node receiving a SIR greater than required. Intuitively the latter method will be more energy efficient because the problem associated with transmitting excess power is resolved.

Assuming a minimum received power, $R_{\min}$, is needed in order to guarantee a maximum BER is not exceeded. The power received, R, is dependent on the transmitted power, P, and the path gain, g; $R = P \cdot g$. The transmission level to guarantee the minimum received power is given by: $P = \frac{R_{\min}}{g}$, and the path gain can be calculated from the received power when the maximum (known) power is transmitted: $g = \frac{R_{\max}}{P_{\max}}$. This information can be combined to give a value for minimum transmit power: $P = \frac{R_{\min} \cdot P_{\max}}{R_{\max}}$

The Periodic Update Protocol (PUP), a method for adapting the parameter N, was proposed as follows:

1. Set the connectivity $N = 2$
2. This value of connectivity is used for a pre-specified number of frames (k)
3. After k frames, the end-to-end throughput, Φ_N, of the particular node is evaluated and broadcast on the dedicated reverse channel (using a contention free MAC scheme)
4. Increase the connectivity by one, the system operates using this new value for the following k frames
5. After the k frames and each node has broadcast their individual end-to-end throughput, calculate the new network throughput. Old Φ_N is now Φ_{N-1}

6. If $\Phi_N > \Phi_{N-1}$ increase the connectivity and goto step 5, otherwise decrease N and goto step 5

This method does seem to have a flaw in that the system could converge to a local maximum, however simulation results have indicated that only a single optimal operating point exists.

Simulation results have indicated that the method of adjusting power within a cluster does indeed improve network throughput and helps lower power consumption. Improvements to the algorithm include the Quasi-Periodic Update Protocol (QPUP), which functions similarly to the PUP differing in that when maximum throughput is sensed the algorithm scales down its attempts to test the current connectivity. With low mobility the network topology will be changing slowly, so control signaling overhead could be reduced this way.

An extension to the PUP allows each node to have a different connectivity parameter N, however this theory has not yet been tested.

2.4.4 Topology control using transmit power adjustment

Ramanathan proposed a set of algorithms (for fixed and mobile packet networks) whereby the transmission power of a node is adjusted to ensure the network remains connected [59]. For fixed networks, two algorithms *CONNECT*, and *BICON-AUGMENT* are proposed. The functioning of the *CONNECT* algorithm is similar to a minimum spanning tree (MST) algorithm, [60] and functions in a *greedy* manner by merging unconnected clusters (connected components) until the entire network is connected. Initially each node is considered to be part of a separate cluster, and the node pairs are parsed in a non decreasing minimum inter-node distance manner. If the two nodes are in different clusters then the transmit power of each node is increased until the two clusters effectively merge into a single connected entity. This process is repeated until the entire network is connected.

It was proven that the resulting connected network will have minimum maximum transmit power. However the process is not necessarily optimal (minimum) per-node, as extra *side-effect* edges get introduced into the graph when the transmit power of a node is increased. The network is said to be per-node-minimal when it is not possible to reduce the power of any single node and still maintain connectivity. The addition of side-effect edges may in fact allow the transmit power of a node to be reduced while still maintaining network connectivity. In order to achieve a network minimal power solution a post-processing procedure is introduced to remove any unnecessary links. This is achieved by lowering the power of the nodes (one at a time) as far as possible while still ensuring connectivity.

A network that is biconnected has a minimum of two paths between any node pair, and has the desirable property that the removal of any single node will result in a network which still has full inter-node connectivity (i.e. network is not partitioned). The extra paths introduced can be used for load balancing and make the network more tolerant to faults.

The *BICON-AUGMENT* algorithm starts with a network that has been *CONNECT*ed by the first algorithm, and then functions in a similar manner to the *CONNECT* algorithm, until all the nodes are biconnected.

These two proposed algorithms require each node to have full knowledge of the positions of all the other nodes in the network, and so are not suitable to implementation in a mobile network. Node mobility leads to a constantly changing network topology, and each node has to make decisions based only on locally available information. Clearly a fully distributed algorithm is necessary, and two mobile algorithms are proposed: Local Information No Topology (LINT) and Local Information Link-State Topology (LILT).

LINT uses information that is available at each node due to the routing protocol. The protocol attempts to keep the desired degree, d_d, of the number of neighbours of a node

constant. The transmit power at each iteration is given by:

$$p_d = p_c - 5 \cdot \varepsilon \cdot \log\left(\frac{d_d}{d_c}\right) \tag{2.21}$$

The information needed to update the transmit power is available at each node: p_c is the current transmit power that results in the degree of neighbours, d_c, whilst the ε corresponds to a path loss exponent. A random time generator is used to determine the power update intervals. The node periodically checks the number of neighbours from information generated by the routing protocol. If the degree of neighbours falls within a hysteresis range then the power is adjusted using (2.21). The greater the difference in connectivity degree, the greater the change in transmission power.

It may however occur that even though the degree of connectivity is satisfied, the network is partitioned. The LINT protocol presented has no method of detecting or correcting network partitions. LILT was developed to overcome this shortcoming of LINT. In addition to the described LINT functioning, LILT also includes a neighbour addition protocol (NAP). Whenever a link-state update is detected then the NAP checks to see if this would result in undesirable connectivity. If the network is connected, but not biconnected, then at least one articulation point[3] exists. The node calculates its distance to the articulation point and sets a timer, t, that is a number randomized with an exponential distribution based on the distance from the articulation point. After time t if the articulation is still not biconnected, then the node increases its transmission power to the maximum allowable power, $\hat{p}$, to quickly reduce the partitioning probability. The aim of the t timer is to give priority to the nodes closer to the danger point, thus giving them the chance of removing the articulation point by adding more available paths. If at any event interval stage the node discovers that the network is partitioned, it increases its transmission power to $\hat{p}$.

Under a simulated mobile network environment, the implementation of LINT and LILT topology control was found to improve network througput.

[3] An articulation point is a node in the network that if removed will result in partitioning

2.4.5 Topology control for multihop packet radio networks

A precursor to the ad hoc network was the tactical radio system. Of importance to the military, this packet switched network architecture was used to connect mobile terminals in a multihop manner. Power control is used in an attempt to achieve a reliable topology that also ensures good throughput, usually two very conflicting requirements. The control needs to be distributed amongst the nodes, as any centralized controller would lead to the network being much more vulnerable, and any decisions would need to be propagated from the controller throughout the network, incurring overhead and reducing network throughput. As the packet radio is susceptible to node failure (due to enemy activity), the topology should be robust in that removal of nodes should not lead to network partitioning. Topological changes should not influence the reliability of data throughput in the network. Hu [61] introduced a topology control mechanism based on transmit power adjustment which is fully distributed and attempts to achieve a reliable, high throughput topology. It is known as the novel topology control (NTC) algorithm. A starting point in the algorithm is a planar graph structure that has the maximum number of edges, i.e. all bounded regions are triangles. By maximising the minimum interior angles of the triangles a structure known as Delaunay triangulation is achieved, and serves as a triangular *backbone* connectivity. A centralized algorithm with the parameters: the maximum degree (number of neighbours), θ, and the maximum transmission range, R, is given:

1. Begin with a Delaunay triangular structure
2. Remove the edges with length greater than R
3. With the remaining edges, in decreasing length, remove if it results in a degree greater than θ at either end node
4. In increasing length, add edges to the graph that do not violate any of the constraints

This centralized scheme was tested in a simulation environment with a CDMA air interface and was noted to outperform networks with regular structures[4].

An implementation would have to be of a distributed nature, and a procedure for topology control with no form of centralized control is given:

1. Through a broadcast, each node is able to determine its neighbours within the distance R
2. A node finds its adjacent Delaunay Triangle neighbours within the distance R
3. In increasing distance order, add an edge as a path until the degree criteria, θ, is satisfied. Notify other nodes about edges rejected, and disregard any edges abandoned by neighbouring nodes
4. Find extra edges through a handshaking process with neighbours. A node will only accept edges from the single node closest to it, and this step continues until the degree is satisfied, or no more nodes are in range are available .

Insight into finding local nodes can be drawn from a Voronoi diagram of the network. Given the Delaunay triangle representation, a Voronoi polygon of node i is the set of all points that are closer to node i than any other node. By tessellating overlapping Voronoi polygons the Voronoi diagram can be obtained, an example of which is given in Fig. 2.4. The dotted lines are the Delaunay triangulation, and the solid lines correspond to the Voronoi polygons constructed from these. Computation of local neighbours can be reduced by considering a radius $r < R$ and increasing r until the neighbouring node degree is satisfied.

It can be shown that the distributed NTC algorithm leads to the same topology as the fully centralized version, and the resultant topology has a greater throughput than regular network structures with the same connectivity degree. In order to maintain

[4] A regular structure is a network that has the same degree for all nodes, and the distance to each neighbour is constant

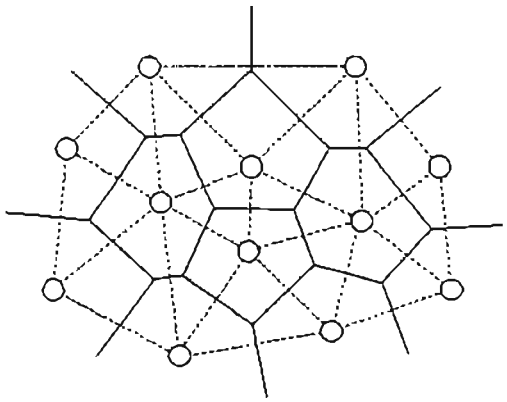

Figure 2.4: Delaunay Triangulation (dotted lines) and corresponding Voronoi diagram

triangulation, θ should be greater than or equal to six, but simulation results show that network throughput decreases as the degree is increased above six, thus $\theta = 6$. It was also shown in [62] that the number of neighbours needed to maximize throughput should be six.

2.4.6 Connectivity

Various papers have proposed different *magic numbers* for neighbouring node connectivity. Initially, Kleinrock proposed that each node should be connected to six neighbouring nodes for optimum performance, and this number was later revised to eight [63]. Other literature suggests different numbers; six and eight were considered optimal when each node had full control over its transmit power [64], and three neighbours was suggested in [65] when the objective was the maximization of transmission efficiency. Simulation carried out by Royer [66] suggested that to maximize network throughput, node density should be an increasing function of node mobility. When network connectivity is studied, [67] showed that the optimum number of neighbouring connected nodes, θ, is in the region of $6 \rightarrow 10$.

More recently, however, it was shown in [68] that when network connectivity is considered, the ideal number of neighbours is not actually a constant. Given a network

consisting of n randomly placed nodes. the connectivity per node should actually be

$$\theta = c(\log n) \tag{2.22}$$

Asymptotically, as the number of nodes increases, if c is greater than $5.1774 \log n$ nodes the network is connected with probability approaching unity. On the other end of the scale, if c is less than $0.074 \log n$ the probability that the network is disconnected tends towards one.

When choosing a connectivity value it should be kept in mind that although a greater connectivity will lead to greater route diversification, it also results in increased interference. The ability to reduce the number of hops a packet has to traverse will result from greater connectivity and may increase throughput, but this is counter balanced by increased interference as a node has to transmit to targets further away, which will reduce capacity. The tradeoff is between network relaying burden and acceptable interference. Work by Gupta [69] proposed that the smaller the range of transmission the better, as the interference burden is of the order of $O(r^2)$, but relaying burden only increases as $O\left(\frac{1}{r^2}\right)$ where r is the broadcast distance. Choosing a r value too small however, can lead to the network becoming disconnected.

In work by Sánchez, [70], the critical transmission radius was investigated. A *critical link* in a network is one which, if removed, will cause partitioning of the network. It is the inter-node distance of this link that is referred to as the critical transmission radius. Using a minimum spanning tree, as provided by, for example, two well known algorithms by Kruskal or Prim [71], the longest edge corresponds to the critical link. If the transmission power is reduced, the longest link will fail first.

Through simulation, and by looking at various mobility models, some statistics of the critical transmission range can be predicted. Results indicate that shorter values of critical link distance produce better throughput, but the probability of network partitioning increases, thus care needs to be exercised when choosing such a value.

If the nodes are uniformly randomly distributed in a disk of unit area, then it was

shown in [72] that a range, $r(n)$, set from $\pi \cdot r^2(n) = \frac{\log n + c(n)}{n}$ would lead to a network that is asymptotically connected if and only if $c(n) \to +\infty$.

A simulation study to determine the effect of the parameter c in (2.22) suggest that the value of c actually lies close to one.

2.4.7 COMPOW

Very little work has been done on actually implementing a power control algorithm in an ad hoc network. The COMPOW protocol [9],[73] is one of the first attempts at providing an implementation that has been tested in a physical system. Central to the algorithm is the argument that every node in the network should use the same (common) transmission power, hence the COMPOW name. In order for the network to have good connectivity properties and to simplify operation the authors suggest that bidirectional links are necessary. A method of ensuring this bidirectionality is to have all nodes transmitting with the same power, and this power should be set as low as possible that guarantees network connectivity.

For each of the i transmit power levels of the node, P_i, a routing table is maintained by sending and receiving *hello* messages at that power level. Each node then selects the transmit power that has the same number of entries in its routing table (number of nodes reachable) as the routing table of the maximum power setting. This newly selected routing table is used by the kernel as the master routing table. Clearly, running extra routing daemons will result in more control information overhead placed on the network. With reasonable connectivity (six nodes within range) the routing information is approximately 60 kbits/s which is only 1 % of the theoretical maximum throughput.

The implementation was done on laptops running Linux. The firmware in the current generation of wireless LAN card needs to be reset every time a new transmission power is selected, and this results in a switching latency of nearly 100 ms. This is clearly not acceptable, and to step around this problem a scheduling algorithm was implemented

that attempts to keep the number of transmission power changes to a minimum. This is done by scheduling consecutively all queued packets that have the same transmission power. A clearing or exhaustive policy can be used to do this, with the power level changed only when no more packets of that power level are present as shown in Fig. 2.5.

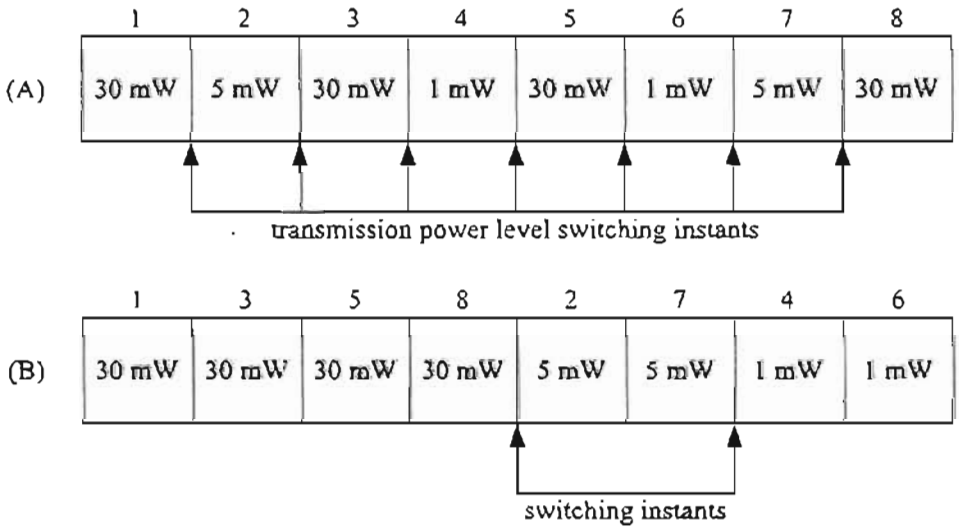

Figure 2.5: (A) Unordered packets, (B) more efficient scheduling (re-ordering of packets) to reduce switching latency

An algorithm for a MAC protocol [74] which can be built into the COMPOW is called SEEDEX. It uses a pseudo-random number generator to allow for channel reservation for the RTS and CTS, and the seeds of the deterministic linear congruence relationship are exchanged with all nodes within a two-hop neighbourhood. The objective is to reduce the overhead and improve throughput-delay and delay jitter performance. Each node knows which time slots it can transmit in because it has knowledge of the state of surrounding nodes, and thus a transmission instant which minimizes the chances of a collision of the MAC signals is used.

The COMPOW algorithm is not without some foreseeable problems and room for improvement. The link gains in both directions due to shadow fading are not always

the same, and so using the same transmit power at each node will not always ensure bidirectional links and full network connectivity. The protocol also ignores the multiple access capabilities that CDMA offers, as it assumes that packet collisions occur when two nodes in close vicinity transmit at the same time. Each transmission power setting needs its own routing daemon running in the node, and although the initial hardware has only a few power settings (for example the Cisco Aironet 340 and the 350 series have four and six transmission power settings respectively) this approach becomes infeasible if the transmission power is allowed to take on many more values. It is also likely that different equipment vendors have different transmit power levels, and thus a calibration will need to be done to ensure that the levels match.

2.4.8 Cone based connectivity

A fully distributed, cone-based topology control algorithm has been proposed by Wattenhofer et al [75]. By using directional information recovered from broadcast transmissions the algorithm attempts to find neighbours in all directions. The algorithm has two phases, initial neighbour discovery and redundant edge removal. The initial phase functioning is as follows: initially each node, u, starts with a small radius and broadcasts a message intended to discover neighbours. All nodes that receive this message transmit an acknowledge back to u. Node u then records all received acknowledgements at node u, noting their incident angle of arrival.[5] The node then runs through the recorded information and determines if at least one neighbouring node in every cone of α degrees is present. Fig. 2.6 shows a cone originating from node u centered around node v. The node continues in this neighbour discovery phase, increasing the transmit power (i.e. increasing the seeking range) until its maximum power is reached, or more satisfyingly, it discovers a neighbour in every direction. This condition is

[5]The incident angle of the signal is commonly termed the Angle-of-Arrival (AOA), and sophisticated techniques using multiple directional antennas [76] can be used to find this angle. If the node is not equipped with the capability of determining this angle then other information, for example gobal positioning system (GPS), can be used and the position of a node included in the transmitted data packet

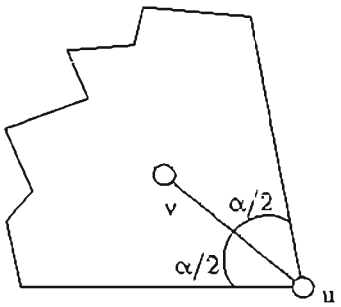

Figure 2.6: Typical cone with angle α

reached when the union of all the cones around u spans the 2π angle around the node. It is shown that for $\alpha \leqslant \frac{2\pi}{3}$ a maximum connected set is guaranteed.

The second phase of the algorithm is then to remove all edges of the connected graph that are redundant. As it is the high-power routes that are removed by this procedure this helps keep interference to a minimum and also reduces the average node degree. Simulation results indicate the algorithm helps improve average node lifetime (indicating a power saving) and the average node degree for $\alpha = 2\pi/3$ and $\alpha = \pi/2$ was 2.8.

2.4.9 Clustering in ad hoc networks

Another method of topology control involves the fragmentation of the network into independent clusters, [77]. A k-hop cluster indicates that any node in a cluster is at most k hops away from any other node (of the same cluster). A special case of this is 2-hop clustering whereby a central node acts as a cluster head (CH), and this emulates a cellular network, with the CH being analogous to the cellular base station. Some of the functioning of the base station is built into the CH, with power and topology control being two of its major functions. Clusters are joined together by nodes which belong to more than one cluster, and these are known as gateway (GW) nodes. The mobile stations (MS) in the network are homogeneous, and any node can become a cluster head or gateway node.

The process of formation of the clusters is briefly described. A cluster head sends out pilot transmissions, and any neighbouring nodes that can detect the pilot with sufficiently strong reception acknowledge back to the CH. If a node does not detect any pilot signals it attempts to become a CH itself by broadcasting an initialization pilot signal (this is different from the normal pilot signal from an already established CH). Open loop power control is employed due to the pilot signal transmitted by a CH. The pilot signal has embedded in it the transmitted power value, and a clustered node can extract that information, along with the actual received strength and set its transmission power equal to the value needed to overcome the path attenuation that the pilot signal experienced. The CH monitors the BER of any signals received from clustered mobile stations, and performs closed loop control to instruct any nodes to either increase or decrease their transmission power, depending on the rate of error achieved. The topology control is done at the CH, where the strength of the pilot

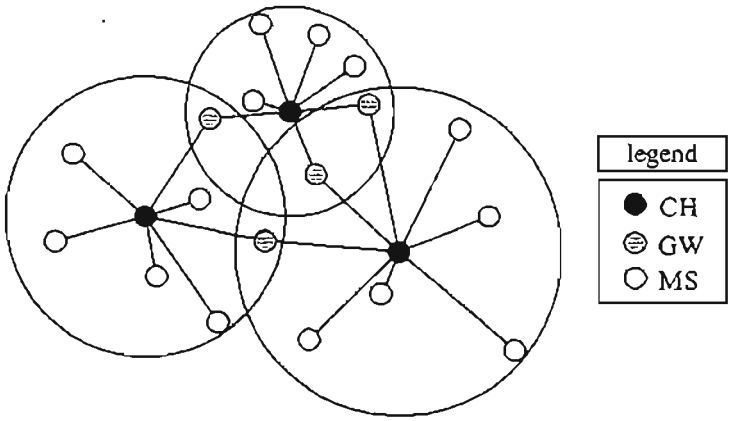

Figure 2.7: Topology control, each cluster head controls 7 mobile stations

signal is adjusted to maintain only a set number of nodes in its cluster. The same transmit power is used by the CH for all the nodes in the cluster, and this is set so as to just reach the furthest node. Fig. 2.7 shows a typical scenario where gateway nodes are used to interconnect various clusters.

This clustering scheme has been shown by simulation to significantly reduce the effects

of mobility on the number of topology changes (link failures due to increased distance), and for a network of 120 nodes randomly placed in a 1 km^2 area the average transmission range was kept below 70 meters. This will lead to energy savings while still maintaining network connectivity and stability.

2.4.10 Minimum energy mobile wireless networks

Attaining a global minimum energy connectivity solution was the goal of the research done by Rodoplu and Meng [78]. Strong connectivity can be guaranteed by a local optimization scheme which can be executed by each node, and this leads to a minimum energy power control solution that is a fully distributed implementation. The algorithm uses a global positioning system that has a spatial resolution of at least 5 m, with each node having its own GPS receiver. Each node knows its own instantaneous position through the GPS capability, but does not know the locations of the other nodes. This extra information is achieved through a broadcast beacon signal, whereby each node transmits its own position, and thus any nearby nodes are able to build a database of the surrounding nodes' positions. A self-configuring protocol is needed to maintain connectivity in the face of the dynamic wireless environment and node mobility.

Central to the algorithm functioning is the concept of a *relay region*. Given three nodes, i, j and k, assuming node i wishes to transmit to node k, then node j is considered to be a *relay* node (of i) if it is more power efficient to transmit to k via j, instead of directly to k. Using j as a relay node will result in a power usage increase at node j due the reception, buffering and processing of the signal, and this needs to be considered when choosing relay nodes. The region around a node that is obtained when the relay regions using the surrounding nodes are intersected is known as the *enclosure* of the node. This can be seen from Fig. 2.8, and is similar to a Voronoi diagram, for example Fig. 2.4. When a node is choosing neighbours it considers only those that lie within its enclosure as these are the most power efficient choices.

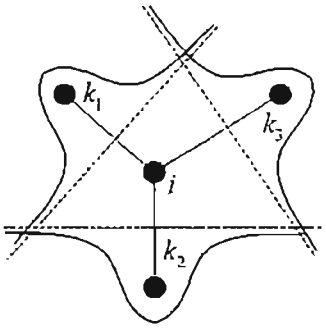

Figure 2.8: The dark solid line is the enclosure of node i

The functioning of the algorithm depends on a two phase process. In the first phase each nodes broadcasts its position, and then each node is able to determine its enclosure regions. Secondly the links are subject to a cost distribution to achieve a global minimum energy solution. A distributed Bellman-Ford shortest path algorithm [79] is used, with the local search area being the enclosure graph, and the cost metric used is power consumption. The enclosure graph contains all the globally optimal links. An iterative procedure is used whereby each node broadcasts its cost[6] which is also a function of its neighbours costs. Each node is then able to calculate the minimum cost it is able to achieve given the costs broadcast by its neighbours. When node i received the cost information from node n, $\text{cost}(n)$, it computes:

$$c_{i,n} = \text{cost}(n) + P_{tx}(i,n) + P_{rx}(n) \tag{2.23}$$

where $P_{tx}(i,n)$ is the required power to successfully transmit to n, and $P_{rx}(n)$ is the extra processing power at n that this transmission would cause. Node i will then calculate a total minimum power:

$$\text{cost}(i) = \min_{n \in N(i)} c_{i,n} \tag{2.24}$$

The node will then use whichever link causes the minimization in (2.24). This process is repeated, and after a finite number of iterations convergence is obtained. Data

[6]The *cost* of a node is the minimum power necessary to establish a path to the master-site, chosen as an arbitrary information sink target for all of the nodes

transmission is then able to proceed to the master-site. Peer-to-peer communication is possible as any node in the network could be thought of as the master-site, and so although only a single topology is generated using the proposed algorithm, it could be run for all the nodes and the resulting optimal topologies superimposed.

2.5 Summary

This chapter has introduced the topic of power control. A few fundamental concepts of power control aspects are presented and this is followed by a brief survey of some of the traditional power control schemes devised for a cellular architecture. Finally some algorithms proposed for power control in an ad hoc network type environment are presented.

Power control in an ad hoc environment has a different end goal to a cellular scheme. In traditional cellular systems, the network consists mainly of a hard-wired backbone, and wireless communication is done only on the last link (base station to mobile or vice versa). The aim of power control in a cellular network is to control the transmission power of mobile and base station such that the communication takes place using the minimum power that will satisfy the target signal-to-interference ratio. In an ad hoc network however the situation is more complicated, as ensuring adequate connectivity on a single link does not guarantee the network will remain strongly connected. A power control algorithm in an ad hoc network has the dual goal of minimizing transmission power, but more importantly ensuring the network does not become partitioned. Due to the mobile nature of terminals a reduction in transmission power will equate to a lengthening of the battery lifetime of the node, a desirable effect of power control.

Chapter 3

Distributed power control algorithm for ad hoc networks

3.1 Introduction

In a homogenous model of an ad hoc network, no node is dominant, the same power control algorithm is running in every node. This chapter investigates some new power control schemes proposed by the author for application in an ad hoc network. A few concepts have been borrowed from traditional cellular networks, and an attempt has been made to adapt them into a fully distributed power control algorithm.

In section 3.2 an introduction into the framework of the algorithm is presented. The various criteria for determining the controlled node set are given in section 3.3. Section 3.4 introduces various proposed methods for adapting the transmit power at a node based on the received control signals, and the derivation of the ideal received power algorithm, as given for a cellular environment [30, 80] is presented in section 3.4.2.

Essentially, the power control algorithm running in node j consists of two parts: the logic used to determine which nodes j should attempt to exert control over, and secondly the way in which j interprets the control signals it receives from its neighbours. It is the combination of both of these methods that will determine the success (or failure)

of the power control algorithm as a whole. One of the most important metrics used in judging the quality of an algorithm is network connectivity. It is vital that the network remains strongly connected so that peer-to-peer communication between any pair of nodes is possible. Another metric is efficiency: defined in terms of transmit power. If two algorithms result in similar connectivities, but one of them uses on average ten times more transmission power, then the algorithm that is able to maintain connectivity with the lowest average node transmit power is better. The system outage, which is a measure of how well an algorithm (after convergence) is able to cope with changing conditions, and also the convergence speed are other metrics, all of which are discussed in more detail in section 4.6.

3.2 Power control algorithm

This section gives a brief overview of the entire power control algorithm, before each of its components is examined in detail. In a cellular environment, the transmission power of a mobile terminal is typically only controlled by the base station to which the mobile is currently connected. However, when the mobile is in soft handoff, the mobile would be receiving a number of power control commands. Handoff is a complicated procedure, for more information refer to [11]. A simplified view is that a node is controlled by the base station from which it is receiving the strongest pilot signal. However, in an ad hoc network the controlling situation is not as clearly defined. Due to the lack of centralized controller, each node has to decide which of the surrounding nodes it is going to attempt to control.

Throughout the description of the algorithm, in order to maintain consistency, the node that is under scrutiny when describing controlling connectivity will be denoted node j, and when the power adaptation of a node is being described, i will be used. Surrounding node j are the other nodes in the network, all transmitting with different powers and to different target nodes. Before node j can attempt to institute some form of

control over the other nodes, it needs to determine its neighbouring controlled subset. In other words, node j needs some *logic* to help it decide which of the other nodes in the network it will try and exert control over. Each node attempting to control over every other node in the network would lead to unacceptable signalling overhead, and probably unstable network behaviour, and is generally not a sensible approach.

Let C_j be the set of all nodes that node j is attempting to control. The criteria for determining which nodes belong in this set are discussed in section 3.3. Node j will only exert control over the nodes in C_j . The signal received from node $m \in C_j$ is compared with some ideal value, τ_j^*, which is a function of $\mathbf{p}$, where $\mathbf{p} = (p_1, p_2, \ldots . p_N)^T$ is the $N \times 1$ vector of each node's transmit power. A decision is made on a link by link basis instructing all $m \in C_j$ respectively to increase or decrease their power. Fig. 3.1

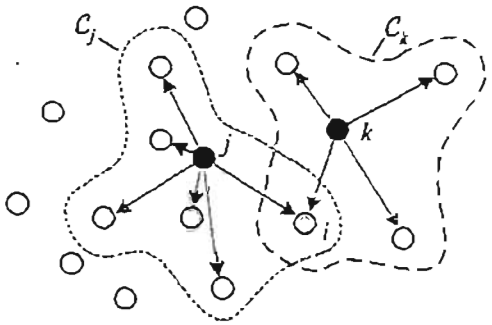

Figure 3.1: Typical controlling node connectivity, showing overlap of sets.

shows a typical scenario indicating the sets of controlled nodes for j and k, C_j and C_k respectively. Another convention that will be used in this dissertation is that in figures, light grey arrows will indicate the control signals whilst a dark arrow depicts the actual signal transmission. As node i is an element of both sets C_j and C_k, it would have two, possibly different, power control commands instructing it. This is analogous to a mobile in soft-handover in a cellular CDMA system. The various methods of selecting C_j are presented in section 3.3.

Node i has to make a decision based on the power control commands (PCCs) it receives.

In Fig. 3.1 node i is being controlled by nodes j and k, and so will have two power control command signals. Consider, for example, node j instructing node i to increase its power, and node k commanding a decrease in power. These two scenarios could possibly have arrived due to the SIR at j from i being below the target SIR, but the SIR at k from i being greater than required for successful communication. Node i would receive the two commands, and would have to make a decision based on the new information, possibly as well as past information. In a cellular system, the node is usually only trying to maintain a communication link to a single base station, and so it should decrease its power if that base station instructs it to, but in an ad hoc network it may be necessary for a node to maintain communication with more than one target. In this case the node should probably not decrease its transmission power if instructed to by a node, especially if a node that is essential for maintaining connectivity is instructing an increase in power. A few proposed power adaptation methods a node can use to decide how to change its transmission power are discussed in section 3.4.

3.3 Connectivity criteria

In order for distributed power control to function, each node needs to know which other nodes it should attempt to control. Each node, j, in the network has associated with it a vector of the nodes it should issue power control commands to, and the controlled node connectivity for the entire network can be represented by a matrix, where $\mathbf{A} = [a_{ij}]$ is an N x N matrix with elements

$$a_{ij} = \begin{cases} 1, & \text{if node } j \text{ is controlling node } i \\ 0, & \text{otherwise} \end{cases}$$

The power control algorithm executing at each node needs to select which nodes it is going to attempt to influence. The question arises as to how a node selects the set of nodes that are to be power controlled. Several methods for determining this controlled node connectivity are now presented.

3.3.1 Power threshold

Node j will attempt to control the transmission power of node k if the signal at j being received from k is greater than some pre-defined threshold, $r_{\min}$. As the algorithm

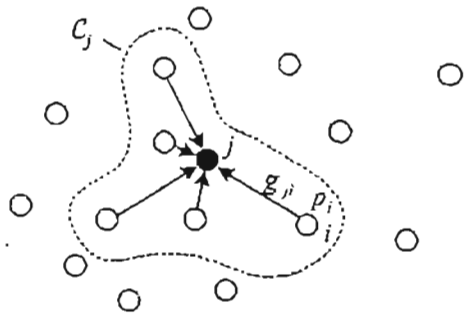

Figure 3.2: Arbitrary region of controlling for node j.

proceeds, the transmit powers of the nodes will evolve and at any instant in time, node j will only attempt to control the nodes, i, that are transmitting with a power great enough such that the signal received at j from i is greater than $r_{\min}$

$$a_{ij}(n) = \begin{cases} 1, & \text{if } r_{ji}(n) \geq r_{\min} \\ 0, & \text{otherwise} \end{cases} \tag{3.1}$$

where the instantaneous received power at node j from node i is

$$r_{ji}(n) = p_i(n) \cdot g_{ji}(n) \tag{3.2}$$

The link gain factor, $g_{ji}(n)$, in (3.2) consists of the attenuation due to distance and slow shadow fading, a more rigorous explanation of the loss model is given in section 4.3.

One of the goals of a power control algorithm is to obtain the minimum system transmit power vector, $\mathbf{p}^* = [p_1^*, p_2^*, \ldots, p_N^*]^T$, that satisfies the SIR targets on the desired links. Clearly a mobile should decrease its transmission power if doing so will still maintain an acceptable connection to its required target nodes. If the transmission power is decreased there will be less interference presented to the rest of the network which can lead to an increase in capacity, or, for the same capacity, allow other nodes to lower

their transmit powers. Thus a power control algorithm should strive for a minimum transmission power solution which will have the added benefit of maximizing battery lifetime.

This scheme for determining the controlling set does however posses a critical flaw. Using this proposed *threshold* method, it is possible that as the algorithm progresses over time a mobile decreases its power (as instructed), and due to attenuation is no longer received at the intended node with a power greater than r_{min}, causing the mobile to be removed from the controlling nodes connectivity set. This could happen for any number of nodes in the entire network, and network partitioning will occur rapidly. Thus considerable insight needs to go into the choosing of this *minimum receive power* system parameter. Selected results using this connectivity method are presented in section 4.7.1.

3.3.2 Distance based connectivity

Another possible method for determining the control connectivity is to use the inter-nodal distances. If the mobile terminals have access to GPS information then a node would have exact knowledge of the position of all the other nodes around it. It is, however, unlikely that this capability would exist in the mobile terminal, and an alternate method would be to use the pilot signals of each mobile. By monitoring the pilot signals, the node is able to determine which are its closest neighbours, as these would have the strongest pilot symbols. The performance of this method is based on the parameter $d_{\max}$. A node, j, will send power control commands to all nodes that are within the distance $d_{\max}$, as depicted in Fig. 3.3. Using a greater value for $d_{\max}$ will lead to increased controlling connectivity, however the overhead introduced will also increase, and a balance needs to be maintained.

$$a_{ij}(n) = \begin{cases} 1, & \text{if } d_{ji}(n) \leqslant d_{\max} \\ 0, & \text{otherwise} \end{cases} \tag{3.3}$$

Clearly the number of nodes that fall within the d_{max} radius is a function of the

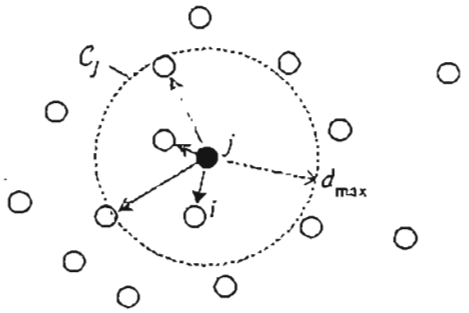

Figure 3.3: Maximum distance based controlling connectivity

distribution of the nodes (assumed uniform), and the node density which, in turn, depends on the number of nodes in the network. Simulation results using this distance based controlling connectivity method are presented in section 4.7.3.

3.3.3 Power received from greatest K nodes

Building on the idea of using the strength of a pilot signal, another connectivity method could be to use actual received signal strength. During each power control iteration node j has a record of all signals received, $\mathbf{r_j} = (r_1, r_2, \ldots, r_N)^T$, with the power received from the node itself defined as zero. The idea behind the *power received from greatest* K method is that the node ranks these received signals, and will only send power control commands to the K nodes from which it is receiving the strongest signal.

It should be noted that the value of K is not the number of nodes controlling node j, rather it is the number of nodes that node j is attempting to control. Even using a K of one could lead to node j being simultaneously controlled by several other nodes.

3.3.4 SIR received from greatest K nodes

Instead of using the actual received signal strength as described in section 3.3.3, a more accurate approach may be to use the SIR received at the node. These two methods

are expected to give very similar results as the received SIR is directly related to the actual received power. Assuming, without loss of generality, that the power received at node j from nodes g, h, and i is ranked as follows:

$$r_j^g \geqslant r_j^h \geqslant r_j^i \tag{3.4}$$

The SIR at j from any node, i, is given by:

$$\gamma_{ji}(n) = \frac{r_i(n)}{R_j(n) - r_i(n)} \tag{3.5}$$

where the total power received from all sources at j is denoted $R_j(n)$ and is:

$$R_j(n) = \sum_{i \neq j}^{N} p_i(n) \cdot g_{ji}(n) + \eta_j \tag{3.6}$$

The iteration time reference (n) will be assumed from now on and omitted from the equations for clarity. Rearranging (3.5) solving for r_i,

$$r_i = \frac{\gamma_{ji} \cdot R_j}{1 + \gamma_{ji}} \tag{3.7}$$

then by the order imposed in (3.4),

$$\frac{\gamma_{jg} \cdot R_j}{1 + \gamma_{jg}} \geqslant \frac{\gamma_{jh} \cdot R_h}{1 + \gamma_{jh}} \tag{3.8}$$

$$\gamma_{jg} \cdot R_j \cdot (1 + \gamma_{jh}) \geqslant \gamma_{jh} \cdot R_h \cdot (1 + \gamma_{jg}) \tag{3.9}$$

$$\gamma_{jg} + \gamma_{jg} \cdot \gamma_{jh} \geqslant \gamma_{jh} + \gamma_{jh} \cdot \gamma_{jg} \tag{3.10}$$

$$\gamma_{jg} \geqslant \gamma_{jh} \tag{3.11}$$

The same method can be used to show that $\gamma_{jg} \geqslant \gamma_{jh} \geqslant \gamma_{ji}$. Clearly using the SIR from the greatest K will lead to equivalent connectivity to using the *greatest K received power*, therefore simulation results are only presented for the SIR method.

Node j will send power control commands to the K nodes from which it is receiving the greatest signal-to-interference ratio:

$$a_{ij}(n) = \begin{cases} 1, & \text{if } \gamma_{ji} \geqslant \bar{\gamma}_j \\ 0, & \text{otherwise} \end{cases} \tag{3.12}$$

where $\bar{\gamma}_j$ is the Kth greatest SIR received at node j.

Table 3.1: Summary of controlling connectivity criteria

Conn. method	Description
Power threshold	control i if $r_{ji} \geqslant r_{\min}$
Maximum distance	control i if $d_{ji} \leqslant d_{\max}$
Power greatest K	control i if r_{ji} is one of the greatest K received powers at j
SIR greatest K	control i if γ_{ji} is one of the greatest K SIRs at j

3.4 Transmit power adaptation

3.4.1 Overview

Once the controlling connectivity has been resolved, the actual power control process is able to proceed. Assume that at any instant in time node j knows what power it should be receiving, $r_j^*(n)$, on any link from a connected node in order to maintain reliable communication (see section 3.4.2 for details). To expand on this, for clarity, the signal-to-interference at node j from node i, γ_{ji}, is given by:

$$\gamma_{ji} = \frac{r_{ji}}{R_j - r_{ji}} \tag{3.13}$$

where R_j is the total received power (including thermal noise) at node j:

$$R_j = \sum_{i \neq j}^{N} p_i \cdot g_{ji} + \eta_j \tag{3.14}$$

in order for reliable communication the SIR, as defined by (3.13), must by greater or equal to some predefined target SIR, γ^*:

$$\gamma^* \leqslant \frac{r_{ji}}{R_j - r_{ji}} \tag{3.15}$$

rearranging and solving for r_{ji},

$$\gamma^* \cdot R_j - \gamma^* \cdot r_{ji} \leqslant r_{ji} \tag{3.16}$$

$$\gamma^* \cdot R_j \leqslant r_{ji} \cdot (1 + \gamma^*) \tag{3.17}$$

$$r_{ji} \geqslant \frac{\gamma^* \cdot R_j}{1 + \gamma^*} \tag{3.18}$$

$$r_j^*(n) = \frac{\gamma^* \cdot R_j(n)}{1+\gamma^*} \tag{3.19}$$

The ideal received power at node j is the same for any node that wishes to be successfully received at j. The value given in (3.19) is one example of a possible method of choosing an ideal received power.

Clearly $r_j^*(n)$ is a function of the system transmit power vector, $\mathbf{p}$. At any given time instant, n, the difference in power received at node j from node i, $\Delta_{ji}(n)$, relative to the ideal received power is:

$$\Delta_{ji}(n) = r_j^*(n) - r_{ji}(n) \tag{3.20}$$

$$= r_j^*(n) - p_i(n) \cdot g_{ji}(n) \tag{3.21}$$

Node j is able to calculate $r_j^*(n)$ using some predefined means, and it can then instruct node i to increase or decrease its transmission power by the amount required, $\Delta_{ji}(n)$. If all the other nodes remain transmitting with the same power then with the next power control iteration (assuming no change in path gain), the ideal received power would be satisfied, i.e. convergence attained in a single iteration. However, all the other nodes are also being instructed to change their powers, and there is a time varying path gain, hence there would be a non-zero $\Delta_{ji}(n)$ at every time instant. The algorithm is repeated infinitely, constantly tracking to the new ideal power.

Several problems exist with the aforementioned scheme. In order for the target node to change its power to match the desired ideal power at node j, the value $\Delta_{ji}(n)$ needs to be transmitted from node j to node i every power control time instant. This leads to a large transmission overhead, especially if there is a high degree of controlling node connectivity. The convergence of the scheme to the optimal value also depends on the accuracy to which the measurements can be achieved, and the precision (word length) of the transmitted power control command.

Another problem still exists, in that a node may be receiving more than one power control command. Embedded in the node must be some logic which determines what

to do in the event that the node receives more than one PCC. Several possible solutions are suggested. The adaptation of transmit power at node i is given by:

$$p_i(n+1) = p_i(n) + \varphi \cdot \varepsilon_i(n) \tag{3.22}$$

It is the choice of the $\varepsilon_i(n)$ function which defines the transmit power adaptation scheme. The power change step-size, φ, is a system constant. Fig. 3.4 shows a typical

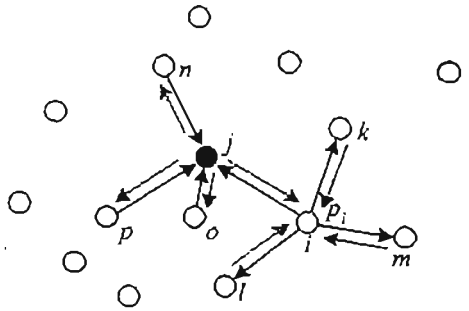

Figure 3.4: Controlling and controlled sets

scenario of controlled and controlling connectivities. The dark arrows indicate a received signal transmission, and the grey arrows indicate the power control commands. Node i is being controlled by nodes j, k, l, m and node j is controlling nodes i, n, o, p

Node j calculates $r_j^*(n)$ and compares this with the actual signal received, $r_i(n)$ from all i it is controlling.

$$\xi_{ji} = \operatorname{sgn}\left(r_j^*(n) - p_i(n) \cdot g_{ji}(n)\right) \tag{3.23}$$

If the signal from node i was received at node j with too little power, then the result of (3.23) will be a positive, indicating that node i should *increase* its transmission power. Similarly, a negative sign indicating a *decrease* in power will result when node i is being received at node j with a power that exceeds $r_j^*(n)$. Only a single bit indicating the desired PCC is needed to be transmitted from node j to node i. This leads to far less overhead than if node j had to transmit the entire $\Delta_{ji}(n)$ value.

The convergence speed of the single-bit control algorithm is directly influenced by the step-size, φ, and the speed at which the algorithm is running.

As mentioned, if a node is receiving more than one PCC, then it has to decide what to do, and some methods for doing so are presented. These different ways that a node can calculate the $\varepsilon_i(n)$ in (3.22) value are presented in section 3.4.3.

3.4.2 Ideal received power

The choice of the method used to determine the ideal received power is crucial. The technique given by (3.19) is a useful starting point, in that the ideal received power is equal to the minimum power necessary to exactly satisfy the target SIR. Borrowing from an idea proposed by Mitra for a bursty transmissions in a cellular environment [30], a new definition of ideal received power is used. At node j, the ideal received power that any signal should arrive at is given by:

$$\bar{r}_j^*(n+1) = \frac{\tilde{\Gamma}}{W}\left[\bar{I}_j(n) + \psi\sqrt{V_j(n)}\right] \tag{3.24}$$

$$\tilde{\Gamma} = \frac{\Gamma \cdot W}{\Gamma + W} \tag{3.25}$$

where Γ is the target de-spread SIR, W is the CDMA processing gain, $\bar{I}_j$ is the mean interference experienced at a node, V_j is the variance of the interference and ψ is a parameter related to the desired outage of the system.

The instantaneous interference at node j is simply the sum of all the received powers, and is given by:

$$I_j(n) = \sum_{k=1}^{N} r_{jk}(n) \cdot X_k + \eta_j \tag{3.26}$$

where the X_k term is a boolean activity indicator, $X_k \in \{0,1\}$, with $X_k = 1$ if the mobile k is transmitting.

The *mean interference* at node j, $\bar{I}_j$, is given analytically by:

$$\bar{I}_j(n) = \sum_{k=1}^{N} p_k(n) \cdot g_{jk}(n) \cdot \omega_k + \eta_j \tag{3.27}$$

where the probability that the k^{th} mobile is transmitting, ω_k is:

$$\omega_k = \Pr\{X_k = 1\} = 1 - \Pr\{X_k = 0\} \tag{3.28}$$

The algorithm also takes the second order statistics of the received interference into account, and thus is better able to adjust to a time-varying environment. The variance of the interference is given by:

$$\text{var}\,[I] = V_j(n) = \sum_{k=1}^{N} p_k^2(n) \cdot g_{jk}^2(n) \cdot \omega_k \cdot (1 - \omega_k) \tag{3.29}$$

When a steady-state condition is reached the variance term would drop to zero and thus have no effect. If node j is receiving a signal at the *ideal received power* value, the SIR at node j is given by:

$$\gamma = \frac{r_j^*}{I - r_j^*} \tag{3.30}$$

If the variance of the interference is zero (steady state), then (3.24) reduces to:

$$r_j^* = \frac{\Gamma}{\Gamma + W} \cdot I_j \tag{3.31}$$

substituting into (3.30):

$$\gamma = \frac{\frac{\Gamma}{\Gamma+W} \cdot I_j}{I - \frac{\Gamma}{\Gamma+W} \cdot I_j} \tag{3.32}$$

$$\gamma = \frac{\frac{\Gamma}{\Gamma+W}}{\frac{\Gamma-W-\Gamma}{\Gamma+W}} \tag{3.33}$$

$$\gamma = \frac{\Gamma}{W} \tag{3.34}$$

thus, as expected, at steady state the SIR is equal to the traditional CDMA spread SIR.

The parameter ψ in (3.24) is related to the tolerable *outage*, δ, of the system. A particular communication link, for example from k to j, is said to be experiencing outage if its SIR drops below a minimum target SIR.

$$\delta_{jk} = \Pr\left\{ \frac{r_{jk}}{I_j - r_{jk}} \leq \frac{\Gamma}{W} \right\} \tag{3.35}$$

It is shown in [30] and [80] that ψ is related to δ by:

$$1 - \delta = \frac{1}{\sqrt{2\pi}} \int_{-\infty}^{\psi} e^{-\frac{x^2}{2}} dx \tag{3.36}$$

Given the maximum allowable outage, δ, a ψ value can be calculated, or looked up from statistical tables. Essentially, the ideal received power is set to slightly greater than actually required so that any increased interference will not cause the SIR of the link to drop below the minimum SIR and result in the system to be in outage. The variance term in (3.24) acts as a damping mechanism, *absorbing* any increased interference. The value of ψ is equal to the x-value at which the area under the standard normal

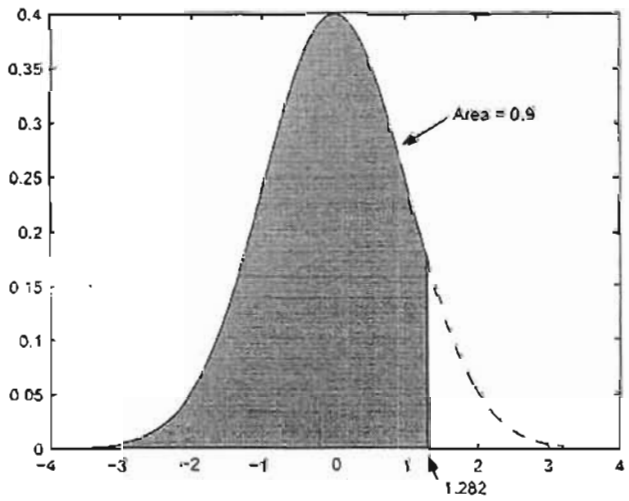

Figure 3.5: Normal distribution with 90% area shaded (10% outage)

distribution is equal to $1-\delta$. From Fig. 3.5 the ψ parameter corresponding to an outage of 10% is 1.282. The tradeoff caused by specifying too stringent an outage requirement is decreased network capacity, as each user transmits with a power slightly greater than what is actually needed.

In essence, (3.24) gives an estimate of the power any signal should arrive at during the $(n+1)^{\text{th}}$ time instant in order for the SIR to be satisfied, based on the signal statistics at time n. Unlike traditional algorithms which only take into account the mean of the interference experienced at a node, (3.24) also relies on the second order statistics (variance) of the interference. This can be used to help in the guarantee the QoS. A similar *padding* of a users SIR was introduced by Bambos in his active link quality

protection call admission scheme [44].

3.4.3 Power adaptation methods

Although based on a cellular system, the quantity defined by (3.24) is used as the r_j^* reference in (3.23). A node is then able to send appropriate increase/decrease PCCs to the terminals it is controlling. After this phase of the algorithm has proceeded, each node will have any number of PCCs (between 0 and $N-1$ of them) instructing it to either increase or decrease its transmission power. Various methods as to how the node chooses which commands to obey are proposed.

Satisfy all links

When a node, j, does the comparison to calculate ξ_{ji} described by (3.23), in essence it is determining if the communication link is deemed satisfactory. For clarity and consistency of description, we assume that when $r_{ji}(n)$ is greater than $r_j^-(n)$ then the minimum SIR target on the i to j link is satisfied and the communication is deemed successful.

Given the connectivity matrix, $\mathbf{A}$, node i will have c_i power control commands, where

$$c_i = \sum_{j=1}^{N} a_{ij} \ , \ 1 < i < N \tag{3.37}$$

Recall, a_{ij} is 1 if node j is controlling node i, and 0 if node j is not controlling node i.

In order to attempt to satisfy the target SIR on *all* the links that are controlling it, node i should use an $\varepsilon_i(n)$ in its power adaptivity, $p_i(n+1) = p_i(n) + \varphi \cdot \varepsilon_i(n)$ where,

$$\varepsilon_i(n) = \begin{cases} +1, & \text{if any } \xi_{ji}(n) \text{ is } +\text{ve} \\ -1, & \text{otherwise} \end{cases} \tag{3.38}$$

That is, increase the transmission power of node i if by a fixed amount, φ, if any other node sends an increase power command.

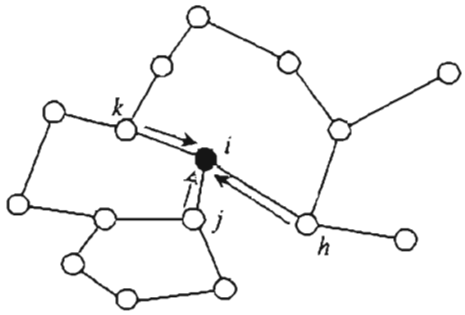

Figure 3.6: Predefined connectivity

Fig. 3.6 gives an example of a strongly connected network where all the links are assumed bi-directional. In the diagram, node i needs to maintain an acceptable communication link with nodes h, j and k, and they are sending control signals to i. In order for the given connectivity to remain in place, i should only decrease its power if all of the controlling nodes are commanding a decrease in power, as by ignoring any of the increase commands, that link would be broken and partitioning of the network may occur.

The problem with this scheme is that in theory a positive feedback effect could occur where all nodes are increasing their power to achieve the target SIR, and this leads to an increase in total interference at all nodes, which requires the nodes to further increase their power. This effect will only stop when all nodes have reached their maximum allowable transmission power, $\hat{p}_i$. If the connectivity criteria algorithm is not carefully chosen, then a node, i, may end up receiving a PCC from a far away node that really should not be attempting to control i.

Satisfy mean of links

Intuitively, a more suitable scheme would be for a node to behave in a manner which would benefit the network as a whole. A seemingly *fair* method would be for the node to increase its transmission power only if the majority of PCCs sent to it indicated an

increase. If the node received more decrease commands than increase commands, then it should lower it transmission power.

$$\varepsilon_i(n) = \text{sgn}\left(\sum_{j\in\{a_{ij}(n)=1\}} \xi_{ji}(n)\right) \tag{3.39}$$

This scheme is also dependent on the connectivity criteria algorithm for the same reasons given previously, however it is a more balanced approach, and should be less susceptible to the positive feedback power saturation problem. If the same number of increase and decrease commands are received then the node will decrease its power, to try and reduce overall interference.

Satisfy best link only

A possible solution to solve the unwanted positive feedback behaviour problem is to instruct the node to only listen to its closest neighbours, and only obey the best power command. Node i should decrease its transmission power if any other node instructs it to, and only if the SIR targets at all of its recipient nodes are not met then i should increase its power by φ.

$$\varepsilon_i(n) = \begin{cases} -1, & \text{if any } \xi_{ji}(n) \text{ is -ve} \\ +1, & \text{otherwise} \end{cases} \tag{3.40}$$

Satisfy weighted arithmetic mean

Another proposed method for calculating φ is the weighted mean approach.

$$\varepsilon_i(n) = \text{sgn}\left(\Omega^+ \cdot \xi_j^+ - \Omega^- \cdot \xi_j^-\right) \tag{3.41}$$

ξ_j^+ is the sum of all the $\xi_{ji}(n)$ that are +ve, and similarly, ξ_j^- is the sum of all the $\xi_{ji}(n)$ that are -ve. A positive scaling factor, Ω^+, and a negative scaling factor,Ω^-, are introduced to emphasize a particular trend. For example setting $\Omega^+ = 2$ and $\Omega^- = 1$ would mean that the increase commands are twice as important as the decrease

commands. Similarly, using $\Omega^+ = \Omega^- = 1$ reduces the weighted arithmetic mean into a standard arithmetic mean as defined by (3.39). If a tie results, i.e. $\Omega^+ \cdot \xi_j^+ - \Omega^- \cdot \xi_j^- = 0$ then the node should decrease its transmission power.

Four methods have been proposed for controlling the transmit power adaptation. A brief summary of the methods is presented in Table 3.2

Table 3.2: Summary of transmit power adaptation algorithms

Adapt. method	Effect
satisfy all	increase power if any node instructs an increase
satisfy mean	network fair? 1:1 ratio
satisfy best	decrease power if any node instructs an decrease
weighted mean	emphasize trend, increase:decrease ratio

Some ideas are common to all the transmit power adaptation schemes described. If a node does not receive any PCCs during an iteration, and the node is currently active, then the node should increase its power by the step-size. Also, if a node is currently not active, then it should ignore any commands received, which may have been sent during the previous iteration when the node was actively transmitting. When a node changes from the inactive to active (transmitting) state it begins transmitting with the same power as it was previously using before it stopped transmission.

3.5 Summary

This chapter introduced the distributed power control method for ad hoc networks. It consists of two separate units: the controlling connectivity algorithm, and the transmit power adaptation algorithm. The connectivity algorithm is used to determine which terminals a node should send control signals to, and four methods have been presented for determining the set of nodes, C_j, that node j will send PCCs to. Node j will attempt to control node i if: the power received at j from i is greater than some threshold ($\tau_{\min}$), the distance between nodes i and j is less than some threshold ($d_{\max}$), the signal received at j is one of the greatest K or the SIR at j from i is one of the greatest K SIRs.

The proposed transmit power adaptation algorithm was also presented. Based on the power control commands received, a node is able to apply some decision logic to determine how it should adapt its transmission power, depending on whether it should attempt to satisfy the best link only, satisfy all the links, or some combination of the two. In order to determine if a particular communication link is acceptable some criteria is needed, and the idea of an *ideal received power* is introduced. An algorithm developed for a cellular system has been used.

The performance of these connectivity schemes in conjunction with the transmit power adaptation algorithms are presented in Chapter 4.

Chapter 4

System and Simulation Model

4.1 Introduction

This chapter focuses on the physical description of the network. The channel loss model is separated into signal attenuation which is a function of distance, and a time varying shadow fading component. Due to the fully distributed nature of the network, each node has to (independently) make power control decisions for the other nodes in the system. The performance of the system was tested through a custom designed computer simulation environment. This chapter describes the model implemented in the simulation and some selected results are presented, comparing the different connectivity and transmit power adaptation schemes.

4.2 Network model

Consider a network consisting of N nodes, with node j transmitting at time instant n with power $p_j(n)$. The *signal-to-interference ratio* (SIR) at node i from node j, $\gamma_{ij}(n)$, is given by:

$$\gamma_{ij}(n) = \frac{p_j(n) \cdot g_{ij}(n)}{\sum_{k \neq i,j}^{N} p_k(n) \cdot g_{ik}(n) + \eta_i} \tag{4.1}$$

The inter-node fading term, $g_{ij}(n)$, includes attenuation due to path loss and shadow fading. Included in the noise at the receiver is a component due to thermal noise, which is modelled as a constant $\eta = N_0 \cdot B$, where B is the spread-spectrum signal bandwidth and N_0 is the single-sided noise power spectral density. In order for reliable communication to be achieved, the SIR received at a node should be greater than some target SIR, γ^*.

4.3 Loss model

The signal transmitted by a node is subject to various forms of fading before it is received at the target node. These include: attenuation due to path loss, shadow-fading as well as fast-fading. The intention is to accurately, and consistently model the total loss a signal will experience once it has been transmitted from a node. The various loss mechanisms are assumed to be independent. Fast fading due to multi-path interference (Rayleigh fading) is not considered in the model or the simulation as it is assumed that time-averaging and a RAKE form of receiver combined with turbo coding will mitigate the effects of fast-fading [1],[81]. The total inter-node loss between nodes i and j at time instant n, $g_{ij}(n)$, due to path loss and shadow-fading can be represented as:

$$g_{ij}(n) = (\text{path loss})_{ij}(n) + (\text{shadow fading})_{ij}(n) \tag{4.2}$$

where the quantities in (4.2) are all in dBs.

4.3.1 Path loss

A simple power law model for path loss has been commonly used in literature [7, 82], where the path loss between nodes i and j at time n, $l_{ij}(n)$, is given by:

$$l_{ij}(n) = -10 \cdot \alpha \log d_{ij}(n) \tag{4.3}$$

where $d_{ij}(n)$ is the Euclidean distance between nodes i and j. It was shown experimentally that the path-loss exponent, α, depends on the type of terrain and also on the height of the base-station antenna above ground [83], so these results are not directly applicable to the case of mobile-to-mobile transmissions which would be typical in an ad hoc network. For a cellular system, empirically α has been show to be in the range of 3 to 5, depending on the type of terrain. A more comprehensive model for the path loss which is widely used in planning cellular networks is the Hata-Okumura model [84, 85], but this model is only useful when the base-station antenna heights are above 30 m. Extensions to this model based were proposed in [83]. A value for α of 4 was used in the simulation.

4.3.2 Shadow fading

The slow fading effects that are evident in a wireless channel have been observed to follow a lognormal[1] distribution. Random features of the terrain such as variable building heights, trees, etc, all contribute to a sequential and independent random fluctuation of the signal. Based on the central limit theorem, these will lead to a Gaussian distribution with zero mean and variance σ^2. Empirical data has show that σ^2 is between 6 and 12 dBs [86].

The dB attenuation due to shadow fading was shown by Gudmundson to exhibit an exponential spatial correlation [87]. Given two points separated by a distance d, the correlation between the shadow fading factors S_1 and S_2 is:

$$E[S_1 \cdot S_2] = \sigma^2 \exp\left(-\frac{d}{D_0}\right) \tag{4.4}$$

D_0 is the correlation distance, and typical values for this range from 20 m for urban areas, to 500 m for suburban areas.

If the velocity of a mobile is v, then the distance travelled by the mobile during the

[1] A function is described as lognormal when the logarithm of the random variable has a Gaussian distribution.

time period τ is $v \cdot \tau$, and the spatial correlation expressed as a time correlation [88]:

$$E\left[S(t) \cdot S(t+\tau)\right] = \sigma^2 \exp\left(-\frac{v \cdot \tau}{D_0}\right) \tag{4.5}$$

The interval between power control updates, τ, varies depending on the system specifications. GSM uses a τ of 480 ms, IS-95 uses 1.25 ms, and UTMS has a power control period of 0.625 ms. The distance change between two mobiles (relative to their actual distance separation) during a single τ duration is insignificant, and d_{ij} is assumed constant to simplify analysis.

A discrete model of the time correlation of the shadow fading is then given by:

$$E\left[S_{ij}^{(n)} \cdot S_{ij}^{(n+1)}\right] = \rho \cdot \sigma^2 \tag{4.6}$$

where ρ, the correlation coefficient, is equal to $\exp\left(-\frac{v \cdot \tau}{D_0}\right)$. From Fig. 4.1 it is clear

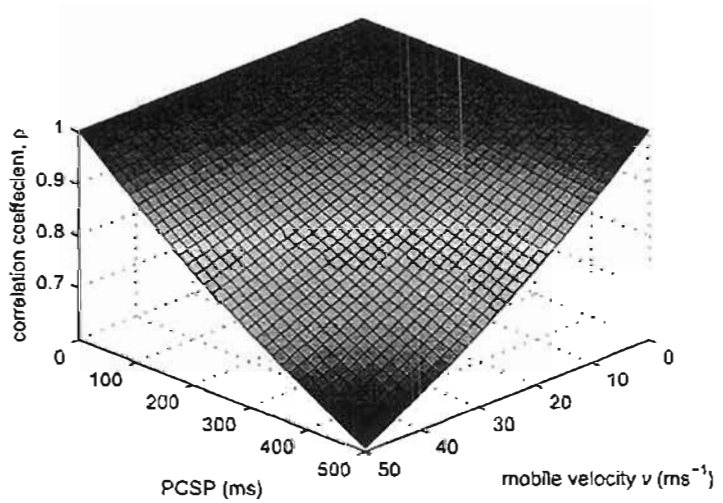

Figure 4.1: Correlation coefficient as a function of mobile velocity and power control sampling period (PCSP) for an urban environment ($D_0 = 50$ m).

that a fast update rate is needed when a mobile is travelling at high velocity in order for the algorithm to be able to track the channel variation.

As the logarithm of the shadow fading has an approximately normal distribution, a generating function for the random variable can be represented by a first-order Gauss-

Markov process:

$$S_{ij}(n+1) = \rho \cdot S_{ij}(n) + \sqrt{1-\rho^2} \cdot Z \tag{4.7}$$

The function Z is a Gaussian random variable with zero mean and variance σ^2, $Z \sim N[0, \sigma^2]$. This variance was set to 6 dB for the simulation. Fig. 4.2 shows a

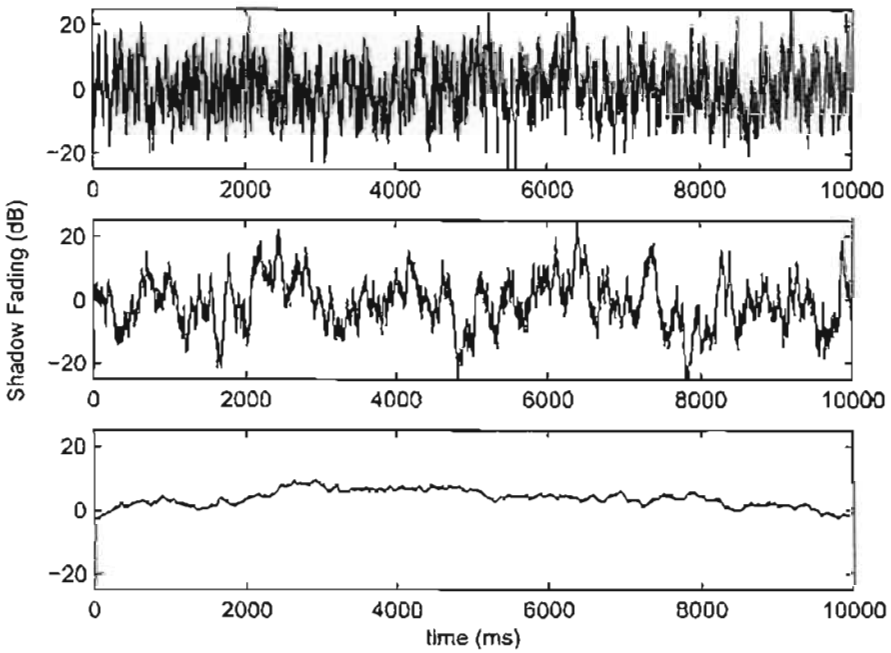

Figure 4.2: Typical random channel variation due to shadowing effects. The correlation coefficients, ρ, are 0.95, 0.99 and 0.9999 respectively.

typical graph of the channel variation due to shadow fading over time.

Recently proposed was an enhanced model for simulating the shadow fading [89]. This method included the correlation between uplink and downlink channels.

4.4 Ideal received power algorithm

The decision logic used by a node when determining if the quality of a received signal is adequate for successful communication depends on the value of r_j^*, the *ideal received*

power. This concept is borrowed from research done for a cellular CDMA system in [30, 80]. The power control algorithm proposed by Mitra was, the *ideal received power*, r_j^*, for any node j in the network at time instant $n+1$ is given by:

$$r_j^*(n+1) = \frac{\tilde{\Gamma}}{W}\left[\bar{I}_j(n) + \psi\sqrt{V_j(n)}\right] \tag{4.8}$$

$$\tilde{\Gamma} = \frac{\Gamma \cdot W}{\Gamma + W} \tag{4.9}$$

where Γ is the target de-spread SIR, set to 10 dB for the simulation, and W is the CDMA processing gain, set to 63.[2] $\bar{I}_j$ is the mean interference experienced at a node, V_j is the variance of the interference and ψ is a parameter related to the desired outage of the system. The ideal received power algorithm was described in more detail in section 3.4.2.

4.4.1 Interference Calculation

The *mean interference* at node j, $\bar{I}_j$, is given analytically by:

$$\bar{I}_j(n) = \sum_{k=1}^{N} p_k(n) \cdot g_{jk}(n) \cdot \omega_k + \eta_j \tag{4.10}$$

For the simulation, $\bar{I}_j$ was calculated using the exact received power from all the transmissions (also including thermal noise) averaged over a time period. The previous L values of $I_j(n)$ are used, achieving a sliding window effect seen in Fig. 4.3, and the mean interference at time n is given by:

$$\bar{I}_j(n) = \frac{1}{L}\sum_{t=n-L+1}^{n} I_j(t) \tag{4.11}$$

4.4.2 Variance calculation

By taking the second order statistics of the received interference into account, the algorithm is better able to adjust to a time-varying environment. When a steady-state

[2] Using a bandwidth of 1.2288 MHz, as specified in the IS-95 standard, this equates to a transmission bit-rate of $R_b = \frac{1.2288\,\text{MHz}}{63} = 19.5\,kb/s$.

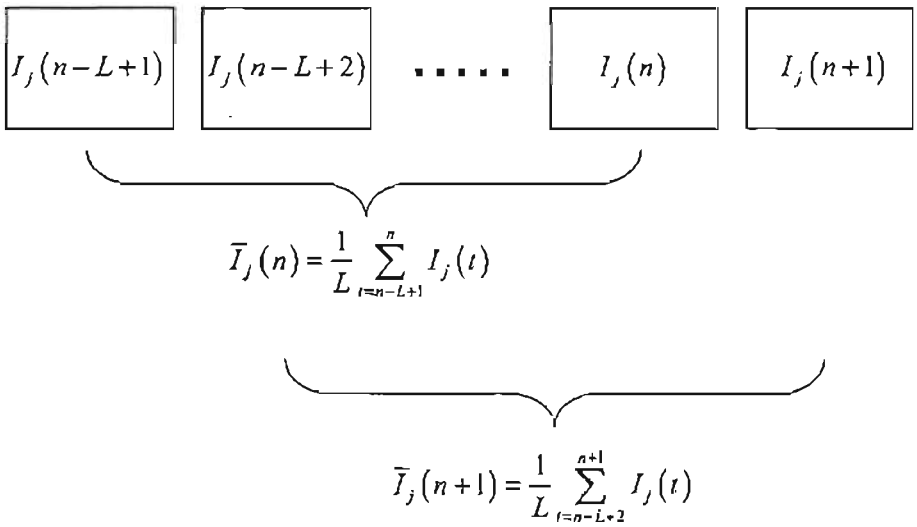

Figure 4.3: Sliding interference window

condition is reached the variance term would drop to zero and thus have no effect. The variance of the interference is given by:

$$\text{var}[I] = V_j(n) = \sum_{k=1}^{N} p_k^2(n) \cdot g_{jk}^2(n) \cdot \omega_k \cdot (1 - \omega_k) \tag{4.12}$$

In the simulation, $V_j(n)$ is calculated by finding the variance of the values of interference stored in the window buffer:

$$V_j(n) = \frac{1}{L} \sum_{t=n-L+1}^{n} \left(\bar{I}_j(n) - I_j(t)\right)^2 \tag{4.13}$$

4.5 Simulation

4.5.1 Description

The power control algorithm was tested in a custom designed simulation environment. The program was written in C++ using the IMSL mathematical and statistical libraries [90] to generate random variables and assist in matrix computations.

A discrete-time implementation with an iteration constant time step of $\tau = 1$ ms was used. This resolution allows for power control iterations to occur at the same resolution, giving a frequency of operation of 1 kHz, compared to 1.6 kHz which is used in UMTS and the much slower rate of 2.083 Hz for GSM. The nodes are initially uniformly randomly situated in a 1000 m $\times$ 1000 m square *cell*. The number of nodes in the network was a variable simulation parameter. It was assumed that the transmitter is able to accurately set its transmission power to the exact value required by the algorithm, and delays due to measurements and signal transmissions were assumed to be negligible. The simulation run time (iterations) is a user definable parameter, *ItsTillStop*.

4.5.2 Mobility model

In order to accurately simulate the network, an algorithm is needed to emulate the mobility of the nodes. There has been a great deal of work done on mobility models for an ad hoc network, see [91] and the references therein. The more detailed mobility models play a greater role in analysing and simulating routing performance. For the simulation of the power control algorithm a simplified model has been implemented. The mean node velocity, v, and mean journey duration, μ, are simulation input parameters. A node travels in a constant direction with a velocity randomly generated using an exponential random variable with a mean of v for a mean duration of μ. The duration is also generated using an exponential random variable. The node direction is a uniform random variable in the range $[0, 2\pi)$.

When the simulation begins a system velocity vector, $\mathbf{v}$, direction vector, $\boldsymbol{\theta}$, and journey duration vector, $\boldsymbol{\mu}$, are generated. Each node, i, has velocity v_i, direction θ_i and journey duration countdown time, μ_i. These represent the random initial mobility conditions of the nodes. Every simulation iteration, each component of the journey duration vector, μ_i, is decremented by 1, and if any of the values drops to zero a new node velocity, direction and duration are generated. All the nodes are then instantly

displaced to their new x and y co-ordinates generated by:

$$\begin{aligned} x_i(n+1) &= x_i(n) + v_i \cdot \cos\theta_i \\ y_i(n+1) &= y_i(n) + v_i \cdot \sin\theta_i \end{aligned} \tag{4.14}$$

Nodes are not allowed beyond the border of the test area, and any calculations of (4.14) that would lead the node to wander outside the boundaries are restricted such that at any time instant, n, all the nodes are within the borders

$$\begin{aligned} 0 \leq x_i(n) &\leq cell\_width \\ 0 \leq y_i(n) &\leq cell\_height \end{aligned} \tag{4.15}$$

4.5.3 Simulation flow

After the initialisation of the input parameters, the necessary number of *node* objects are created in memory with random starting positions and mobilities. The flow of the simulation is a fairly linear progression, and is self explanatory upon looking at the approximate flow diagram of the process, Fig. 4.4.

The initialisation routine extracts the default initialisation parameters and stores them in memory for use during the simulation. The N nodes are scattered over the system area using x and y coordinates generated with a uniform random variable, and the initial inter-node attenuation due to simple path loss is calculated using (4.3) and stored in the L matrix, which has dimensions $N \times N$. The fading model includes slow shadow fading and a matrix of shadow fading factors, S, is generated for time $n = 0$ where $S_{ij}(0)$ is calculated using (4.7), with $S_{ij}(n = -1) = 0$ and a channel correlation coefficient calculated using the mean node velocity and the correlation distance simulation input parameter.

Instead of calculating new values for the shadow fading on each inter-node link every simulation instant, a new N by N matrix, S^t, representing the time until the next shadow fading link change is also introduced. ${S_{ij}}^t(n)$ contains the time in milliseconds

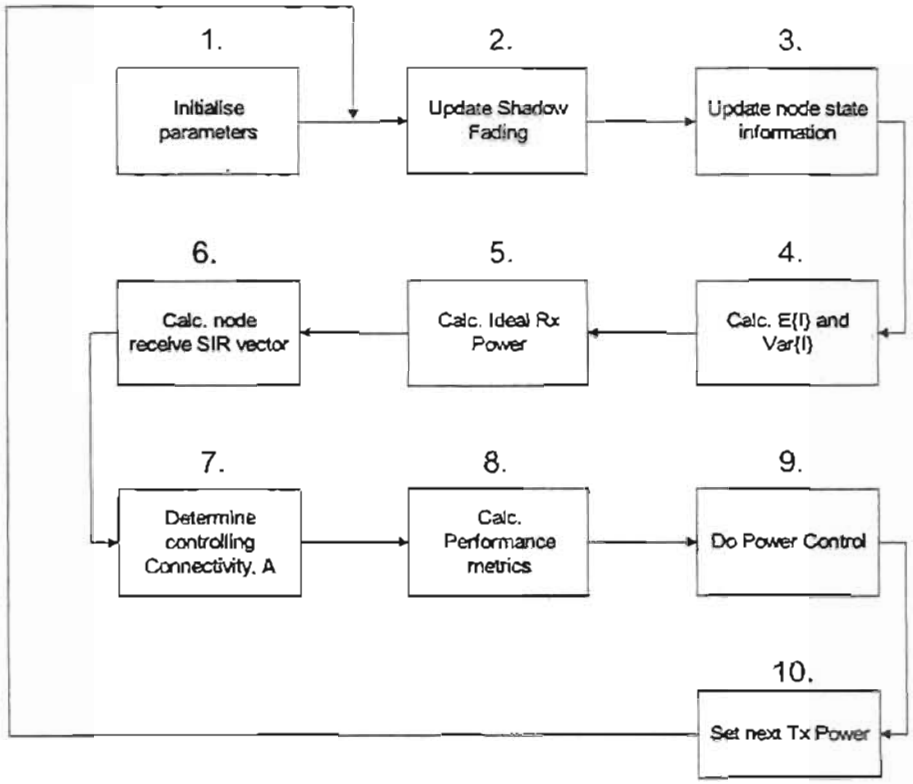

Figure 4.4: Simulation flow diagram

until the link undergoes its next fade. Every simulation iteration all the S_{ij} are decremented by one, and if any value reaches zero a new S_{ij} and $S_{ij}{}'$ are generated. An exponentially distributed random variable with mean τ_s, where τ_s is a simulation input parameter, is used to generate the random times of S'.

The stochastic on/off behaviour of each node is simulated in a method similar to that used for the node mobility and shadow fading. A vector, T , with element T_i containing the random time for node j before the node switches state. The node is on for *mean_on*, and off for a time of *mean_off*, where both of these are simulation input parameters. Every simulation iteration T is parsed and decremented, and if any node reaches a zero count then its state is changed.

The simulation is able to exactly determine the total interference experienced at a node, as required by (4.8). The new interference value is added to the sliding window vector, replacing the oldest stored value, and a new mean interference, $\bar{I}_j$, is calculated based upon the previous L interference values. After the calculation of $\bar{I}_j$, the engine calculates the instantaneous variance, V_j, of the interference over the $I_j(n)$ values stored in the window. This is repeated for each node, j, in the network.

Equation (4.8) is used to obtain the ideal received power, $r_j^*(n-1)$. This value is what any signal at node j should be received at in order for the SIR target, as well as the QoS outage specifications to be satisfied.

Each node, j, is able to calculate an SIR vector, γ_j, where the i^{th} element of γ_j is $\gamma_{ji}(n)$ as given by (4.1), and this vector is sorted so that node will easily be able to determine which the greatest K SIRs are if necessary for the connectivity algorithm.

The inter-node controlling connectivity matrix, A, is calculated depending on the connectivity criteria set at the beginning of the simulation. For each *connected* node, node j then either sends an increase or decrease power control command to the necessary nodes depending on the result of (3.23). Each node i then adapts its transmission power according to the adaptation method set in the initialisation (refer to 3.4). The actual transmission power is only updated at the very end of the iteration of the algorithm. Any further calculations that are done this iteration are based upon the values obtained before the actual power change.

4.6 Performance metrics

In order for the different connectivity and adaptation algorithms to be compared and ranked, some meaningful statistics need to be observed for the conditions under test. These statistics include system outage, mean SIR value and convergence speed, as well as the total connectivity of the network. A mean SIR value for node i, γ_i^{avg}, is obtained

by averaging the best SIR value of node i over every iteration after convergence is believed to have been achieved. This convergence condition is somewhat difficult to calculate in the simulation, so instead a trend is manually monitored and is available as a user input parameter, *ItsTillConv*, indicating the number of iterations until convergence is assumed. Although there are more sophisticated methods of determining the convergence, if this parameter is made sufficiently large relative to the time-step, but small compared to the total number of iterations, it is an accurate, although generous way of specifying convergence. The system mean SIR is taken by averaging γ_i^{ave} over all N nodes in the network.

In order to calculate the system outage the simulation contains an outage count vector, δ. Every simulation iteration the best SIR of all the nodes is (sequentially) compared to the target SIR, and if it is below this target the outage count for that node is incremented:

$$\delta_i(n) = \delta_i(n-1) + 1 \tag{4.16}$$

A running count is also kept of the number of iterations that each node has been transmitting, otherwise when a node is inactive (not transmitting), its SIR will drop to zero and the simulation will think the node is experiencing outage. Once the particular simulation run has completed the total system outage is calculated by taking the average outage of all the nodes. The outage for a single node is only tested after *convergence* has been attained, which is the number of iterations specified as described previously, by the *ItsTillConv* input parameter. As mentioned the convergence is difficult to accurately quantify, as it varies dramatically between nodes and initial starting conditions (node placement etc.). Human input is used here to get a *feel* of the speed of the algorithm.

True network connectivity is also a very important metric to see how a particular combination of connectivity and transmit power adaptation fare. At the end of each simulation run, the total connectivity for each node is calculated. The true connectivity for node j is a boolean vector indicating which other nodes are receiving from j with a SIR that is acceptable. All these true connectivity vectors are combined to form a

true connectivity matrix indicating which nodes are successfully being received at other target nodes. An example network showing final connectivity is given in Fig. 4.5: By

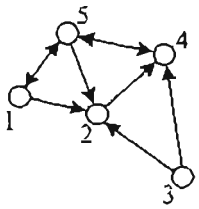

Figure 4.5: Sample ad hoc network with connectivity after convergence as indicated, an arrow pointing from node i to node j indicates that $\gamma_{ji} \geqslant \gamma^*$

direct observation of the diagram the true connectivity matrix can be extracted:

$$\mathbf{A} = [a_{ij}] = \begin{bmatrix} 0 & 0 & 0 & 0 & 1 \\ 1 & 0 & 1 & 0 & 1 \\ 0 & 0 & 0 & 0 & 0 \\ 0 & 1 & 1 & 0 & 1 \\ 1 & 0 & 0 & 1 & 0 \end{bmatrix} \tag{4.17}$$

However, by noting, for example, that node 1 can communicate to node 4 through the use of an intermediate node, 2, it is possible to loop through this single link connectivity matrix and obtain the total networks' global true connectivity matrix, $\mathbf{A}^*$.

$$\mathbf{A}^* = [a_{ij}] = \begin{bmatrix} 0 & 1 & 1 & 1 & 1 \\ 1 & 0 & 1 & 1 & 1 \\ 0 & 0 & 0 & 0 & 0 \\ 1 & 1 & 1 & 0 & 1 \\ 1 & 1 & 1 & 1 & 0 \end{bmatrix} \tag{4.18}$$

Clearly node 3 cannot be reached by any other node, and so this would be an example of poor topology control.

From this $\mathbf{A}^*$ matrix it is easy to obtain the total average node connectivity, χ:

$$\chi = \frac{1}{N(N-1)} \sum_{i}^{N} \sum_{j}^{N} a_{ij} \tag{4.19}$$

A network which has a path between every node pair (connected network) would lead to $\chi = 1$, which is the ideal value for an ad hoc network. The maximum number of hops between any node pair is $N - 1$.

In order to get accurate statistics, the simulation needs to be run for lengthy periods of time using a Monte-Carlo approach, where the same input parameters are tested for many different initial node conditions, random shadow fading and mobilities.

4.7 Results

It is very difficult to easily summarize and quantify the effect that many of the input parameters have on the system performance and it is impossible to present results from every logical permutation of the parameters, so instead a general overview is presented. Some of the actual results obtained may appear unrealistic in terms of real-world values, but as this work is an initial foray into power control in ad hoc networks the results are more useful in portraying trends than obtaining exact values.

One of the properties of a power control algorithm is the convergence of the node SIR. The SIR of a node i is defined as:

$$\gamma_i(n) = \max_j \gamma_{ji}(n) \tag{4.20}$$

That is γ_i is taken at the node, j, which has the greatest SIR from node i. Two important properties when discussing the convergence of the SIR are: speed and final value. The speed of convergence to the final value is difficult to quantify as it varies substantially from node to node. The best way is to give an approximate *worst-case* scenario.

4.7.1 Connectivity: Received power threshold

For an explanation of this connectivity method refer to section 3.3.1. Starting off with the most basic model of an ad hoc network, the nodes are kept stationary and the atten-

uation due to shadow fading is set to 0 dB. Thus the only signal loss mechanism is due to distance attenuation, and this remains constant for every inter-node link throughout the duration of the simulation. The best method of visualizing the performance of the network in terms of SIR convergence is a a plot of the SIR of a node over time. This enables an accurate description of the functioning of the algorithm (with specific

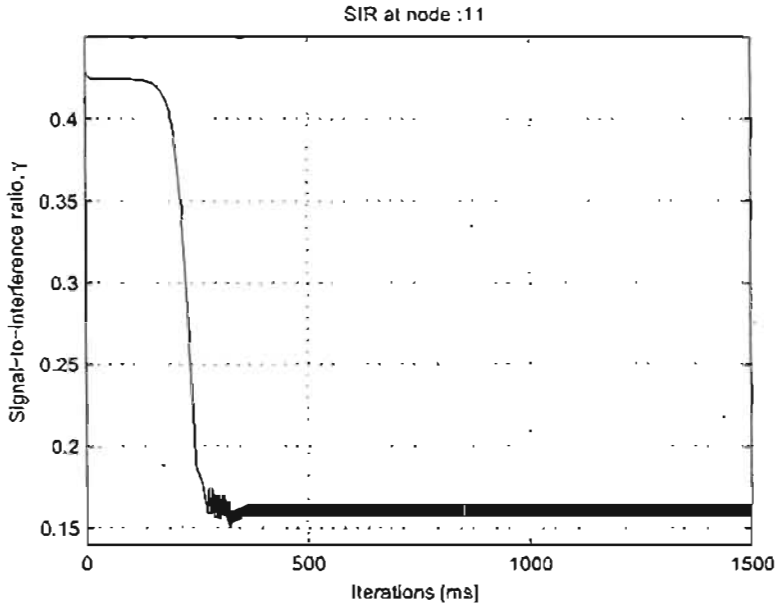

Figure 4.6: SIR over course of simulation run, no mobility: $v = 0\,\mathrm{ms}^{-1}$

input parameters) over time. The time taken until convergence can be easily read off such a graph. Fig. 4.6 shows the temporal adaptation of the node's SIR, as defined by (4.20). This was using a $\tau_{\min} = 10^{-16}\,W$ and the *satisfy best link* transmit power adjustment scheme. Again it should be noted that although this may seem like an unrealistically small value to use, the aim is to show that the algorithm works (under particular conditions), not to exactly quantify all simulation parameters.

Zooming in on the area of interest from approximately $200 \rightarrow 400$ iterations, as shown in Fig. 4.7, it can be seen that convergence occurs (for this particular node) after approximately 360 iterations. The node maintains this converged value indefinitely.

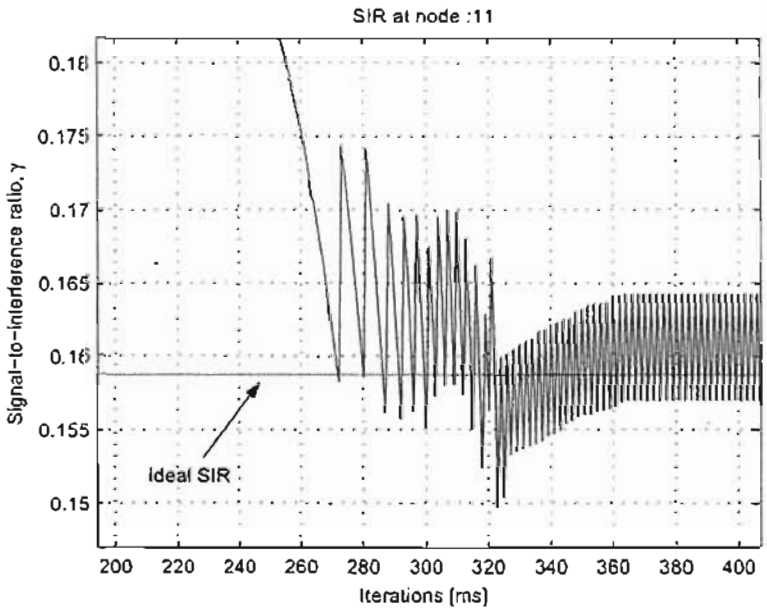

Figure 4.7: Zoomed in SIR showing iterations 200 → 400

It was noted that when the SIR did converge to the correct target, an oscillatory behaviour was observed. With Γ set to 10 dB and a processing gain, W, of 63 this corresponds to an ideal SIR of:

$$\gamma^* = \frac{\Gamma}{W} = \frac{10}{63} = 0.159 \tag{4.21}$$

The magnitude of the oscillations depends on the value of the power adaptation step-size parameter, φ. Recall, the outage is calculated by comparing γ to some target SIR, γ^*, and if $\gamma < \gamma^*$ the node is considered to be in outage. The actual SIR bounces around the target SIR and this leads to an outage of approximately 50 % which is obviously not satisfactory.

A solution to this is to *pad* the target SIR slightly, i.e. introduce a guard zone so that even with the oscillation γ remains above γ^*.

Increasing the Γ by φ leads to a target SIR of

$$\gamma^* = \frac{\Gamma \cdot \varphi}{W} \tag{4.22}$$

With φ set to 0.25 dB the new target spread SIR is

$$\gamma^{*} = \frac{10 \cdot 10^{\frac{0.25}{10}}}{63} = 0.168 \tag{4.23}$$

By increasing the target SIR a small amount the outage target SIR can be kept the same. In a system implementation where the target SIR is set to, for example 10 dB, the nodes think they should be attempting a target of 10.25 dB thus even when taking the SIR oscillation into account, the outage specifications will be satisfied. Hence this *modified* SIR of $\Gamma = 10.25$ dB is used as the target despread SIR for the nodes in all the simulations.

It can be seen from Fig. 4.8 that even though the node is below its new target spread SIR of 0.168, because of the padding the SIR does not drop below the actual required spread SIR of 0.159, and so the outage is much lower. Another issue that arises is

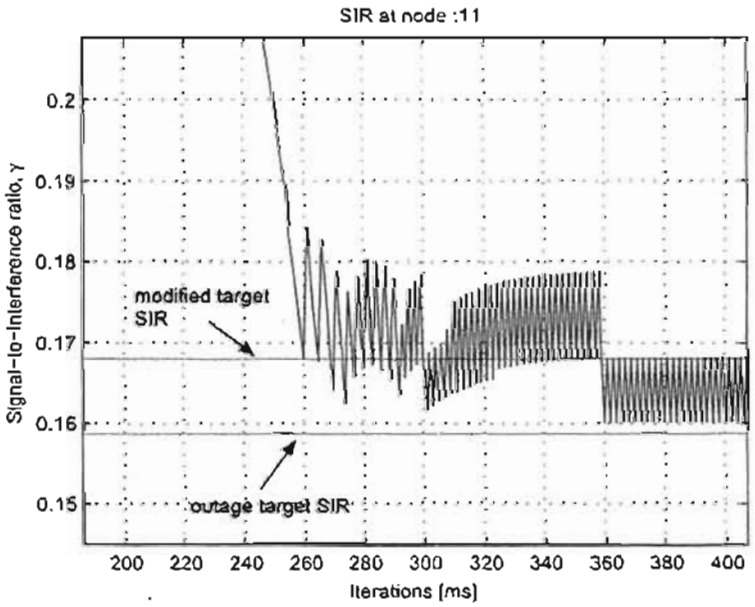

Figure 4.8: SIR over time, with modified SIR target

the necessity to cap the SIR of a node. Consider the situation where two nodes are grouped close together but spatially displaced from the rest of the network, as shown

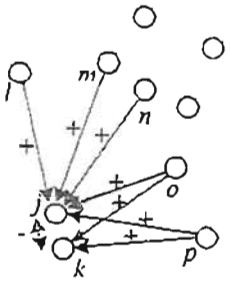

Figure 4.9: Situation where average SIR would be affected

by Fig 4.9. As the distance between, for example, nodes j and l is large, any signal transmitted by node j will experience significant attenuation before it is received at l. In some instances, a subset of the other nodes will instruct j and k to increase their power. Even though node j will probably instruct node k to decrease its power and vice versa the majority of nodes will be instructing an increase in power. Unless the *satisfy best link only* is used as the transmit power adjustment scheme, nodes j and k will end up increasing their power. Thus the SIR at k from j will be much greater than required, often by several orders of magnitude. When taking the average SIR over the whole network, a pair of nodes as in the example, would cause the mean SIR to be greatly skewed, and it would exhibit a very large variance. This is not a meaningful result, and so an upper limit is imposed. In the output statistics of the simulation, the maximum SIR of a node is upper limited to $\hat{\gamma} = 0.5$.

As an example, with no mobility or shadow fading and the interference window length set to 1 iteration, the average SIR of the nodes using the different controlling connectivity schemes is presented in Fig. 4.10. As can be seen, the range of the SIR is almost 50 dB!

It would initially appear that the *satisfy best link only* performs the best, with the mean node SIR approximately equal to the ideal target SIR[3] of -7.743 dB when the $r_{\min}$ parameter is kept below 10^{-16} W. However, examining the true network con-

[3]The target SIR as given by (4.23) in decibels is: $(\gamma^*)_{dB} = 10\log\left(\frac{10.69}{63}\right) = -7.743\,dB$

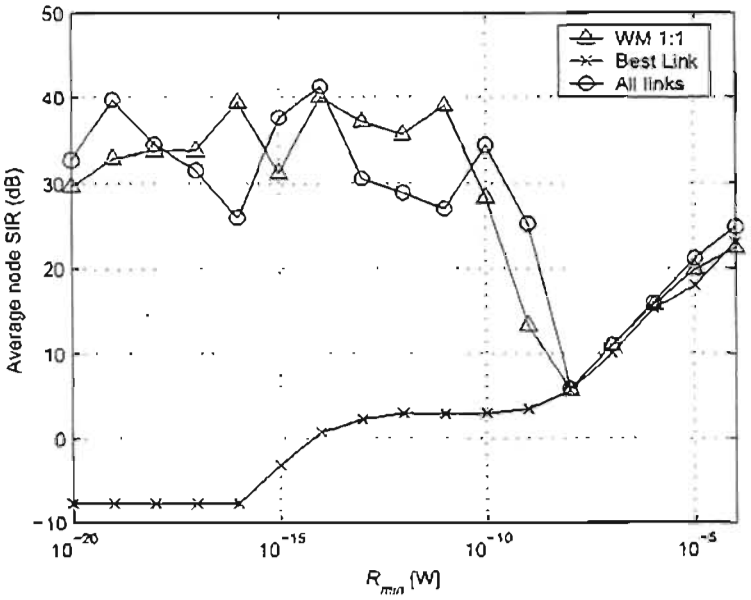

Figure 4.10: Mean node SIR (dB)

nectivity graph, as given in Fig. 4.11 indicates that the performance of this connectivity scheme is poor for this range of $r_{\min}$. The best connectivity is achieved for $10^{-14} \leqslant r_{\min} \leqslant 10^{-8}$ W, and all the connectivity schemes appear to achieve maximum network connectivity when $r_{\min} = 10^{-8}$ W. It is clear from Fig. 4.12 that the *weighted arithmetic mean_1:1* and *satisfy all links* connectivity schemes result in positive feedback effects that cause the transmit power to ramp up continuously for values $r_{\min} \leqslant 10^{-11}$ W. In these simulation runs, the transmit power was limited to a maximum output of 1 W, or 0 dB. Using too small a $r_{\min}$ parameter will lead to a node sending power control commands to many other nodes, and this will cause the positive feedback effect that results in the ramping of the nodes' transmit powers.

The *satisfy best link only* scheme performs the best in terms of average node transmit power, as a node is able to ignore this feedback effect and essentially only be controlled by its nearest neighbour, however the true network connectivity, χ_t of the scheme suffers, with a peak value of approximately 28 %. As can be seen from Fig. 4.13 the

average node outage is also minimized when this connectivity scheme is used, and zero outage was experienced when $r_{\min}$ was in the range of $10^{-15} \leqslant r_{\min} \leqslant 10^{-10}$ W.

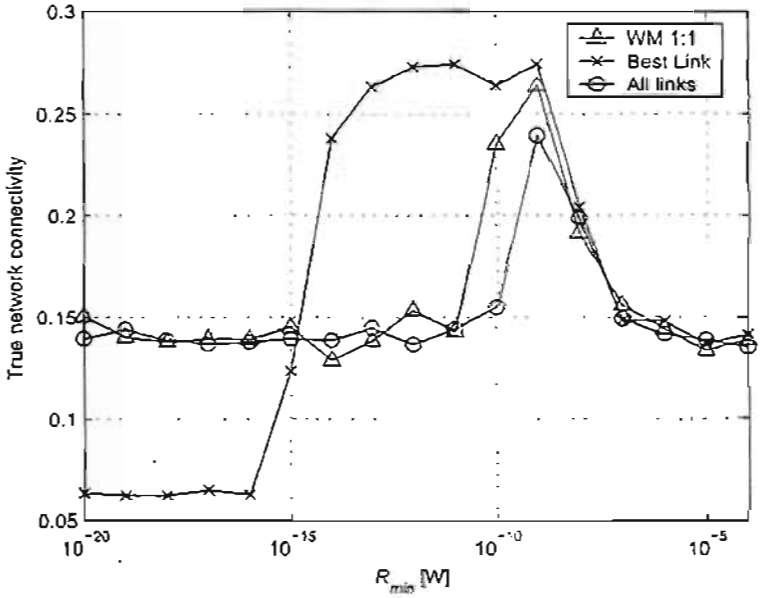

Figure 4.11: Average true node connectivity

Another method of visualising the SIR is a probability density function (pdf) which characterizes the distribution of the SIR. The simulation is set to execute for multiple runs with the same input parameters (but different initial placements) and the γ value for every node and every simulation iteration is stored in memory on the computer. This is averaged over all the runs done, and a histogram of the SIR is produced using MATLAB, which is then normalized by the sum of all the bins to obtain a pdf. With the mobile velocity set to vehicular speeds 60 kmh^{-1}, equivalent to $v = 16.7\,\text{ms}^{-1}$ the SIR distribution, as depicted in Fig. 4.14 has a clearly *Gaussian* type distribution, with the mean situated around 0.168. These distributions were obtained using $r_{\min} = 10^{-16}$ W. The transmit power adaptation method, *satisfy best link only*, is functioning appropriately as the average node SIR is clearly around the target SIR, however the network connectivity is poor.

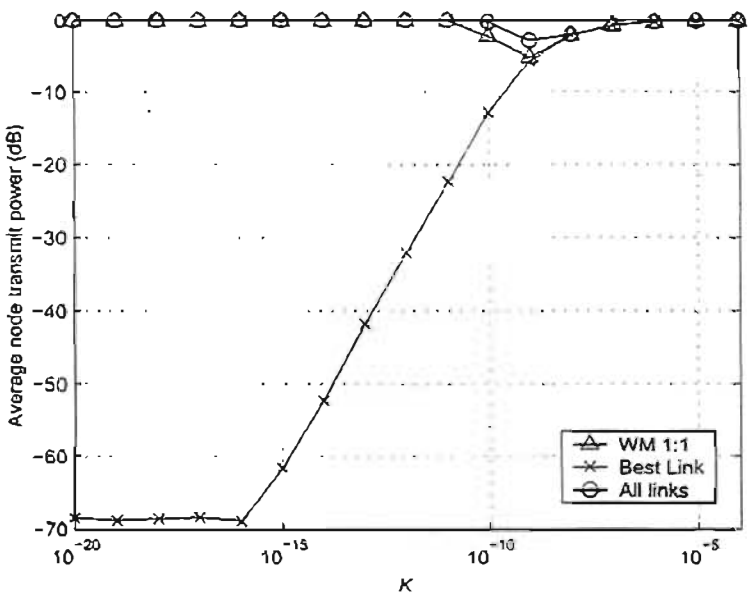

Figure 4.12: Average node transmit power

Clearly, central to this power control connectivity method is the r_{min} parameter. Recall that a node, j, will send power control commands to another node, i, if the power received at j from any i is greater than r_{min}. It is apparent that this parameter depends in turn on the number of nodes in the network, N. The greater N, the higher the node density becomes, and the mean distances from a node to its neighbours will decrease. The algorithm was tested for $N = 10$, $N = 25$ and $N = 50$ nodes.

As the minimum received power threshold is decreased, the controlling node connectivity rises, and as r_{min} approaches zero the controlling connectivity tends towards unity, refer to Fig. 4.16. The controlling connectivity is defined as the number of nodes a single node is sending power control commands to, expressed as a percentage by dividing this count by the total number of controllable nodes, i.e. $N - 1$. It is not realistic to have a node controlling every other node in the network, rather it should be a small subset of its closest neighbouring nodes. Usually in CDMA fast power control commands are sent by puncturing the transmit data bit-stream, and are not passed through

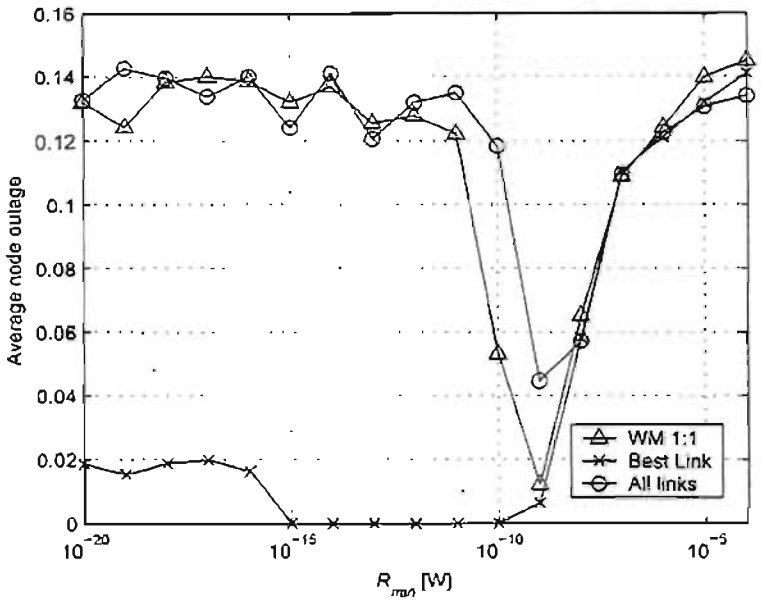

Figure 4.13: Average node outage

any forward error correction to reduce delay. However, this does have an impact on the chances of the power control command being received incorrectly due to interference. With a high controlling connectivity then if the controlled node is far away, in order for the command to be received without error at the node destination it may have to be transmitted on a pilot channel at a much greater power, and this would have a detrimental impact on the battery lifetime of the terminal. This is counter-productive to one of the goals of power control which is to extend as much as possible the terminal lifetime.

Recall that the SIR of a node is only capped in the output data statistics and has no effect on the system performance. A value of 0.5, nearly three times the ideal SIR, was used for $\hat{\gamma}$, and as $r_{\min}$ is increased beyond a certain value the average node SIR tends rapidly towards $\hat{\gamma}$. This particular algorithm trait is explained as follows. After some time, n, node i is transmitting with a power $p_i(n)$ such that it is being received with a power greater than $r_{\min}$ *only* at it closest node, j . This leads to node j sending power

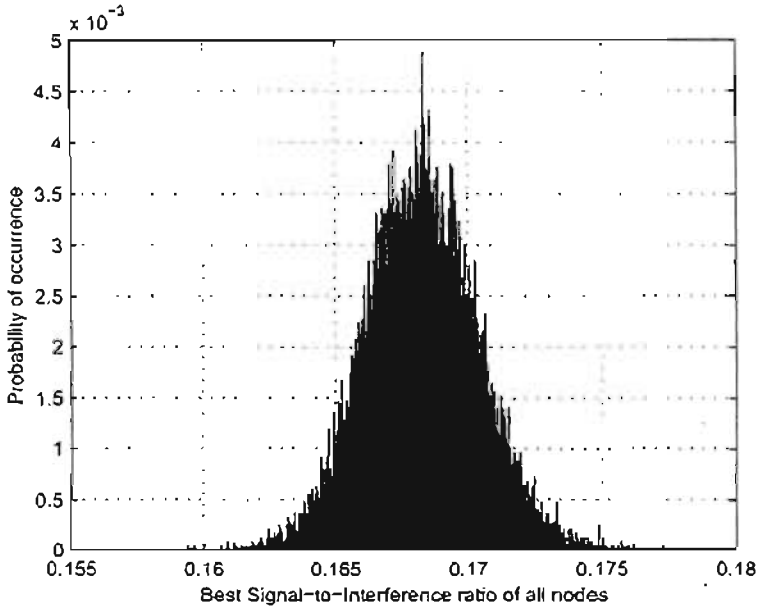

Figure 4.14: pdf of SIR, fast mobility: $v = 16.7\,\mathrm{ms}^{-1}$

control commands to node i as required and expected. However, assume there are a few other nodes around node j that are transmitting such that they are received at j with power slightly less than $r_{\min}$, hence j will not attempt to control them. Due to the received signal strength dropping off with an exponential factor of 4 as the inter-node distance increases there will be only a few dominant nodes interfering with node j. Assuming there are M dominant nodes nearby j, each being received at j with a power $\frac{r_{\min}}{M}$, then the SIR at j from i is:

$$\gamma_{ji} = \frac{r_{\min}}{M\frac{r_{\min}}{M} + \eta_j} \tag{4.24}$$

A value of $r_{\min}$ approximately the same as the background noise, η_j, leads to an SIR of:

$$\gamma_{ji} = \frac{\eta_j}{M\frac{\eta_j}{M} + \eta_j} = \frac{1}{2} \tag{4.25}$$

Clearly this would lead to node j instructing node i to decrease its power, which i would dutifully do. However by doing so, at the next iteration the decrease in transmission power could lead to the signal arriving at j with a power less than $r_{\min}$, which would

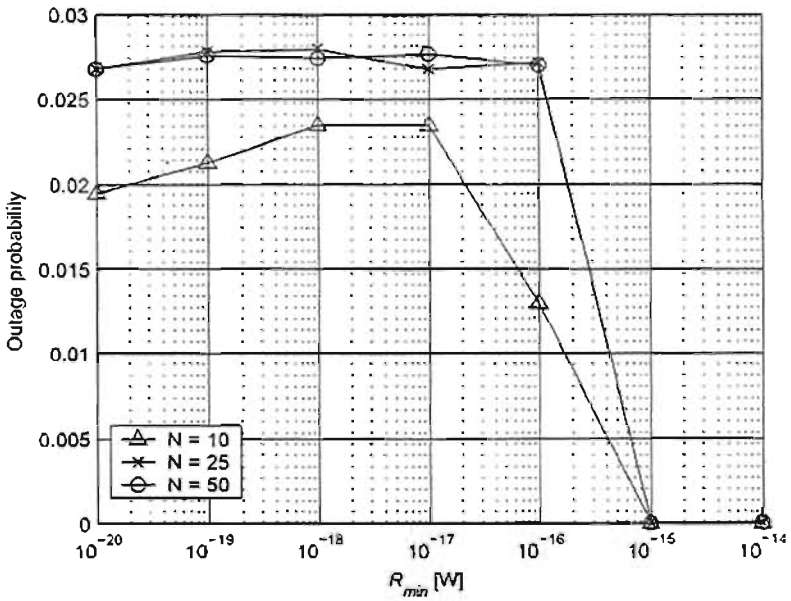

Figure 4.15: Effect of $r_{\min}$ on system outage, shadow fading disabled

mean than j would not control the power of i. If there were no other nodes sending power control commands to i then it would increase its power, and then be picked up again by j. Clearly this oscillatory cycle could continue indefinitely, with γ_{ji} oscillating around a value greater than the desired target γ^*. There could also be other nodes that are receiving from i with a signal less than $r_{\min}$, but actually with an SIR of greater than γ^*.

Clearly the value of $r_{\min}$ should not be made too large otherwise although the average node SIR will be met and the system outage is zero, there will be resources wasted in that the nodes are transmitting with a power greater than required. However, setting a value of $r_{\min}$ that is too small could lead to unnecessary controlling node connectivity, requiring nodes to control nodes far away from them, which is not power efficient.

Different permutations of parameters produce similar results, and it is not possible to present them all. Some conclusions can however be drawn. The minimum received *power threshold* method can not guarantee 100 % network connectivity, but when com-

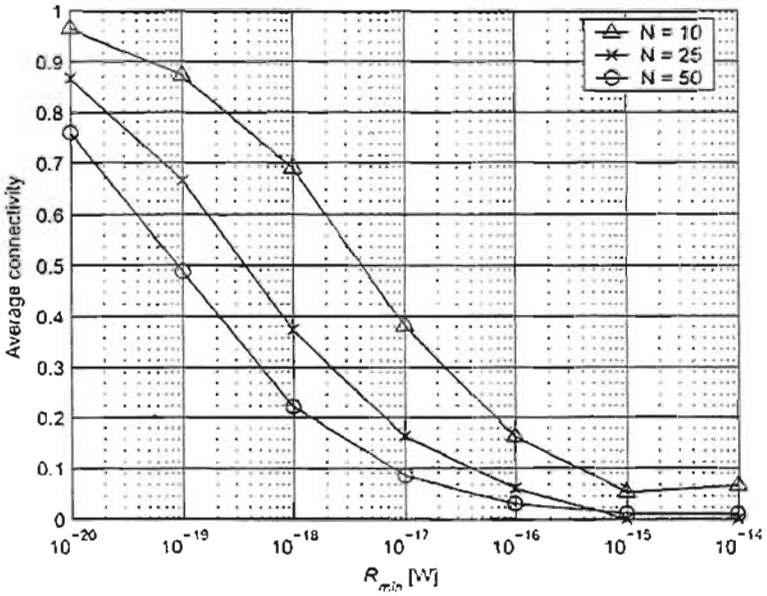

Figure 4.16: Effect of $R_{\min}$ on controlling connectivity, shadow fading disabled

bined with the *satisfy best link only* transmit power adaptation scheme the transmit power of each node can be greatly reduced while still maintaining partial network connectivity. In order to obtain full connectivity some other, higher level, network function needs to be present.

4.7.2 Connectivity: SIR received from greatest K nodes

One of the disadvantages of the threshold based method described previously is the hardwired value of $r_{\min}$. As the algorithm proceeds in time an adaptive method is ideally required to determine controlling node connectivity. Instead of using a threshold, another proposed method is for node j to send power control commands to the nodes from which it is receiving the most power. This number of nodes is determined by the simulation input parameter, K. During each power control iteration node j sorts through a vector of the power received from all the other nodes, $\mathrm{r_j} = (r_1, r_2, \ldots, r_N)^T$, and updates its connectivity vector such that it will work with the greatest K of these.

The power received from the node itself is defined to be zero.

Another method that a node could use to determine its controlling connectivity would be to use the SIR from the greatest K nodes. As the SIR is directly related to the received signal power it is surmised that this will lead to the same connectivity.

Initially the system was tested with no node mobility or shadow fading. The average node transmit power gives an indication of the ability of the algorithm to find a feasible power solution. From Fig. 4.17 it is clear that the only transmit power scheme that

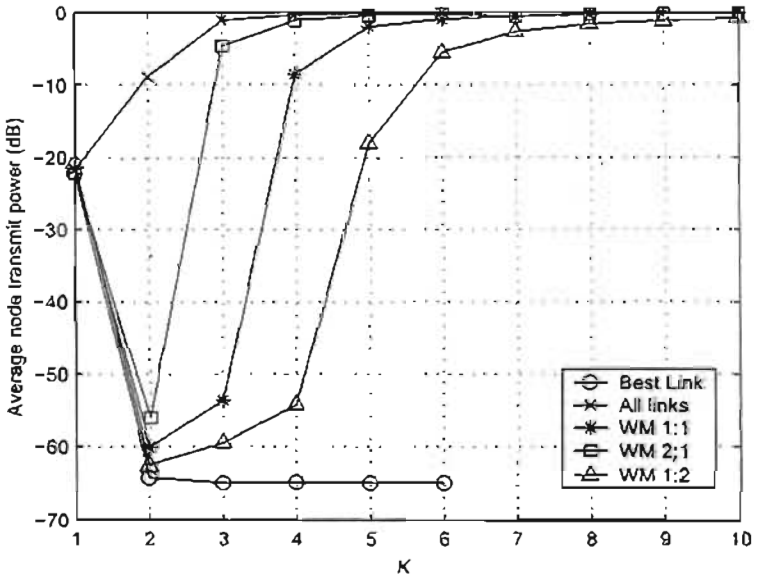

Figure 4.17: Effect of K on average transmit power (dB), shadow fading disabled

maintains stability is the *satisfy best link only* scheme. All the other methods lead to a positive feedback effect which causes the transmit power to continuously ramp up until the maximum allowable power, set in the simulation parameters to 0 dB, is reached. As the number of controlled nodes, K, is increased beyond 2 there is no effect on the average connectivity and outage. With the connectivity parameter, K, set to one it was noticed that there was a large variance in the average node transmission powers between simulation runs. For the majority of the simulation runs the average power

would usually be in the region of approximately -50 dB, but occasionally the average would be much greater at around -8 dB. The result is that these occasional non-ideal[4] runs skew the average greatly. As K is increased, and the transmission power of a node affected by a single dominant decrease power control command, the network is more likely to converge to a minimum power solution. A connectivity control parameter of $K \geqslant 2$ leads to the lowest average node transmit power, but this is subsequently negatively offset by the lowest true connectivity of the power adaptation schemes. The true connectivity and outage graphs are given respectively by Figures 4.18 and 4.19.

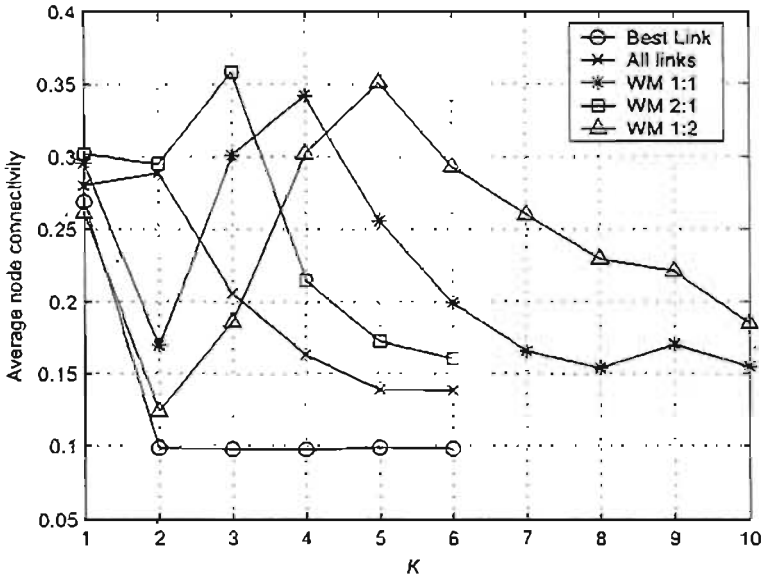

Figure 4.18: Effect of K on average node true connectivity

The worst functioning power adaptation algorithm is the *satisfy all links* method. Recall the functioning of this transmit power adaptation scheme: a node will increase its power if it receives any increase commands. As K is increased a node will send control signals to nodes further away, leading to a positive feedback effect that causes all the nodes to saturate their transmit power at the upper limit. With K set to one not all the nodes are transmitting with the maximum power, and this leads to the maximum

[4]Some or all of the nodes are transmitting at maximum power

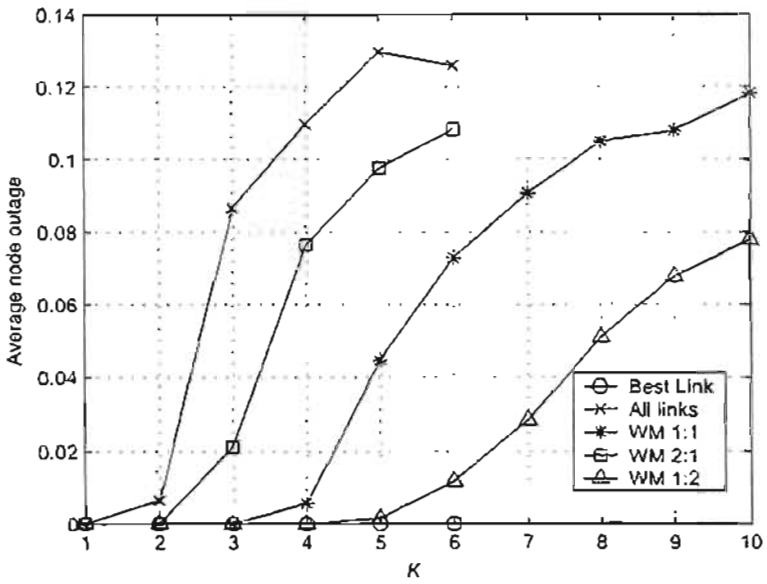

Figure 4.19: Effect of K on average node outage

true connectivity for this connectivity/adaptation combination.

The *weighted mean* approach was tested using three different combinations: WM 1:1, WM 2:1 and WM 1:2. The format of this nomenclature is increase:decrease, so a 2:1 ratio means that the increase commands are twice as important as the decrease commands. As an example to enhance clarity, if a node is using WM 1:2 and assuming it is receiving two decrease commands, it will increase its power only if it is being instructed to by more than four other nodes. The *satisfy best link only* can be seen as a special cases of the weighted mean approach where the scaling factor is infinite, i.e. WM 1:∞, and similarly the *satisfy all links* could be interpreted as WM ∞:1. These relationships can be seen from the average transmit power graph, Fig. 4.17, with the WM 1:2 algorithm being less susceptible to the positive feedback effect that leads to transmit power saturation. On the other end of the scale, WM 2:1 performs slightly better than the *satisfy all links* algorithm in terms of transmit power saturation. Whereas the *satisfy all links* method saturates for any value of K greater than 2 (with a maximum network connectivity at $K = 2$), WM 2:1 achieves a greater peak connectivity

(35 % when $K = 3$) and only saturates when $K \geqslant 4$. All three weighted mean variants produce similar peak connectivity values. Considering only average transmit power and true network connectivity, the apparent best scheme is the WM 1:2 method with a K value of five, as this leads to peak connectivity. If connectivity is not as important as saving energy in the mobile device, then using WM 1:2 and a K of four leads to only a slight decrease in connectivity (approximately 30 %) but a 35 dB decrease in average node transmit power. By looking at the outage graph of Fig. 4.19, the trend indicates that a lower value of K produces smaller outage results, which is desired. The WM 1:1 method results in a connectivity peak in between the WM 2:1 and WM 1:2 method, and a transmit power saturation with similar properties. It is surmised that with a WM $x : y$ as $\frac{x}{y} \rightarrow \infty$ the behaviour will mimic the *satisfy all links* algorithm, i.e. the transmit power graph will tend toward saturation at $K = 3$, and peak connectivity will occur when $K = 2$. Similarly, as $\frac{y}{x} \rightarrow \infty$ the behaviour will tend towards the *satisfy best link only* transmit power adaptation scheme. The average node SIR results were capped at $\hat{\gamma} = 0.5$ and generally do not contain meaningful value, so they are not presented. The node controlling connectivity has also not been shown for this connectivity method, as it is clearly a straight line with a defining equation $y = \frac{K}{N-1}$.

Enhancing the realism of the simulation by introducing shadow fading and fast mobility, the results generated are very similar to the case of no mobility or shadow fading. The $K = 1$ point which seemed to cause instability under the latter set of conditions is removed, and produces the lowest average node transmission for all transmit power adaptation algorithms except the *satisfy best link only* scheme, as can be seen from Fig. 4.20. The true network connectivity and outage results, Fig. 4.21 and Fig. 4.22 respectively, are very similar to the when the algorithm was tested without shadow fading or mobility. The best transmit power adaptation scheme appears to be WM 1:1 with $K = 3$, as this achieves a network connectivity (33%) nearly equal to the maximum observed connectivity (approximately 35%), with an outage of around 0.1% using only an average transmit power of -53 dB.

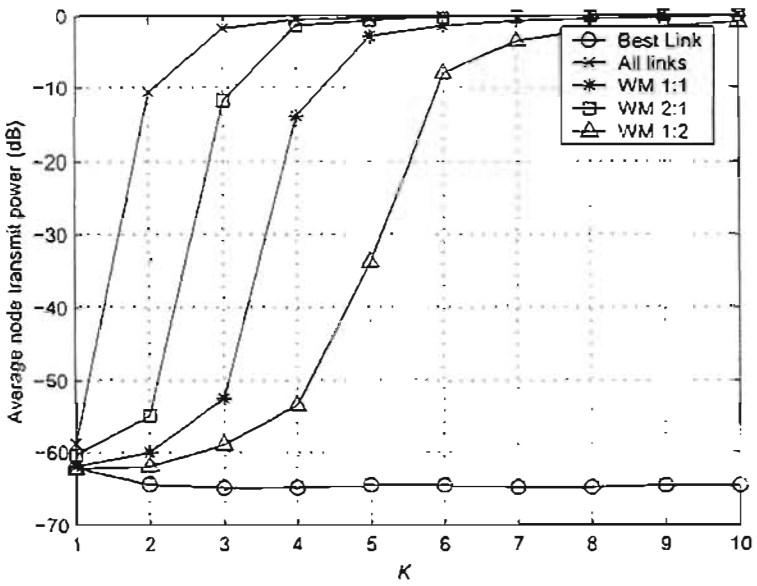

Figure 4.20: Effect of K on average transmit power (dB)

Effect of interference window length, L

The mean interference defined by (4.11) averages the previous L values of the instantaneous interference, and is repeated here for convenience.

$$\tilde{I}_j(n) = \frac{1}{L} \sum_{t=n-L+1}^{n} \tilde{I}_j(t)$$

The effect of this L parameter is tested for the system where the connectivity criteria is *SIR from greatest K nodes*, and the transmit power adaptation algorithm used is WM 1:1 which, from the previous graphs and discussion, appeared to give the best overall performance. The average node transmit power, as depicted in Fig. 4.23, is lowest when L is set to one. It is desirable to have the transmission power as low as possible, as this helps conserve the valuable resources of the mobile terminals, however by examining the network connectivity of Fig. 4.24 and the outage as given in Fig. 4.25 indicates that using $L = 1$ is not the best approach. This value of the interference window length leads to the lowest average network connectivity and also the greatest average outage. As mentioned earlier, the ideal received power algorithm, defined

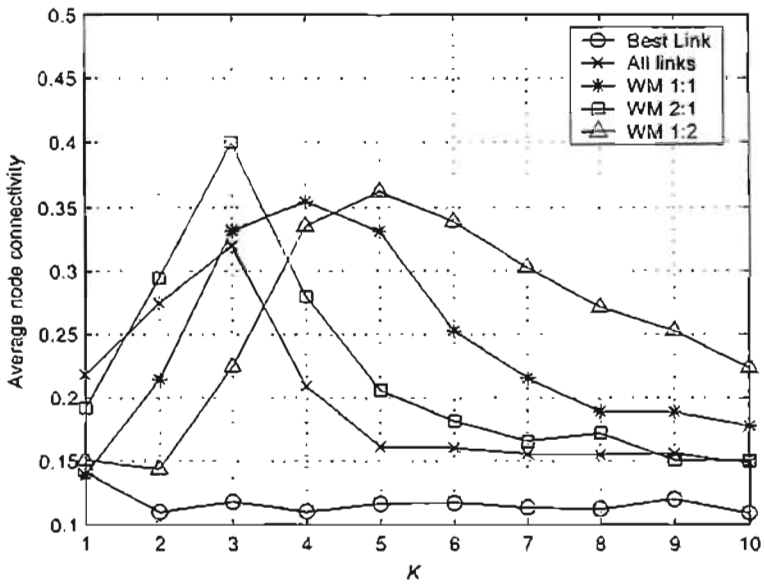

Figure 4.21: Effect of K on average node true connectivity

by (4.8) includes a term which is dependent on the variance of the interference. With the L parameter is set to unity, the mean interference will always be equal to the instantaneous interference and this has the result that the calculated variance will always be equal to zero, so the benefit of the increased algorithm complexity is lost. The zero variance also explains why the average node transmit power is a minimum, as there is essentially no extra *padding* of the SIR target, but this leads to an increased outage, very noticeable in Fig. 4.25. As the interference window length is increased the outage drops slightly and there is also a minor increase in average node transmission power. Essentially, increasing L above two has no major benefit to the network. If a value of $L = 2$ is used, then the effect of the signal oscillation around the ideal point will be reduced, as an average of the low and high point of the oscillation will be used.

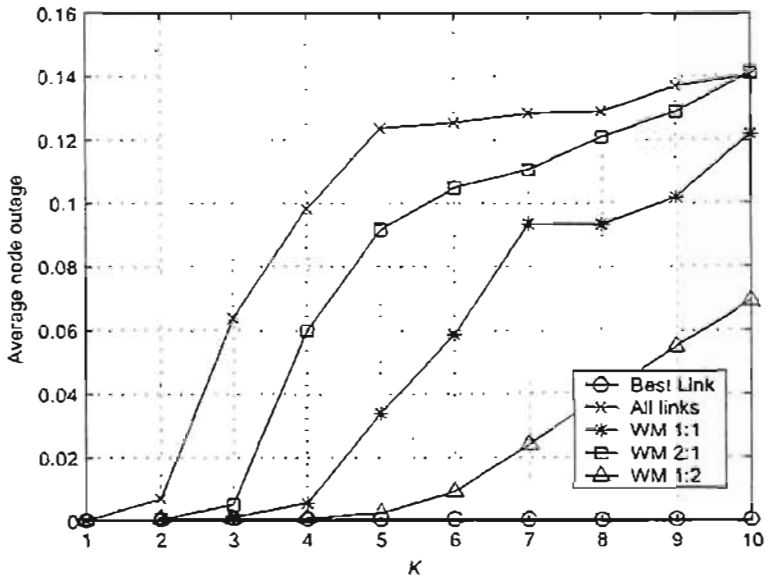

Figure 4.22: Effect of K on average node outage

Effect of initial transmit power

When the simulation is started, and the network generated, each node has an initial transmit power value, which is variable via a simulation input parameter, but constant for each node in the network for that set of runs. The results thus far have mostly been generated with the initial transmit power, $p(0)$, equal to 1 W, or 0 dB. Using the *SIR from greatest K nodes* connectivity criteria, and the WM 1:1 power adaptation routines, the effect of $p(0)$ was tested using an initial transmit power of: 0 dB, -10 dB, -20 dB and -30 dB. The average node transmit power, given in Fig. 4.26, indicates that a smaller value of $p(0)$ leads to a smaller average power. The minimum power solution (assuming the system is feasible) should be independent of the initial transmit powers, and thus another conclusion that can be drawn from this graph is that the algorithm does not always converge to the exact ideal solution for values of $K \leqslant 3$. This is typical of an iterative, decentralized, approach. The average power is however approximately the same for values of $p(0) \leqslant -10$ dB. If shadow fading and mobility are disabled,

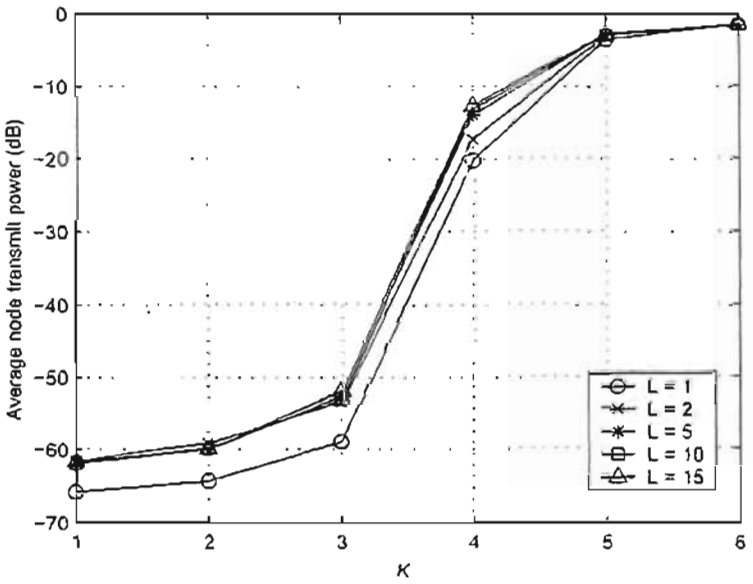

Figure 4.23: Effect of interference window length, L, on average node transmit power

then through direct observation of the *ideal received power* temporal adaptivity graph the convergence time (iterations) an be obtained for a single run. Convergence for a particular node is indicated by a region on the graph with zero gradient for a large period of time, as shown for example by Fig. 4.29. By observing the IRP graph for each node in the network, it is possible to ascertain the time at which which the node with the slowest convergence reaches this constant value. Fig. 4.29 was generated using a $p(0)$ value of -20 dB with shadow fading and mobility disabled. Using the same initial transmit power, but including shadow fading and fast node movement, a similar graph, Fig. 4.30, was obtained. The main difference is that due to the constantly varying path gain (due to shadow fading and fast mobility), the IRP does not actually settle at a value, rather it exhibits a region of convergence.

It was mentioned in section 2.4.6 that a node should be connected to approximately six other nodes to ensure that network partitioning does not occur. From the average connectivity results that have been presented it is clear that partitioning is indeed occurring. Using the various transmit power adaptation methods and an interference

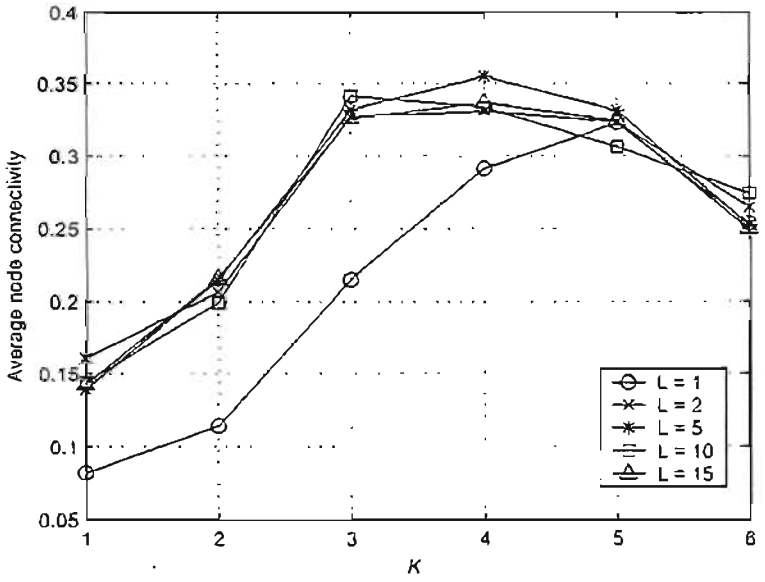

Figure 4.24: Effect of interference window length, L, on average node connectivity

window length of $L = 2$, Fig. 4.31 is a graph of the average node degree of connectivity (number of nodes that are receiving a signal from a node which satisfies the target SIR). It is clear from this graph that the best average connectivity is significantly less than six, and this explains the poor network connectivity results.

4.7.3 Connectivity: maximum inter-node distance

The final method of controlling node connectivity tested is based on inter-node distances, as discussed in section 3.3.2. A node will issue power control signals to all the other nodes that are within $d_{\max}$ m of the controlling node. Initially shadow fading was disabled and the nodes were stationary. The average node transmission power graph, Fig. 4.32, indicates that using $d_{\max}$ values greater than 450 m leads to saturation of the nodes' transmission powers. This occurs for all the power adaptation schemes except the *satisfy best link only* method. As $d_{\max}$ is increased, controlling nodes will issue a larger number of *increase power* commands, and this leads to an unstable network con-

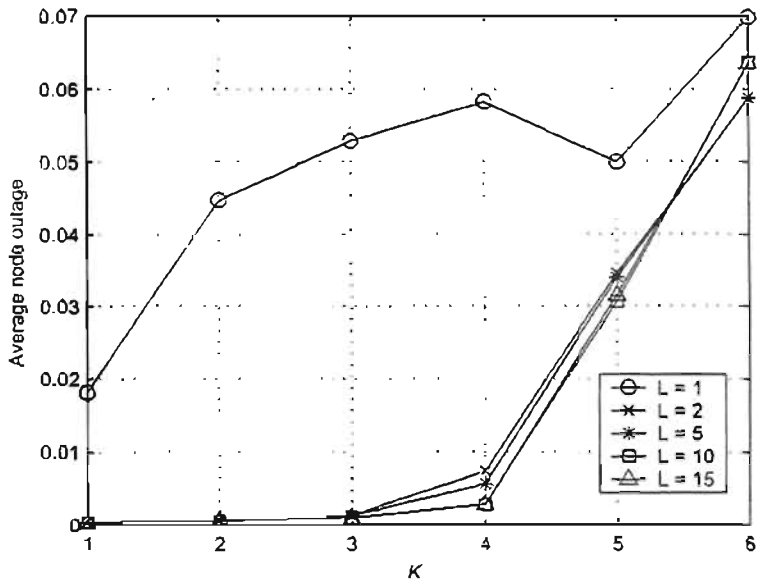

Figure 4.25: Effect of interference window length, L, on average node outage

figuration (positive feedback effect). When considering the performance of the schemes, and choice of $d_{\max}$, the network connectivity also needs to be examined. Fig. 4.33 shows that a maximum average connectivity of approximately 34 % can be achieved using any of the *weighted mean* power adaptation approaches. The best operating point would appear to be using the WM 1:2 method with $d_{\max} = 250$ m. The system outage, given in Fig. 4.34, is also minimized using this combination, with an average value of approximately 0.52 %. When the effect of shadowing and mobility are introduced into the model, the results are similar to the more simple scenario, the only major difference lies in the average node transmit power, Fig. 4.35, with $d_{\max} \geq 450$ m. By observing individual runs it was noted that for $d_{\max} < 450$ m most of the simulation runs would result in an average transmit power of approximately -65 dB. However, a small number of runs (one or two out of one hundred) would result in a solution where some of the nodes would be transmitting at maximum power, making the average transmit power for that run fairly high. These *bad* runs tend to skew the transmit power average when taken over all the runs. If a node is substantially removed from all the other nodes,

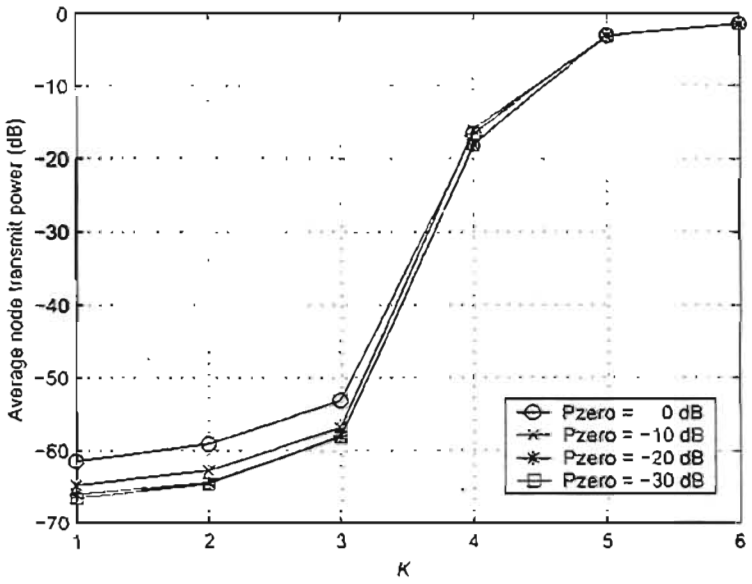

Figure 4.26: Effect of initial transmit power, $p(0)$, on average node transmit power

then it would constantly be receiving increase commands, and since its initial transmit power is set to 0 dB, the upper limit for power (set as a simulation parameter), its power will remain at 0 dB for the duration of the run. When the $d_{\max}$ parameter is made large enough (greater than 400 m) there is enough interaction between all the nodes to ensure that these far away nodes receive some decrease signals.

The addition of shadow fading and mobility does not affect the connectivity or outage significantly.

4.8 Summary

This chapter has introduced the mathematical model for the system, and described the custom designed simulation environment. The important metrics for evaluating and comparing the performance of the different combinations of controlling and power adaptation algorithms are: average network connectivity and average transmit power.

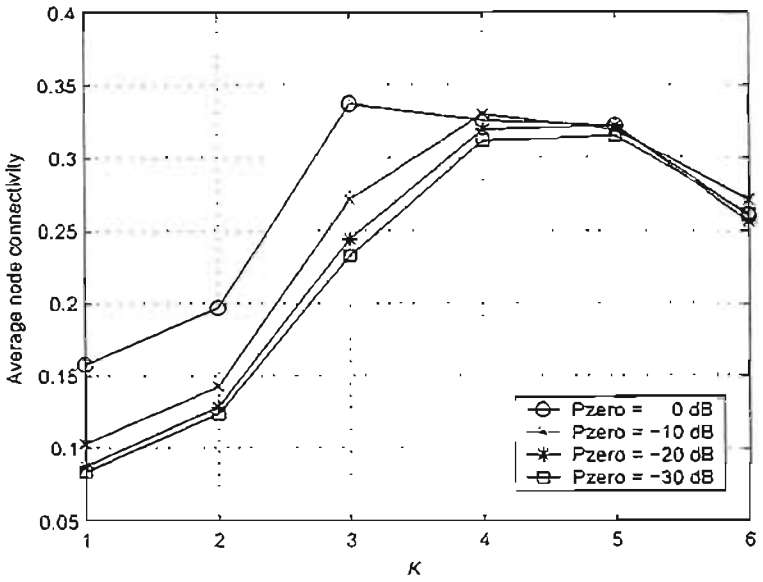

Figure 4.27: Effect of initial transmit power, $p(0)$, on average node connectivity

A large selection of results and graphs have been presented, and a short summary is as follows:

- Due to the oscillatory nature of system, the target SIR should be slightly padded
- When using the minimum receive power threshold connectivity method the best balance between connectivity and average node power occurs with WM 1:1, and a $\tau_{min} = 10^{-9}$ W. Outage is also minimized when this is used
- Using the *satisfy all links* power adaptation method is typically very unstable, and leads to positive feedback effect that causes the node transmission power to saturate
- Using *satisfy best link only* method leads to the lowest average transmission power, but conversely also produces the worst connectivity results
- The WM 1:1 method results in a connectivity peak in between the WM 2:1 and WM 1:2 method, and a transmit power saturation with similar properties. It is

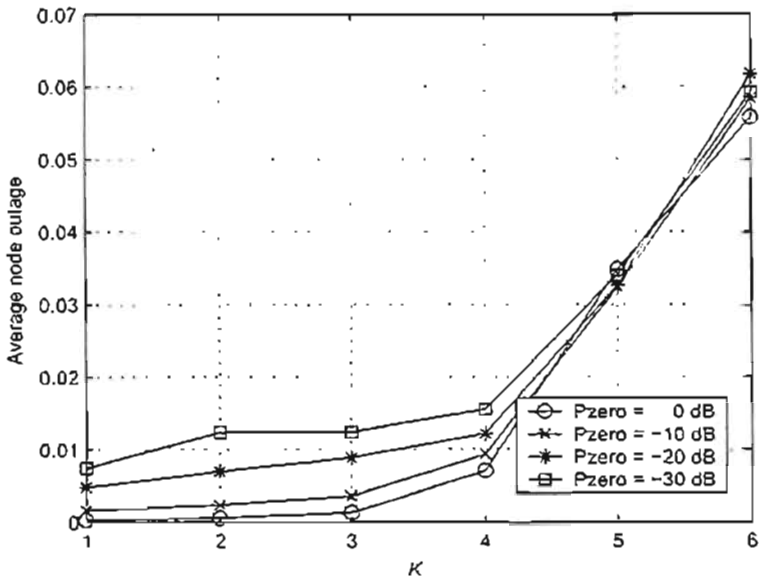

Figure 4.28: Effect of initial transmit power, $p(0)$, on average node outage

surmised that with a WM $x : y$ as $\frac{x}{y} \rightarrow \infty$ the behaviour will mimic the *satisfy all links* algorithm.

- Similarly, as $\frac{y}{x} \rightarrow \infty$ the behaviour will tend towards the *satisfy best link only* transmit power adaptation scheme.

- WM 1:2 power adaptation routine, when used in conjunction with the *SIR from greatest K* controlling connectivity criteria, produces the maximum network connectivity when a K value of five is used

- If the average transmit power is more important, a slightly lower network connectivity can be achieved if WM 1:1 is used with $K = 2$.

- The average node transmission power can be decreased by using an interference window length of greater than two samples, however there is no benefit to increasing the length beyond this

- The greater than initial transmit power the longer the algorithm takes to converge,

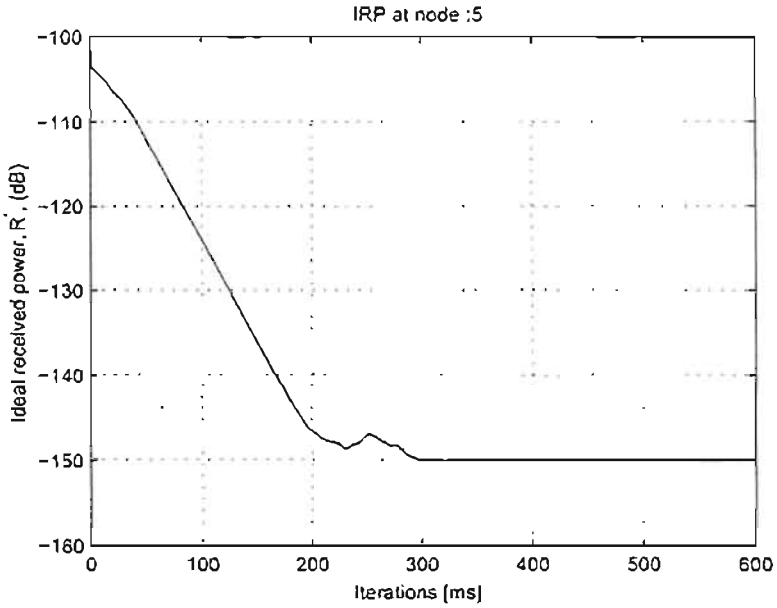

Figure 4.29: Ideal received power temporal adaptation, no shadow fading or mobility

and using a smaller initial value can also lead to slight gains in reducing the average transmission power

- Using the maximum distance connectivity method, the best combination of parameters is to use a WM 1:2 power adaptation method with a maximum internode distance of 250 m.
- The maximum average connectivity achieved from all combinations appears low, at around 35 %, however the outage in most circumstances was below the 1 % specified by the QoS parameter

In an ad hoc network the connectivity should be high, ideally 100 % to ensure point-to-point communication between any node pair, and some other measures need to be taken to ensure this. If the controlling connectivity matrix (which had full connectivity) was present, then the transmit power adaption portion of the algorithm could be tested. This is investigated in chapter 5.

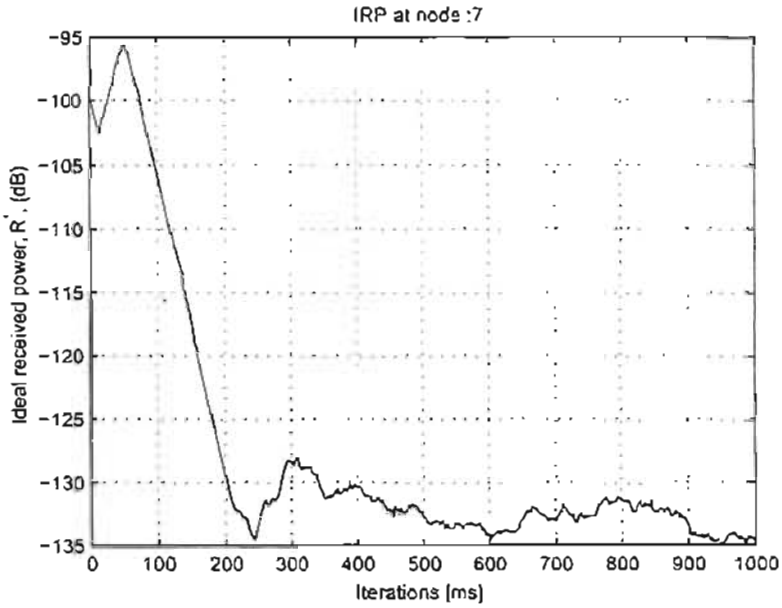

Figure 4.30: Ideal received power temporal adaptation

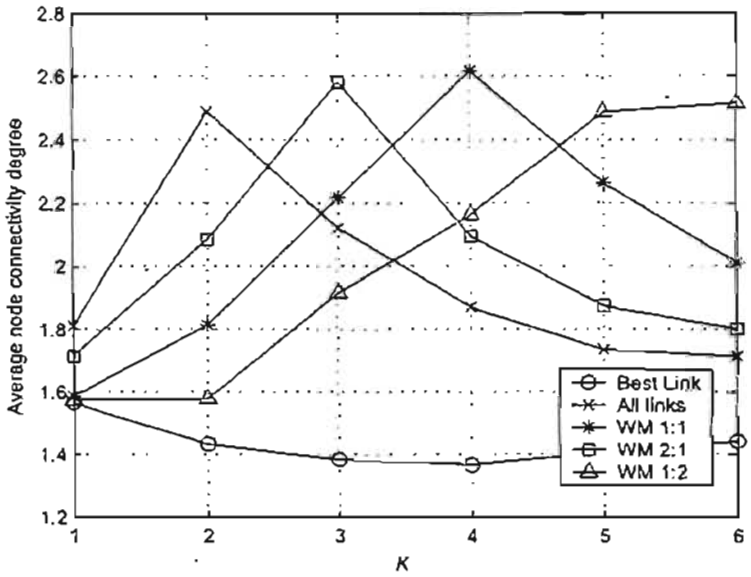

Figure 4.31: Average node degree connectivity, WM 1:1, $L = 2$

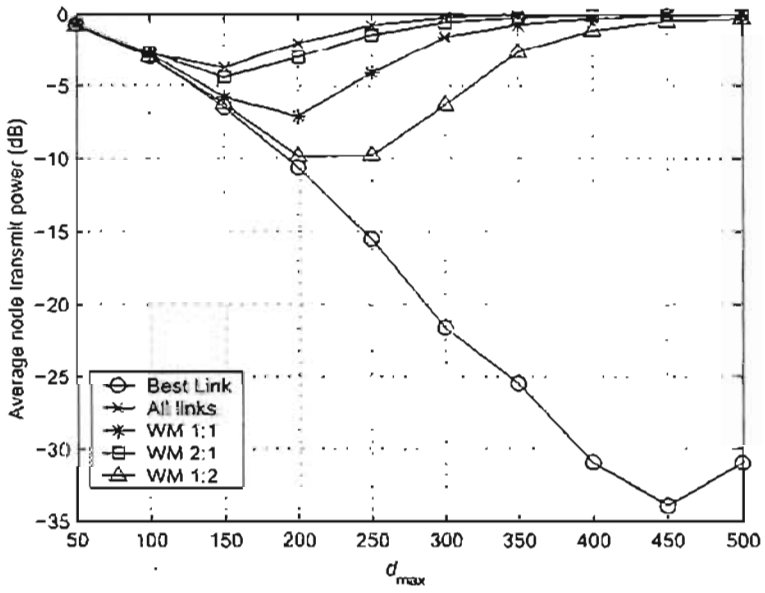

Figure 4.32: Effect of $d_{\max}$ on average node transmit power, shadow fading and mobility disabled

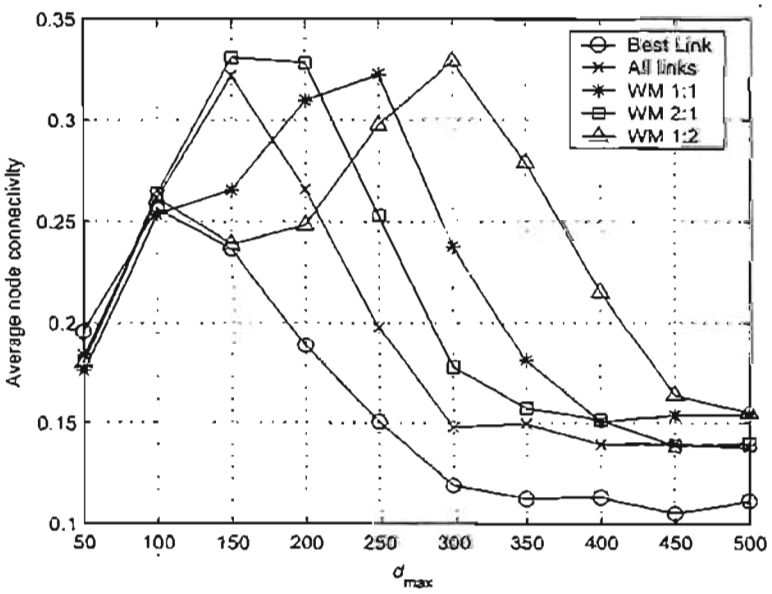

Figure 4.33: Effect of $d_{\max}$ on average node connectivity, shadow fading and mobility disabled

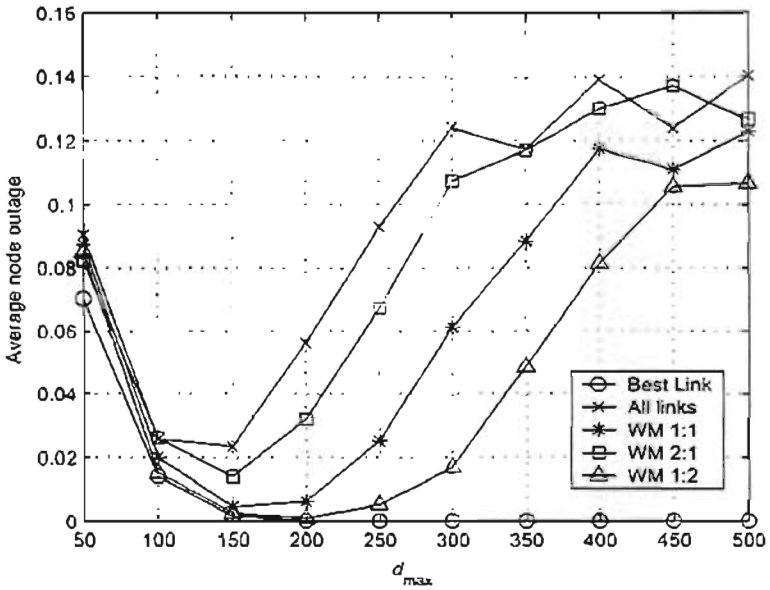

Figure 4.34: Effect of $d_{\max}$ on average node outage, shadow fading and mobility disabled

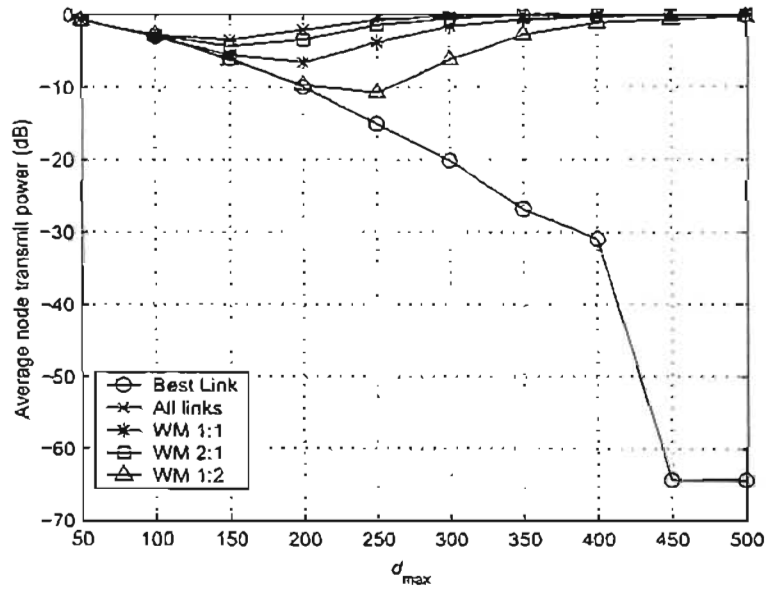

Figure 4.35: Effect of $d_{\max}$ on average node transmit power, shadow fading and mobility enabled

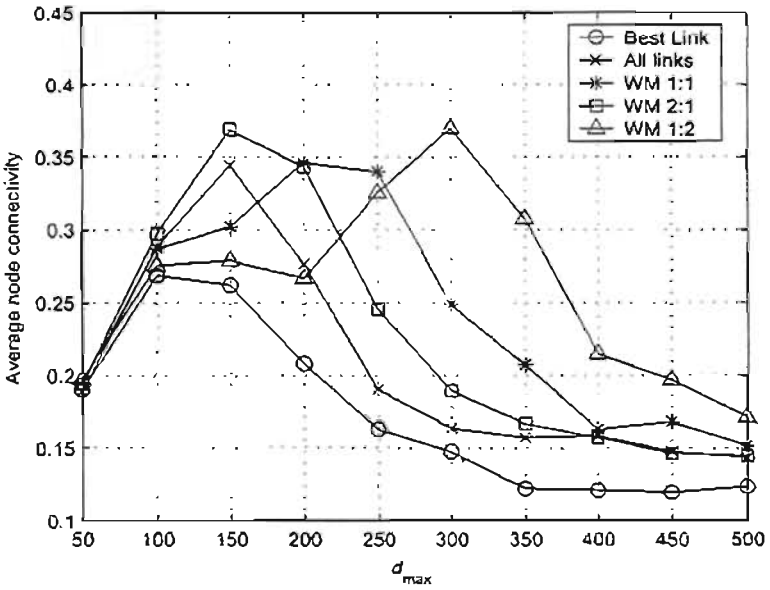

Figure 4.36: Effect of $d_{\max}$ on average node connectivity, shadow fading and mobility enabled

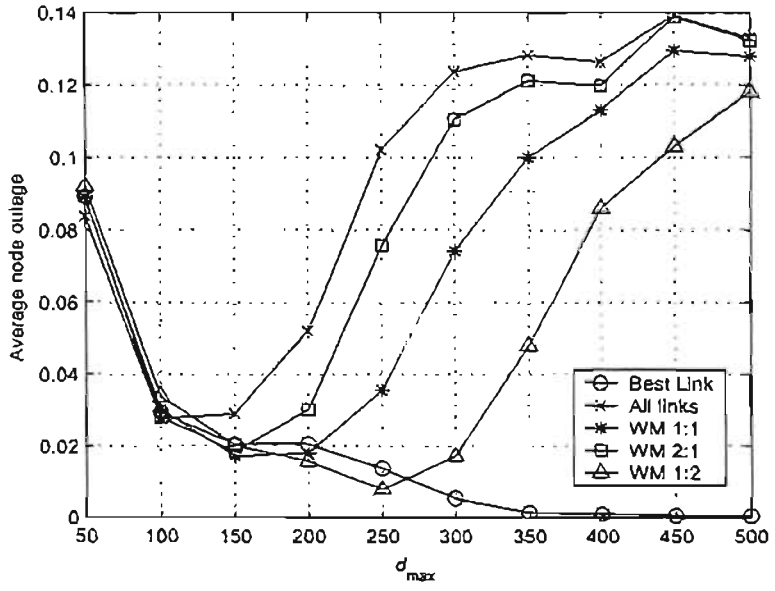

Figure 4.37: Effect of $d_{\max}$ on average node outage, shadow fading and mobility disabled

Chapter 5

Connectivity and convergence analysis

5.1 Introduction

One of the most basic goals of a power control algorithm is to regulate the transmission power of a mobile terminal so that the quality of the signal received at the intended destination is acceptable for reliable transmission. Usually this requirement translates directly into the received SIR being above some pre-specified target value. Due to time varying channel gains and the changing transmit powers of all the other nodes in the network, a power control algorithm will continuously operate, striving to maintain an acceptable connection. In a traditional cellular system, the mobile needs only to maintain a connection with its corresponding base station. If every mobile (and base station) satisfies this single link condition, then the network is guaranteed to be strongly connected, i.e. point-to-point communication between any node pair is possible. The situation in an ad hoc network is rather different however. In order to ensure full network connectivity a node may have to maintain an acceptable connection at more than one target node. So far very little research has been done on analyzing the impact that connectivity issues in an ad hoc network have on transmit power. This chapter attempts to gain some initial insight into the existence of a feasible power solution given

an arbitrary connectivity. Using an example network with pre-specified connectivity, the ability of the various transmit power adaptation schemes introduced in chapter 3.4 to evolve to the final (desired) network is presented.

5.2 Interference functions

5.2.1 Overview

In wireless communication systems the power control problem can be reduced to finding a system transmit power vector, p, that achieves the SIR target of each node. This SIR requirement can be modelled as an *interference function*, I(p), which is dependent on all the other users' transmit powers. The SIR target of node m will be satisfied if m transmits with a power greater than that defined by the interference function

$$p_m \geqslant I_m(\mathbf{p}) \tag{5.1}$$

The system transmit power vector, p, is given by:

$$\mathbf{p} = (p_1, p_2, \ldots, p_N)^T \tag{5.2}$$

If p satisfies the interference function for every index, then the solution is said to be feasible.

Under the assumption that the other users do not change their transmit powers, the output power of node i in the next power control iteration is given by:

$$p_m(n+1) = I_m(\mathbf{p}(n)) \tag{5.3}$$

This sets the transmit power of the node to exactly what is required to satisfy the SIR requirements at the target. If the other nodes were to not change their power and all the path gains were to remain constant then this would be the final solution, as the interference function for node m would not change. However, as this algorithm is run at all the nodes any change in node m's transmit power would affect the interference

function of all the other nodes, so they would also adapt their transmit powers. This, coupled with the stochastic nature of the path gains, ensures the algorithm will operate continuously.

Given an traditional cellular system with fixed base station assignment (possibly specified by base station pilot signals or other extrinsic means), the SIR target of node m at base station f, γ_{fm}, is given by:

$$\gamma_{fm}(\mathbf{p}) \leqslant \frac{p_m \cdot g_{fm}}{\sum\limits_{k \neq m}^{N} p_k \cdot g_{fk} + \eta_f} \tag{5.4}$$

Defining μ_{fm} as:

$$\mu_{fm}(\mathbf{p}) = \frac{g_{fm}}{\sum\limits_{k \neq m}^{N} p_k \cdot g_{fk} + \eta_f} \tag{5.5}$$

and having node m assigned to base station a_m, the SIR target power requirement can be written:

$$p_m \geqslant \frac{\gamma_m}{\mu_{a_m m}(\mathbf{p})} \tag{5.6}$$

which gives the the *interference function* for node m under a fixed assignment.

$$I_m^{\mathrm{FA}}(\mathbf{p}) = \frac{\gamma_m}{\mu_{a_m m}(\mathbf{p})} \tag{5.7}$$

5.2.2 Standard interference functions

A technique first proposed by Yates [23] is used to evaluate the convergence properties of an algorithm that uses the iteration defined by (5.3). A special class of interference functions are termed *standard interference functions* if they satisfy the following requirements:

- Positivity
- Monotonicity

- Scalability

The positivity property states that the transmit power of every node must be greater than zero:

$$\text{positivity}: \ \mathbf{I}(\mathbf{p}) > 0 \tag{5.8}$$

This property is necessary to overcome receiver noise, and to stop the all zero power vector which is feasible in a completely impractical way. The vector inequality is taken over every component.

Given two arbitrary power vectors, $\mathbf{p}$ and $\mathbf{p}'$, with $\mathbf{p} \geqslant \mathbf{p}'$, the monotonicity property is satisfied if the interference function using system transmit power vector $\mathbf{p}$ is greater than when using $\mathbf{p}'$

$$\text{monotonicity}: \ \text{if } \mathbf{p} \geqslant \mathbf{p}', \ \text{then } \mathbf{I}(\mathbf{p}) \geqslant \mathbf{I}(\mathbf{p}') \tag{5.9}$$

The *scalability* criteria is based on the premise that if under a power vector $\mathbf{p}$ a node i has achieved its target SIR, then if all transmit powers are uniformly scaled i will have a greater than acceptable connection with its target. As the receiver noise, η, is not influenced by $\mathbf{p}$, any increase in transmit power will reduce the effect that the noise has on the SIR.

$$\text{scalability}: \ \text{for all } \alpha > 1 \ , \ \alpha \cdot \mathbf{I}(\mathbf{p}) > \mathbf{I}(\alpha \cdot \mathbf{p}) \tag{5.10}$$

5.2.3 Proof of synchronous standard power control algorithm

If the interference function is standard, then the transmit power adaptation iteration of (5.3) is termed a *standard power control algorithm*. Beginning with a system transmit power vector, $\mathbf{p}$, iterating the standard power control algorithm n times produces the vector $\mathbf{I}^n(\mathbf{p})$. Assuming that the interference function, $\mathbf{I}(\mathbf{p})$, is feasible, the convergence properties of the *standard power control algorithm* are presented.

Theorem 1 *If a fixed point of a standard power control algorithm exists, the fixed point is unique*

Proof: Theorem 1 Given that $\mathbf{p}$ and $\mathbf{p}'$ are different fixed points, then since $\mathbf{I}(\mathbf{p}) > 0$ (positivity property of standard interference function) for all $\mathbf{p}$, there must be $p_i > 0$ and $p_i' > 0$ for all i. Without loss of generality it can be assumed that there exists an i such that $p_i < p_i'$, and hence an $\alpha > 1$ exists such that $\alpha \cdot \mathbf{p} \geqslant \mathbf{p}'$. Also, for some i, $\alpha \cdot p_i = p_i'$. Applying the monotonicity and scalability properties implies

$$p_i' = I_i(\mathbf{p}') \leqslant I_i(\alpha \cdot \mathbf{p}) < \alpha \cdot I_i(\mathbf{p}) = \alpha \cdot p_i \tag{5.11}$$

However, since $p_i' = \alpha \cdot p_i$ this is a contradiction, and this implies the fixed point must be unique. □

Lemma 1 *If a feasible power vector* $\mathbf{p}$ *exists, then* $\mathbf{I}^n(\mathbf{p})$ *is a monotone decreasing sequence of feasible power vectors that converges to the fixed point,* $\mathbf{p}^*$*, which is unique.*

Proof: Lemma 1 Assume the initial transmit power vector (time $n = 0$) is $\mathbf{p}(0) = \mathbf{p}$, and $\mathbf{p}(n) = I^n(\mathbf{p})$. The feasibility of $\mathbf{p}$ leads to $\mathbf{p}(1) \leqslant \mathbf{p}(0) = \mathbf{p}$. Suppose $\mathbf{p}(n) \leqslant \mathbf{p}(n-1)$, then by the monotonicity property $\mathbf{I}(\mathbf{p}(n)) \leqslant \mathbf{I}(\mathbf{p}(n-1))$. Then

$$\mathbf{p}(n) \geqslant \mathbf{I}(\mathbf{p}(n)) = \mathbf{p}(n+1) \tag{5.12}$$

so $\mathbf{p}(n)$ is a monotone decreasing sequence of feasible power vectors, and since $\mathbf{p}(n)$ is bounded from below by the zero vector, Theorem 1 implies that the sequence generated by $\mathbf{I}^n(\mathbf{p})$ converges to $\mathbf{p}^*$, the unique fixed point. □

Lemma 1 implies that for any initial (feasible) starting vector $\mathbf{p}$, the fixed point $\mathbf{p}^*$ is the solution to the interference function definition, $\mathbf{p} \geqslant \mathbf{I}(\mathbf{p})$. Also, $\mathbf{p} \geqslant \mathbf{p}^*$ and so the solution uses the minimum transmission power.

Lemma 2 *Given a feasible standard interference function,* $\mathbf{I}(\mathbf{p})$*, then starting from the all zero power vector,* $\mathbf{z}$*, the standard power control algorithm produces a monotone increasing sequence of power vectors that converges to the unique fixed point* $\mathbf{p}^*$*.*

Proof: Lemma 2 Clearly $\mathbf{z}(0) < \mathbf{p}^*$, and $\mathbf{z}(1) = \mathbf{I}(\mathbf{z}(0)) = \mathbf{I}(\mathbf{z}) \geqslant \mathbf{z}$. If $\mathbf{z} \leqslant \mathbf{z}(1) \leqslant \ldots \leqslant \mathbf{z}(n) \leqslant \mathbf{p}^*$ and from the monotonicity property

$$\mathbf{p}^* = \mathbf{I}(\mathbf{p}^*) \geqslant \mathbf{I}(\mathbf{z}(n)) \geqslant \mathbf{I}(\mathbf{z}(n-1)) = \mathbf{z}(n) \tag{5.13}$$

So, $\mathbf{p}^* \geqslant \mathbf{z}(n+1) \geqslant \mathbf{z}(n)$. Thus the sequence of $\mathbf{z}(n)$ is nondecreasing and upper bounded by $\mathbf{p}^*$. Then, from Theorem 1, $\mathbf{z}(n)$ has to converge to the fixed point $\mathbf{p}^*$. □

Theorem 2 *Given a feasible standard interference function,* $\mathbf{I}(\mathbf{p})$*, then for any initial transmit power vector* $\mathbf{p}$*, the standard power control algorithm converges to* $\mathbf{p}^*$*, a unique fixed point.*

Proof: Theorem 2 If the standard interference function is feasible, then a unique fixed point $\mathbf{p}^*$ exists. This unique point has to be positive for every i, $p_i^* > 0$, and for any initial $\mathbf{p}$ there exists an $\alpha > 1$ such that $\alpha \cdot \mathbf{p}^* \geqslant \mathbf{p}$. Due to the scalability property the existence of $\alpha \cdot \mathbf{p}^*$ is guaranteed to be feasible. Then, $\mathbf{z} \leqslant \mathbf{p} \leqslant \alpha \cdot \mathbf{p}^*$ and due to monotonicity:

$$\mathbf{I}^n(\mathbf{z}) \leqslant \mathbf{I}^n(\mathbf{p}) \leqslant \mathbf{I}^n(\alpha \cdot \mathbf{p}^*) \tag{5.14}$$

where $\mathbf{z}(n) = \mathbf{I}^n(\mathbf{z})$. From lemmas 1 and 2,

$$\lim_{n \to \infty} \mathbf{I}^n(\alpha \cdot \mathbf{p}^*) = \lim_{n \to \infty} \mathbf{p}^* = \mathbf{I}^n(\mathbf{z}) = \mathbf{p}^* \tag{5.15}$$

and thus for any $\mathbf{p}$ the standard power control algorithm produces a sequence of power vectors that converges to the unique fixed point $\mathbf{p}^*$. □

In the preceding proof, it is assumed that all the nodes update their powers simultaneously, however an asynchronous extension to the standard power control algorithm has also been proven [23].

5.3 Ad hoc networks

When considering an ad hoc network it is useful to first look at a simple example, such as that depicted in Fig. 5.1 where 5 nodes are randomly placed, and the connectivity has

already been defined. This predetermined connectivity may have been obtained from routing information or some external input. Once the desired connectivity is defined it is possible to set up a system of equations describing the network behavior. Specifically, for each node that node m is connected to, an SIR inequality can be obtained.

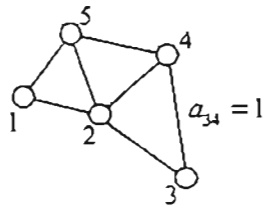

Figure 5.1: Sample ad hoc network with pre-defined connectivity

For example, the SIR at node 1 as a result of node 2, γ_{12}, is given by:

$$\gamma_{12} = \frac{p_2 \cdot g_{12}}{\sum_{k \neq 1,2}^{5} p_k \cdot g_{1k} + \eta_1} \tag{5.16}$$

By introducing a minimum SIR target, γ^*, and replacing the equality with an inequality the minimum transmit power for node 2 if it is to successfully communicate with node 1 is given by:

$$\gamma^* \leqslant \frac{p_2 \cdot g_{12}}{\sum_{k \neq 1,2}^{5} p_k \cdot g_{1k} + \eta_1} \tag{5.17}$$

Rearranging and solving for p_2:

$$p_2 \geqslant \frac{\gamma^*}{g_{12}} \cdot \left(\sum_{k \neq 1,2}^{5} p_k \cdot g_{1k} + \eta_1 \right) \tag{5.18}$$

Similar equations can be written for every node that node 2 is communicating with. Thus the minimum power that node 2 needs to transmit at in order for the signal to be successfully received at node 3 is given by:

$$p_2 \geqslant \frac{\gamma^*}{g_{32}} \cdot \left(\sum_{k \neq 3,2}^{5} p_k \cdot g_{3k} + \eta_3 \right) \tag{5.19}$$

And similarly for nodes 4 and 5:

$$p_2 \geqslant \frac{\gamma^*}{g_{42}} \cdot \left(\sum_{k \neq 4,2}^{5} p_k \cdot g_{4k} + \eta_4 \right) \tag{5.20}$$

$$p_2 \geqslant \frac{\gamma^*}{g_{52}} \cdot \left(\sum_{k \neq 5,2}^{5} p_k \cdot g_{5k} + \eta_5 \right) \tag{5.21}$$

Introducing the connectivity matrix, $\mathbf{A}$, where each element $a_{ij} = 1$ if the SIR target at node i is to be satisfied by j, and $a_{ij} = 0$ otherwise. For the network given in Fig. 5.1 the defined connectivity matrix is given by

$$\mathbf{A} = [a_{ij}] = \begin{bmatrix} 0 & 1 & 0 & 0 & 1 \\ 1 & 0 & 1 & 1 & 1 \\ 0 & 1 & 0 & 1 & 0 \\ 0 & 1 & 1 & 0 & 1 \\ 1 & 1 & 0 & 1 & 0 \end{bmatrix} \tag{5.22}$$

The transmit power requirements of node 2 ensuring that the SIR target at node n are satisfied can be re-written as:

$$p_2^{(n)} \geqslant \frac{a_{n2} \cdot \gamma^*}{g_{n2}} \cdot \left(\sum_{k \neq n,2}^{5} p_k \cdot g_{nk} + \eta_n \right), \text{for all } 1 < n < 5 \tag{5.23}$$

The connectivity element, a_{ij}, acts as a boolean switch, indicating whether that particular constraint is to be met or not. If $a_{ij} = 1$ then node j needs to satisfy the SIR target at node i. The connectivity matrix always has zeros down diagonal, i.e. $a_{ii} = 0$. To determine the transmit power of the node, the minimum transmit power which satisfies all the connectivity constraints should be used:

$$p_2 = \max_n \left[\frac{a_{n2} \cdot \gamma^*}{g_{n2}} \cdot \left(\sum_{k \neq n,2}^{5} p_k \cdot g_{nk} + \eta_n \right) \right], \text{for all } 1 < n < 5 \tag{5.24}$$

More generally, the transmit power of any node, m, in a network of N nodes is given by:

$$p_m = \max_{n \in \mathcal{N}} \left[\frac{a_{nm} \cdot \gamma^*}{g_{nm}} \cdot \left(\sum_{k \neq n,m}^{N} p_k \cdot g_{nk} + \eta_n \right) \right], \text{for all } 1 < m < N \tag{5.25}$$

The set, $\mathcal{N}$, from which a node can choose its constraints is given in this instance by all the other nodes in the network, however under certain circumstances it may be necessary to limit this set.

Looking more closely at (5.23), it can be expressed as

$$p_m^{(n)} \geqslant \frac{a_{nm} \cdot \gamma^*}{g_{nm}} \cdot \left(\sum_{k \neq n}^{N} p_k \cdot g_{nk} - p_m \cdot g_{nm} + \eta_n \right), \text{for all } 1 < m < N \tag{5.26}$$

$$p_m^{(n)} \geqslant \frac{a_{nm} \cdot \gamma^*}{g_{nm}} \cdot \left(\sum_{k \neq n}^{N} p_k \cdot g_{nk} + \eta_n \right) - \frac{a_{nm} \cdot \gamma^*}{g_{nm}} \cdot (p_m \cdot g_{nm}), \text{for all } 1 < m < N \tag{5.27}$$

$$p_m^{(n)} \cdot (1 + a_{nm} \cdot \gamma^*) \geqslant \frac{a_{nm} \cdot \gamma^*}{g_{nm}} \cdot \left(\sum_{k \neq n}^{N} p_k \cdot g_{nk} + \eta_n \right), \text{for all } 1 < m < N \tag{5.28}$$

$$p_m^{(n)} \geqslant \frac{a_{nm} \cdot \gamma^* \cdot \left(\sum_{k \neq n}^{N} p_k \cdot g_{nk} + \eta_n \right)}{g_{nm} \cdot (1 + a_{nm} \cdot \gamma^*)}, \text{for all } 1 < n < N \tag{5.29}$$

$$p_m^{(n)} \geqslant \frac{a_{nm} \cdot \gamma^* \cdot R_n}{g_{nm} \cdot (1 + a_{nm} \cdot \gamma^*)}, \text{for all } 1 < n < N \tag{5.30}$$

where R_n term is the total received power at node n.

If node m is to satisfy the SIR targets on all its defined links, then the minimum transmit power for the node is given by:

$$p_m = \max_{n \in \mathcal{N}} \left[\frac{a_{nm} \cdot \gamma^* \cdot R_n}{g_{nm} \cdot (1 + a_{nm} \cdot \gamma^*)} \right], \text{for all } 1 < m < N \tag{5.31}$$

From (5.31) it is possible to define the interference function for any node, j, in the system.

$$I_m(\mathbf{p}) = \max_{n \in \mathcal{N}} \left[\frac{a_{nm} \cdot \gamma^* \cdot R_n}{g_{nm} \cdot (1 + a_{nm} \cdot \gamma^*)} \right], \text{for all } 1 < m < N \tag{5.32}$$

If the power control iterations given by (5.32) can be shown to be *standard*, then convergence to the unique optimal operating point, $\mathbf{p}^*$, is assured assuming a solution exists.

The positivity criteria will always be satisfied, as all of the quantities in the RHS of (5.32) are real, positive values, and only when a node, m, is not connected to any other nodes (all $a_{im} = 0$), or the SIR target is set to zero will the interference function be equal to zero. These two situations are not meaningful, so positivity is assured. The non-zero, positive, receiver noise will also always ensure that $I_m(\mathbf{p}) > 0$

Given two system transmit power vectors, $\mathbf{p}$ and $\mathbf{p}'$, with $\mathbf{p} \geqslant \mathbf{p}'$ for at least one element (excluding node m), the total received power at node m will be greater under vector $\mathbf{p}$ than $\mathbf{p}'$, and so consequently the interference functions will satisfy the *monotonicity* property, $I_m(\mathbf{p}) \geqslant I_m(\mathbf{p}')$

For any $\alpha > 1$, testing the scalability property, substitution into (5.32) and expanding R_n gives:

$$\alpha \cdot I_m(\mathbf{p}) = \max_{n \in \mathcal{N}} \left[\frac{\alpha \cdot a_{nm} \cdot \gamma^* \cdot \sum_{k \neq n}^{N} (p_k \cdot g_{nk}) + \alpha \cdot a_{nm} \cdot \eta_n}{g_{nm} \cdot (1 + a_{nm} \cdot \gamma^*)} \right], \text{for all } 1 < m < N \tag{5.33}$$

Using power vector $\alpha \cdot \mathbf{p}$, substituting into (5.32) results in:

$$I_m(\alpha \cdot \mathbf{p}) = \max_{n \in \mathcal{N}} \left[\frac{\alpha \cdot a_{nm} \cdot \gamma^* \cdot \sum_{k \neq n}^{N} (p_k \cdot g_{nk}) + a_{nm} \cdot \eta_n}{g_{nm} \cdot (1 + a_{nm} \cdot \gamma^*)} \right], \text{for all } 1 < m < N \tag{5.34}$$

When using this new scaled power vector the receiver noise is not affected by the increase in transmit power, so the relationship $\alpha \cdot I(\mathbf{p}) > I(\alpha \cdot \mathbf{p})$ holds. A result of this is that if a node has an acceptable connection under $\mathbf{p}$, then if all the nodes' powers are scaled up uniformly the node will have a better connection than before. Thus the *scalability* criteria is also satisfied and the interference function defined by (5.32) is

proven to be *standard*.

Given a fixed assignment A matrix where each node needs to satisfy an SIR target at only *one* other node, (5.32) reduces to a scenario analogous to a cellular system:

$$p_m \geqslant \frac{\gamma^* \cdot R_n}{g_{a_m m} \cdot (1+\gamma^*)}, \text{for all } 1 < m < N \tag{5.35}$$

where a_m indicates the node to which m is communicating. Cellular systems with similar defining equations have been widely studied, and in vector notation the system power equations can be expressed as:

$$\mathbf{p} \geqslant \mathbf{H}\mathbf{p} + \eta \tag{5.36}$$

where $\mathbf{H}$ and $\mathbf{s}$ represent the normalized gain matrix and the normalized noise vector respectively.

$$\mathbf{H} = [h_{ij}] = \begin{cases} \frac{\gamma^* \cdot g_{a_i j}}{g_{a_i i}} & \text{if } j \neq i, a_i \\ 0 & \text{otherwise} \end{cases} \tag{5.37}$$

$$\eta = [s_i] = \frac{\gamma^* \cdot \eta_{a_i}}{g_{a_i i}} \tag{5.38}$$

If the system is feasible, the solution for $\mathbf{p}$ can be derived from (5.36). The minimum power solution, $\mathbf{p}^*$, is obtained by replacing the inequality with an equality, and solving for $\mathbf{p}$:

$$\mathbf{p}^* = \mathbf{H}\mathbf{p}^* + \eta \tag{5.39}$$

$$\mathbf{p}^* (\mathbf{I} - \mathbf{H}) = \eta \tag{5.40}$$

$$\mathbf{p}^* = (\mathbf{I} - \mathbf{H})^{-1} \eta \tag{5.41}$$

where $\mathbf{I}$ represents the N by N identity matrix.

The normalized gain matrix, $\mathbf{H}$, is nonnegative in that every element of $\mathbf{H} \geqslant 0$. The $\mathbf{H}$ matrix is also primitive as $\mathbf{H}^2 > 0$, and these two conditions imply that $\mathbf{H}$ is irreducible. From the theory of Perron and Frobenius in matrix theory, [42], a nonnegative and

irreducible matrix has an eigenvalue known as the Perron-Frobenius eigenvalue, or more commonly the spectral radius, ρ_H, which is the maximum eigenvalue of $\mathbf{H}$.

Given a system of equations, $\mathbf{p} = \mathbf{H}\mathbf{p} + \eta$, and the fact that $\mathbf{H}$ is a square, nonnegative, irreducible matrix, a nonnegative solution for $\mathbf{p}$ exists only if $\rho_H < 1$. If the constant SIR target, γ^*, is factored out of $\mathbf{H}$, leaving a new matrix, $\bar{\mathbf{H}}$, with $\mathbf{H} = \gamma^* \cdot \bar{\mathbf{H}}$, then the feasibility of the system (nonnegative power vector $\mathbf{p}^*$) can be derived from (5.39) and the Perron and Frobenius condition for the spectral radius of $\mathbf{H}$:

$$\rho_H = \rho(\mathbf{H}) = \rho\left(\gamma^* \cdot \bar{\mathbf{H}}\right) \tag{5.42}$$

$$\rho\left(\gamma^* \cdot \bar{\mathbf{H}}\right) < 1 \tag{5.43}$$

$$\gamma^* < \frac{1}{\rho\left(\bar{\mathbf{H}}\right)} \tag{5.44}$$

Existence of a feasible solution for $\mathbf{p}^*$ is assured when the inverse of the maximum eigenvalue of the $\bar{\mathbf{H}}$ matrix is less than the desired target SIR. If the *standard power control algorithm* is used then convergence to an optimal power vector is assured.

Concentrating on an ad hoc network with arbitrary connectivity matrix, the transmission power of node m is given by (5.25), repeated here for convenience:

$$p_m = \max_{n \in \mathcal{N}} \left[\frac{a_{nm} \cdot \gamma^*}{g_{nm}} \cdot \left(\sum_{k \neq n,m}^{N} p_k \cdot g_{nk} + \eta_n \right) \right], \text{for all } 1 < m < N$$

Separating the total received power into received signal and noise components:

$$p_m = \max_{n \in \mathcal{N}} \left[\frac{a_{nm} \cdot \gamma^*}{g_{nm}} \cdot \left(\sum_{k \neq n,m}^{N} p_k \cdot g_{nk} \right) + \frac{a_{nm} \cdot \gamma^* \cdot \eta_n}{g_{nm}} \right], \text{for all } 1 < m < N \tag{5.45}$$

In pseudo-vector form, the transmit power of node m is given by $p_m = \mathbf{h}_m \mathbf{p} + \eta_m$, which consists of a normalized path row vector term, $\mathbf{h}_m$, and a normalized noise term, η_m. The noise term is given by:

$$\eta_m = \frac{\gamma^* \cdot \eta_n}{g_{nm}} \tag{5.46}$$

where the index n is the node that is used in the maximization in 5.45. Node n_m is the transmit destination of node m which maximizes the power requirements.

$$n_m = \arg\max_{n \in \mathcal{N}} \left[\frac{a_{nm} \cdot \gamma^*}{g_{nm}} \cdot \left(\sum_{k \neq n,m}^{N} p_k \cdot g_{nk} \right) + \frac{a_{nm} \cdot \gamma^* \cdot \eta_n}{g_{nm}} \right], \text{for all } 1 < m < N \tag{5.47}$$

The n vector has element n_i indicating which target node dominates the transmit power equations for node i.

The $\mathbf{h}_m$ row vector is the particular set of normalized path gains that (along with the noise term) leads to the maximization of (5.45).

$$\mathrm{h}_m = [h_j] = \begin{cases} \frac{\gamma^* \cdot g_{nj}}{g_{nm}} & \text{if } j \neq m, n \\ 0 & \text{otherwise} \end{cases} \tag{5.48}$$

Taken over all the nodes, the system power vector $\mathrm{p} = \mathbf{H}\mathrm{p} + \eta$ can be solved in the same manner as described earlier, with $\mathbf{H}$ and η as:

$$\mathbf{H} = [h_{ij}] = \begin{cases} \frac{\gamma^* \cdot g_{nj}}{g_{ni}} & \text{if } j \neq i, n \\ 0 & \text{otherwise} \end{cases} \tag{5.49}$$

$$\eta = [\eta_i] = \frac{\gamma^* \cdot \eta_n}{g_{ni}} \tag{5.50}$$

where once again the n index indicates which is the critical equation requiring the greatest transmit power.

Conditions for the existence of a feasible power vector are as before, except the definition of the normalized path gain matrix, $\mathbf{H}$, and the normalized noise vector, η, are as given by (5.49) and (5.50) respectively, however as the n index, given by (5.47), is dependent on the system transmit power it is not immediately apparent how this could be analytically solved. However, through the use of the custom designed simulation tool $\mathbf{H}$ and η can be calculated and then used to determine an optimum minimum power solution given by:

$$\mathrm{p}^* = (\mathrm{I} - \mathbf{H})^{-1} \eta \tag{5.51}$$

5.4 Connectivity analysis

Using the pre-defined strongly connected network of Fig. 5.2, the various transmit power adaptation algorithms introduced in chapter 3.4 are tested for their ability to achieve the desired input network.

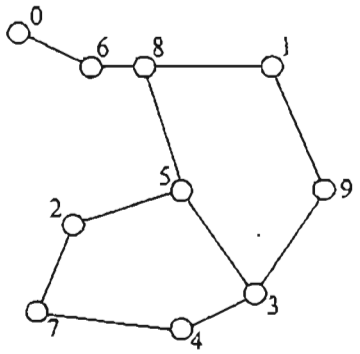

Figure 5.2: Sample ad hoc network with pre-defined connectivity (#1)

Two separate algorithms were tested with the networks defined in Figures 5.2 and 5.9. Using the pre-defined connectivity, the various transmit power adaptation algorithms defined in Chapter 3 are tested for their ability to converge to the desired network topology.

5.4.1 Satisfy best link only

Initially, a stationary network was simulated, and the shadow fading term of the loss model was constant at 0 dB. Using the *satisfy best link only* transmit power adaptation scheme resulted in the algorithm converging to a solution after approximately 290 iterations. This convergence was observed to occur last at node 8. The mean average transmit power of the nodes was 1.6×10^{-6} W, with an average SIR of 0.208 achieved. This indicates that a minimum power solution has been found, but the true network connectivity, $\chi = 0.22$, is low; which based on the results presented in chapter 4 is typical of this power adaptation scheme. The calculated outage was observed to be

zero. The topology after the algorithm has run for 600 iterations is shown in Fig. 5.3, the very fragmented resulting network can be clearly seen. A half-link between nodes i and j mean that j is successfully communicating with i, but not vice-versa. For example, in Fig. 5.3, node 5 is being received[1] at node 2, but the SIR at node 5 from node 2 does not exceed the minimum target SIR. When node mobility and shadow

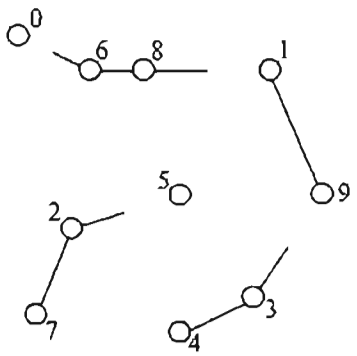

Figure 5.3: Network #1, satisfy best link only

fading were introduced into the model, the outage increased slightly, but was still less than 0.01 % and the mean SIR and average true network connectivity both decreased slightly. All of these are indicative of the time varying channel interfering with the algorithms ability to converge to a solution and to accurately track it after convergence has been attained.

Using this transmit power adaptation scheme, even in conjunction with desired topology information still results in a network that is disconnected and thus not suitable for implementation in an ad hoc network.

5.4.2 Satisfy all links

Given the same desired input topology combined with the *satisfy all links* transmit power adaptation results in much better performance. The network topology resulting is almost identical to the desired input topology, as can be seen from Fig. 5.4. The

[1] SIR is above pre-specified target

only difference is the addition of a few extra links: node 8 is able to communicate directly with node 0, and similarly node 5 is able to reach node 1. Without any

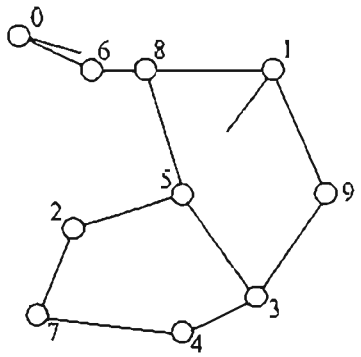

Figure 5.4: Network #1, satisfy all links

SIR cap (described in section 4.7.1 page 85) the mean despread SIR of the system was 18.33 dB, which compared to the ideal of 10 dB is much greater than required, however this is to be expected, as a node will increase its power given any increase command. A minimum power solution is achieved, with an average node transmit power of 2.376×10^{-5} W (-46 dB). Although this is an order of magnitude increase over the *satisfy best link only* method, the network is in a strongly connected state, with point-to-point communication possible between any node pair.

The addition of fast mobility and shadow fading, resulted in a decrease in the average true connectivity, as although the vast majority of simulation runs resulted in a mean transmit power of approximately -50 dB, occasionally a run would converge to a much greater average power, around -15 dB with some of the nodes transmitting at maximum power. Clearly, this large variance is a result of an algorithm with unstable regions, indicative of the positive feedback effect that is inherent with the method whereby a node increases its power if any other nodes demands an increase.

5.4.3 Satisfy arithmetic mean

Using the satisfy arithmetic mean and a 1:1 increase:decrease ratio results in the final topology displayed in Fig. 5.5. The mean connectivity is 46 % and the average transmit power is 3.152×10^{-6} W (-55 dB). Node 5 is able to communicate through a multihop fashion to any other node in the network, but the algorithm fails in terms of maintaining network connectivity.

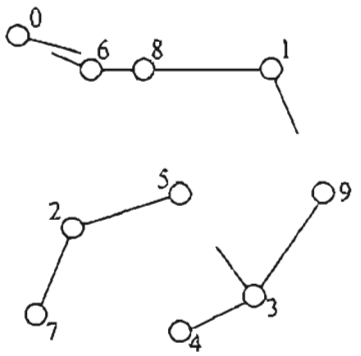

Figure 5.5: Network #1, weighted mean 1:1

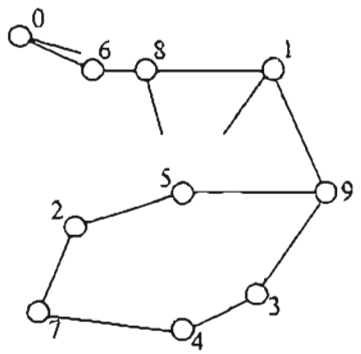

Figure 5.6: Network #1, weighted mean 2:1

Emphasizing the importance of the *increase* commands, the WM 2:1 transmit power adaptation algorithm produces the topology of Fig. 5.6. Clearly the resulting topology is strongly connected, and the average transmit power is 1.08×10^{-5} W (-49.7 dB). The

resulting topology differs slightly from the desired input topology, but with the only negative factor being the absence of the dual link $3 \rightarrow 5$.

5.4.4 Optimum power algorithm

The previous methods all used the single bit controlling connectivity scheme described in chapter 3 in conjunction with the pre-specified connectivity matrix. Based on the algorithm derived in section 5.3 the same connectivity was tested using the new algorithm.

Given the connectivity information the simulation calculates (for every node in the network) the power required to satisfy the desired connectivity. The maximum of these calculates powers is then set as the new transmission power, and the next iteration proceeds similarly. In essence, the simulation does the calculation defined by (5.49) for every node in the network to obtain the normalized gain matrix, $\mathbf{H}$.

By determining the spectral radius of the H matrix, the given topology can be analyzed to determine if a feasible solution exists. Recall the condition for a feasible solution: the spectral radius of the normalized gain matrix must be less than unity: $\rho_H < 1$

The maximum modulus eigenvalue of the network given in Fig. 5.2 was found to be 0.736 which satisfies the feasibility solution. This value is constant over the course of the simulation as their is no change in the path gains.

Using the new optimum power algorithm the transmission power adaptation of the system was noted to be much quicker, achieving convergence in approximately 50 iterations. The average node transmission power was 1.337×10^{-5} W (-48.7 dB), which is approximately the same value as obtained using the single-bit controlling scheme. The final topology obtained is identical to that given in Fig. 5.4.

As the $\mathbf{H}$ matrix and the η vector are both calculable, the ideal minimum power solution, as given by (5.51) can be determined. For the given network, the minimum

power vector was obtained (calculated), and it was observed that the optimal power control algorithm was able to exactly achieve the analytic solution. Fig. 5.7 shows the adaptation of the calculated optimal transmit power and actual adaptation of transmit power for node 5. Convergence to the solution is achieved after approximately 70 iterations, and this value is maintained indefinitely. The ideal transmit power vector remains constant over the course of the simulation except for the first few iterations where it quickly adjusts to the final value. All nodes exhibit the same trends.

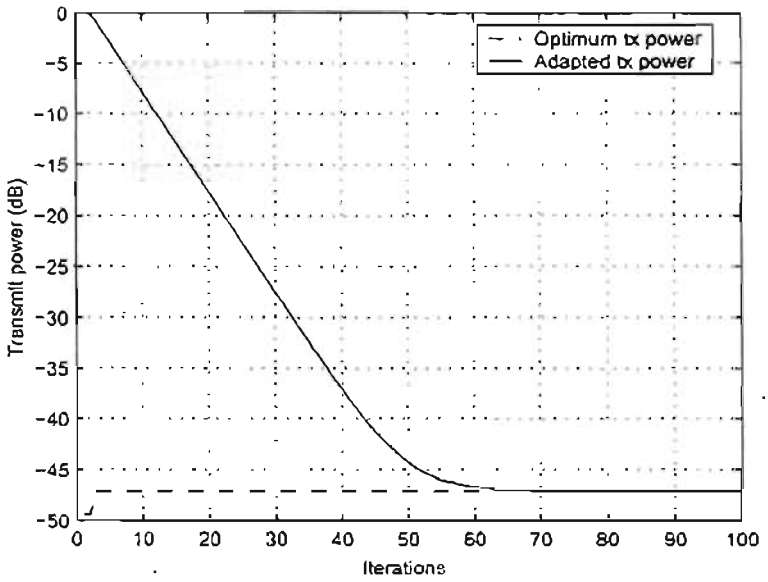

Figure 5.7: Adaptation of optimum and actual transmit power over time for node 5

When shadow fading and mobility are included in the model, the spectral radius is no longer constant, but varies over the course of a simulation run, and typically was in the range of between 0.72 and 0.9. Every simulation iteration the calculated ideal power vector also varies, and exact convergence to this vector is not possible, however the algorithm is able to accurately track the changes, as indicated in Fig. 5.8.

Introducing a slightly more stringent topology, given in Fig. 5.9 leads to vastly different results. The spectral radius was calculated to be 3.061, which would imply that the

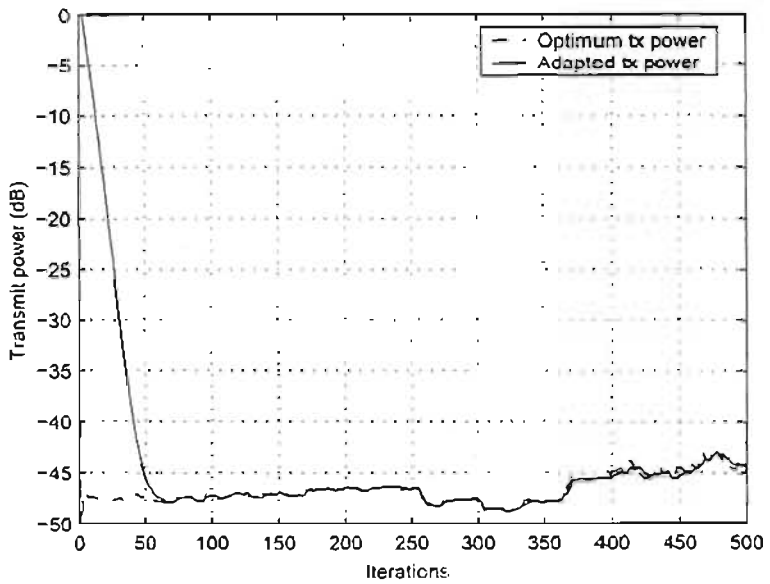

Figure 5.8: Adaptation of optimum and actual transmit power over time for node 5, shadow fading and node mobility included

desired topology is not feasible. The calculated optimum transmit power vector contained components with negative values, indicative of the infeasibility of the proposed topology. Upon running the algorithm, all the nodes start to ramp up their transmission power until the majority of them reach their upper limit, the average power was 0.956 W (-0.195 dB). This resulting topology, depicted in Fig. 5.10, shows the network becomes partitioned.

Although not exhaustively tested, the two sample networks confirm the theory. If the given topology has a feasible solution, i.e. $\rho_H < 1$, then the *standard power control* algorithm given by (5.45) is able to achieve a minimum power solution in finite time. When the system is not feasible the algorithm is quickly able to detect the infeasibility, and then the problem becomes one of ideal topology selection.

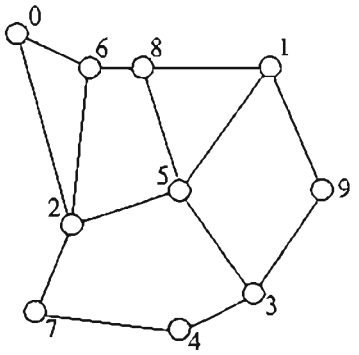

Figure 5.9: Sample ad hoc network with pre-defined connectivity (#2)

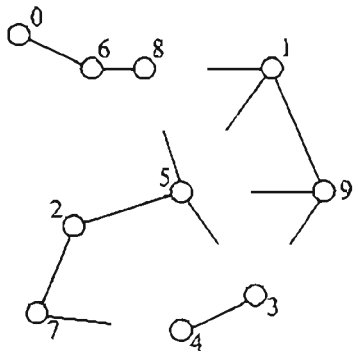

Figure 5.10: Network #2, using optimal transmit power algorithm

5.5 Summary

This chapter introduced the concept of an interference function, a tool that can be used in the analysis of a power control algorithm. It was shown that if a power control algorithm conforms to a class defined as a *standard power control* algorithm then convergence to a minimum power solution is assured.

A model for an ad hoc network where the connectivity is known (pre-specified by some other means) was derived and the conditions for the existence of a feasible solution presented. Using the pre-defined connectivity matrix and the *satisfy all links* transmit power adaptation algorithm, the desired topology was achieved for the test case, however when shadow fading and node mobility were introduced the average node transmit

power was noted to exhibit a large variance between simulation runs, indicating that the algorithm is not stable.

An adaptive power control algorithm for ad hoc networks was proposed, and it was shown to conform to the definition of a *standard power control* algorithm. This algorithm was tested using two sample networks, and where the topology was feasible the algorithm was able to exactly obtain the minimum power solution. In the second case, the desired topology was infeasible, and the algorithm quickly saturated.

Chapter 6

Conclusions

This dissertation focused on power control in ad hoc networks. Power control is a crucial element in any wireless communication system (especially CDMA based), as it allows the shared channel capacity to be maximized while striving for minimum energy solutions. Power control is also useful in extending node lifetime due to the mobile nodes battery limitations. All the results generated were produced with various custom designed software simulation environments.

6.1 Dissertation summary

The introductory chapter discussed the concept of a wireless network, and introduces the notion of an *ad hoc network*. The subject of power control was also elaborated upon, and its necessity in a wireless network explained. Current ad hoc network implementation such as WLAN and Bluetooth were also briefly covered.

Chapter 2 provided a more in depth discussion of power control, explaining some of the pertinent concepts. A literature survey of selected power control techniques used in cellular and ad hoc networks was also presented.

A distributed power control algorithm was described in Chapter 3. The algorithm

consists of two separate components: controlling connectivity criteria, and transmit power adaptation. One of the problems in an ad hoc network is the lack of defined connectivity. It is the aim of power control to establish a strongly connected topology, and the goal of the controlling connectivity criteria is to select which nodes a single node should control. A node will send power control commands to the nodes which it deems suitable, i.e. those that pass the connectivity criteria. Four methods of determining this criteria were proposed: signal received above some predefined threshold, maximum inter-node distance based, control the K nodes received with the greatest power and control the K nodes received with the greatest SIR. The decision as to issue an increase or decrease control signal is based upon an ideal received power (borrowed from a cellular system) which takes into account second order signal statistics to guarantee QoS requirements. The transmit power adaptation portion of the algorithm determines how a node should interpret its received power control commands. The methods proposed include: increase power if any node commands an increase *(satisfy all links)*, decrease power if any node commands a decrease *(satisfy best link only)*, do majority command *(network fair)* and emphasize trend *(weighted mean)*.

The system model for the ad hoc network was presented in Chapter 4. Mathematical models for the total path loss, including distance attenuation and shadow fading were formulated. A method of calculating the ideal received power factor, as described in section 3.4.2, was presented and a general description of the simulation environment given. The results indicate that no combination of connectivity criteria and transmit power adaptation are able to guarantee that the network remains strongly connected. Typically, using the *satisfy best link only* power adaptation method achieves the lowest average transmit power but also has the worst resulting connectivity; rendering it unusable for implementation in an ad hoc network. A connectivity of approximately 35 % is achievable if the *SIR from greatest K* nodes is used in conjunction with the WM 1:1 transmit power adaptation method.

Chapter 5 introduced the concept of an *interference function*, which is a tool devel-

oped to aid in the analysis of a power control algorithm. A special type of interference function known as a *standard* interference function was presented, and the proof of a synchronous system given. A mathematical model for an ad hoc network was developed. Given a desired (known) topology, a distributed iterative algorithm was derived and shown to be *standard*. An optimal power vector was derived, and the conditions given for convergence of the system to the ideal system transmit vector. Using a predefined network with known desired connectivity, the various transmit power adaptation algorithms proposed in chapter 4 were tested for their ability to converge to the proposed topology. The *satisfy best link only* algorithm was shown to lead to large scale partitioning of the network, confirming it as an inappropriate choice for an ad hoc network. The *satisfy all links* power adaptation algorithm was able to achieve the desired topology, but when shadow fading and fast mobility were introduced into the system it was observed that occasionally the transmit power of some of the nodes in the system would saturate at the maximum power, indicative of the unstable positive feedback nature. Using the iterative method proposed, the same network topologies were tested, and it was found that when the system was feasible the algorithm was able to adapt to the calculated optimum power vector. An unfeasible topology input resulted in the calculated optimum power vector containing negative components, and the algorithm quickly saturated for most of the nodes.

6.2 Future directions

Due to the packet based nature of all the transmissions, a node can switch power levels depending on how the data packet needs to be routed. Thus the node uses only the minimum power required to transmit that particular packet to the node, and 100% connectivity at every time instant would not be necessary, as the node could buffer the data and transmit at a later stage. Testing the performance of such a scheme however would need an accurate traffic generation algorithm, as well as the implementation of one of the established ad hoc routing protocols, and is beyond the scope of this research.

Bibliography

[1] J. G. Proakis. *Digital Communications.* McGraw-Hill International Edition, 4th ed., 2001.

[2] S. Das, *Multiuser Information Processing in Wireless Communication.* PhD thesis, Electrical and Computer Engineering, Rice University, Houston, Texas, September 2000. `http://www-ece.rice.edu/~cavallar/theses/suman_phd.pdf`.

[3] "GSM World - the web-site of the GSM Association." `http://www.gsmworld.com/index.shtml`.

[4] D. Pandian, "Channel allocation & power control in IS-136," Master's thesis, Graduate School, Rutgers University, New Brunswick, New Jersey, May 1999.

[5] A. J. Viterbi, *CDMA: Principles of Spread-Spectrum Communications.* Reading, Mass.: Addison-Wesley Publishing Company, 1995.

[6] F. Simpson and J. M. Holtzman, "Direct sequence CDMA power control, interleaving, and coding," *IEEE J. Select. Areas Commun.*, vol. 11, no. 7, pp. 1085–1095, 1993.

[7] K. S. Gilhousen, I. M. Jacobs, R. Padovani, A. J. Viterbi, L. A. Weaver, and C. E. Wheatley, "On the capacity of a cellular CDMA system," *IEEE Trans. Veh. Technol.*, vol. 40, pp. 303–311, February 1991.

[8] T. Ojanperä and R. Prasad, "An overview of air interface multiple access for IMT-2000/UMTS," *IEEE Commun. Mag.*, vol. 36, pp. 82–95, September 1998.

[9] S. Narayanaswamy, V. Kawadia, R. S. Sreenivas, and P. R. Kumar, "The COMPOW protocol for power control in ad hoc networks: Theory, architecture, algorithm, implementation, and experimentation.".

[10] The Bluetooth Special Interest Group, *Specifications of the Bluetooth System 1.1*, February 2001. `http://www.bluetooth.com`.

[11] H. Holma and A. Toskala, eds., *WCDMA for UMTS: Radio Access for Third Generation Mobile Communications*. John Wiley & Sons, 2nd ed., 2002.

[12] Iridium satellite failure `http://www.ee.surrey.ac.uk/Personal/L.Wood/constellations/iridium.html`.

[13] "A conversation with Claude Shannon," *IEEE Commun. Mag.*, vol. 22, pp. 123–126, May 1984.

[14] J. Broch, D. A. Maltz, D. B. Johnson, Y.-C. Hu, and J. Jetcheva, "A performance comparison of multi-hop wireless ad hoc network routing protocols," in *Proc. ACMI/EEE International Conference on Mobile Computing and Networking (MOBICOM)*, (Dallas, TX), pp. 85–97, October 1998. `http://citeseer.nj.nec.com/broch98performance.html`.

[15] S. Chen and K. Nahrstedt, "Distributed quality-of-service routing in ad hoc networks," *IEEE J. Select. Areas Commun.*, vol. 17, pp. 1488–1505, August 1999.

[16] S.-J. Lee, *Routing and Multicasting Strategies in Mobile Ad Hoc Networks*. PhD thesis, University of California, 2000. `http://www.cs.ucla.edu/~sjlee/diss.ps.gz`.

[17] E. M. Royer and C.-K. Toh, "A review of current routing protocols for ad-hoc mobile networks," *IEEE Personal Communications*, vol. 6, pp. 46–55, April 1999.

[18] J. L. Sobrinho and A. S. Krishnakumar, "Quality-of-service in ad hoc carrier sense multiple access wireless networks," *IEEE J. Select. Areas Commun.*, vol. 17, pp. 1353–1368, August 1999.

[19] S. Jiang, J. Rao, D. He, X. Ling, and C. C. Ko, "A simple distributed PRMA for MANETs," *IEEE Trans. Veh. Technol.*, vol. 51, pp. 293–305, March 2002.

[20] Z. Y. Tang and J. J. Garcia-Luna-Aceves, "Hop-reservation multiple access (HRMA) for ad hoc networks," in *Proc. IEEE INFOCOM*, (New York), pp. 194–201, March 21–25 1999.

[21] L.Kleinrock and J.Silvester, "Spatial reuse in multihop packet radio networks," *Proc. Of the IEEE*, vol. 75, pp. 156–166, January 1987.

[22] R. Prasad and T. Ojanperä, "An overview of CDMA evolution toward wideband CDMA," *IEEE Communications Surveys*, vol. 1, no. 1, Fourth Quarter 1998.

[23] R. D. Yates, "A framework for uplink power control in cellular radio systems," *IEEE J. Select. Areas Commun.*, vol. 13, pp. 1341–1347, July 1995.

[24] J. B. Whitehead, "Space-time multiuser detection of multi-carrier DS-CDMA systems," Master's thesis, University of Natal, Durban, 2001.

[25] D. M. Novakovic and M. L. Dukic, "Evolution of the power control techniques for DS-CDMA toward 3G wireless communication systems," *IEEE Communications Surveys*, Fourth Quarter 2000.

[26] S. Glisic and B. Vucetic, *Spread Spectrum CDMA Systems for Wireless Communications*. Norwood, MA: Artech House, Inc., 1997.

[27] T. A. Elbatt, S. V. Krishnamurthy, D. Connors, and S. Dao, "Power management for throughput enhancement in wireless ad-hoc networks," in *Proc. IEEE International Conference on Communications, ICC'2000*, (New Orleans, LA), pp. 1506–1513, June 2000. `http://www.cs.ucr.edu/~krish/icc1hrl.pdf`.

[28] A. Chockalingam, P. Dietrich, L. B. Milstein, and R. R. Rao, "Performance of closed-loop power control in DS-CDMA cellular systems," *IEEE Trans. on Vehicular Technology*, vol. 47, pp. 774–789, August 1998.

[29] T. W. Charbonneau and J. H. Gass, "Connectivity analysis for a tactical radio network," in *Proc. MILCOM 2001*, (Washington D.C.), October 2001.

[30] D. Mitra and J. A. Morrison, "A distributed power control algorithm for bursty transmission on cellular, spread spectrum wireless," in *Wireless Information Networks* (J. Holtzman, ed.), pp. 201–212, Kluwer, 1996. `http://cm.bell-labs.com/cm/ms/who/mitra/papers/powers.ps`.

[31] C. Y. Huang and R. D. Yates, "Rate of convergence for minimum power assignment algorithms in cellular radio systems," *Submitted to Wireless Networks*, September 1996.

[32] S. V. Hanly and D. N. Tse, "Power control and capacity of spread-spectrum wireless networks," *Automatica*, vol. 35, pp. 1987–2012, December 1999.

[33] J. D. Herdtner and E. K. P. Chong, "Analysis of a class of distributed asynchronous power control algorithms for cellular wireless systems," *IEEE J. Select. Areas Commun.*, vol. 18, pp. 436–446, March 2000.

[34] N. R. Pate and F. Takawira, "Power control in ad hoc networks," in *Proc. South African Telecommunications, Networks and Applications Conference (SATNAC) 2001*, (Wild Coast Sun, Kwa-Zulu Natal, South Africa), September 2001.

[35] N. R. Pate and F. Takawira, "Adaptive distributed power control in ad hoc networks with different controlling node connectivity criteria," in *Proc. South African Telecommunications, Networks and Applications Conference (SATNAC) 2002*, (Champagne Sports, Drakensberg, Kwa-Zulu Natal, South Africa), September 2002.

[36] C.-J. Chang and F.-C. Ren, "Centralized and distributed downlink power control methods for a DS-CDMA cellular mobile radio system," *IEICE Trans. Commun.*, vol. E80-B, pp. 366–371, February 1997.

[37] J. M. Aein, "Power balancing in systems employing frequency reuse," *COMSAT Tech. Rev.*, vol. 3, no. 2, pp. 277–299, 1973.

[38] J. Zander, "Performance of optimum transmitter power control in cellular radio systems," *IEEE Trans. Veh. Technol.*, vol. 42, pp. 57–62, February 1992.

[39] S. A. Grandi, J. Zander, and R. Yates, "Constrained power control," *International Journal of Wireless Personal Communications*, vol. 1, no. 4, 1995. `http://www.winlab.rutgers.edu/~ryates/papers/cpc.ps`.

[40] N. Bambos, "Towards power-sensitive network architectures in wireless communications:concepts, issues and design aspects," *IEEE Personal Communication Systems*, vol. 5, pp. 50–59, June 1998.

[41] S. V. Hanly, *Information Capacity of Radio Networks*. PhD thesis, University of Cambridge, 1993. `http://www.ee.mu.oz.au/staff/hanly/publications.html`.

[42] E. Seneta, *Non-Negative Matrices and Markov Chains*. Springer-Verlag, 2nd ed., 1981.

[43] G. J. Foschini and Z. Miljanic, "A simple distributed autonomous power control algorithm and its convergence," *IEEE Trans. Veh. Technol.*, vol. 42, pp. 641–646, November 1993.

[44] N. Bambos, S. C. Chen, and G. J. Pottie, "Radio link admission algorithms for wireless networks with power control and active link quality protection," in *Proc. IEEE INFOCOM '95*, vol. 1, (Boston, MA), pp. 97–104, April 1995.

[45] Z. Uykan, R. Jäntti, and H. N. Koivo, "A PI - power control algorithm for cellular radio systems," in *Proc. IEEE 6th Int. Symp. on Spread-Spectrum Tech. & Appli.*, (New Jersey, USA), pp. 782–785, September 2000. `http://wooster.hut.fi/RAVE/C/Zekeriya_Uykan_publication_05.pdf`.

[46] R. Jäntti and S.-L. Kim, "Second-order power control with asymptotically fast convergence," *IEEE J. Select. Areas Commun.*, vol. 18, pp. 447–

458, March 2000. http://www.s3.kth.se/radio/Publication/Pub2000/SeongLyunKim2000_2.pdf.

[47] F. Gunnarsson and F. Gustafsson, "Power control with time delay compensation," in *Proc. IEEE Vehicular Technology Conference*, (Boston, MA), pp. 646–653, September 2000.

[48] Z. Uykan and H. N. Koivo, "A sigmoid-basis nonlinear power control algorithm for mobile radio systems," in *Proc. IEEE-VTC2000 (Vehicular Technology Conference)*, (Boston, MA), pp. 1556–1560, September 2000.

[49] A. Abrardo, G. Benelli, G. Giambene, and D. Sennati, "An analytical approach for closed-loop power control error estimations in CDMA cellular systems," in *Proc IEEE ICC-2000*, (New Orleans, Louisiana, USA), pp. 1492–1496, June 18-22 2000. http://www-dii.ing.unisi.it/~abrardo/p48swed-pm9.pdf.

[50] R. Yates and C.-Y. Huang, "Integrated power control and base station assignment," *IEEE Trans. Veh. Technol.*, vol. 44, pp. 638–644, August 1995. http://www.winlab.rutgers.edu/~ryates/papers/power12.ps.

[51] D. Kim, "Setting SIR targets for CDMA mobile systems in the presence of SIR measurement error," *IEICE Trans. Commun.*, vol. E82-B, pp. 196–199, January 1999. http://search.ieice.or.jp/1999/pdf/e82-b_1_196.pdf.

[52] D. W. Paranchych, "On the performance of fast forward link power control in IS-2000 CDMA networks," in *Proc. Wireless Communications and Networking Conference (WCNC) 2000*, (Chicago, IL), pp. 603–607, September 2000.

[53] T. Chulajata and H. M. Kwon, "Combinations of power controls for cdma2000 wireless communications system," in *Proc. IEEE Fall Vehicular Technology Conference 2000*, (Boston, MA), pp. 638–645, September 24-28 2000.

[54] M. Stemm and R. H. Katz, "Measuring and reducing energy consumption of network interfaces in hand-held devices," *IEICE Transactions on Communications, vol.E80-B, no.8, p. 1125-31.* vol. E80-B, no. 8, pp. 1125–31, 1997.

[55] T. O. Ks, "Adaptive energy-conserving routing for multihop ad hoc networks." `http://citeseer.nj.nec.com/310126.html`.

[56] Y.-C. Tsen, C.-S. Hsu, and T.-Y. Hsieh, "Power-saving protocols for IEEE 802.11-based multi-hop ad hoc networks," in *Proc. IEEE INFOCOM 2002*, pp. 200–209, 2002.

[57] J.-H. Chang and L. Tassiulas, "Energy conserving routing in wireless ad-hoc networks," in *Proc. IEEE INFOCOM 2000*, pp. 22–31, March 2000. `http://citeseer.nj.nec.com/chang00energy.html`.

[58] S. Agarwal, R. H. Katz, S. V. Krishnamurthy, and S. K. Dao, "Distributed power control in ad-hoc wireless networks," in *Proc. PIMRC 2001*, (San Diego), pp. 59–66, 2001. `http://www.cs.ucr.edu/~krish/SharadPIMRC01.pdf`.

[59] R. Ramanathan and R. Rosales-Hain, "Topology control of multihop wireless networks using transmit power adjustment," in *Proc. INFOCOM 2000: Nineteenth Annual Joint Conference of the IEEE Computer and Communication Societies.*, vol. 2, pp. 404–413, 2000.

[60] Minimum Spanning Trees `http://ciips.ee.uwa.edu.au/~morris/Year2/PLDS210/mst.html`.

[61] L. Hu, "Topology control for multihop packet radio networks," *IEEE Trans. Commun.*, vol. 41, pp. 1474–1481, October 1993.

[62] L. Kleinrock and J. Silvester, "Optimum transmission radii for packet radio networks or why six is a magic number," in *Proc. National Telecommunications Conference*, (Birgmingham, Alabama), IEEE, December 1978.

[63] H. Takagi and L. Kleinrock, "Optimal transmission ranges for randomly distributed packet radio terminals," *IEEE Trans. Commun.*, vol. COM-32, pp. 256–257, 1984.

[64] T. Hou and V. Li, "Transmission range control in multihop packet radio networks," *IEEE Trans. Commun.*, vol. COM-34, pp. 38–44, January 1986.

[65] B. Hajek, "Adaptive transmission strategies and routing in mobile radio networks," in *Proc. Conference on Infomation Sciences and Systems*, pp. 373–378, March 1983.

[66] E. M. Royer, P. Michael-Smith, and L. E. Moser. "An analysis of the optimum node density for ad hoc mobile networks."
`http://www.parc.xerox.com/zhao/stanford-cs428/readings/Networking/Royer_icc01_opt_density_2001.pdf`.

[67] J. Ni and S. Chandler, "Connectivity properties of a random radio network," *Proc. IEE Proc.-Commun.*, vol. 141, pp. 289–296, August 1994.

[68] F. Xue and P. R. Kumar, "The number of neighbors needed for connectivity of wireless networks." `http://citeseer.nj.nec.com/xue02number.html`.

[69] P. Gupta and P. Kumar, "The capacity of wireless networks," *IEEE Trans. Infor. Theory*, vol. IT-46, pp. 388–404, March 2000.
`http://decision.csl.uiuc.edu/~piyush/capacity.ps`.

[70] M. Sánchez, P. Manzoni, and Z. J. Haas, "Determination of critical transmission range in ad-hoc networks," in *Proc. of Multiaccess Mobility and Teletraffic for Wireless Communications 1999 Workshop (MMT'99)*, (Venice, Italy), October 6-8 1999. `http://www.ee.surrey.ac.uk/Personal/G.Aggelou/PAPERS/mmt99.pdf`.

[71] R. Prim, "Shortest connection networks and some generalizations," Bell Syst. Techno. J. 36, 1957.

[72] P. Gupta and P. Kumar, "Critical power for asymptotic connectivity in wireless networks," in *Stochastic Analysis, Control, Optimization and Applications: A Volume in Honor of W.H. Fleming* (W. McEaneany, G. Yin, and Q. Zhang, eds.), (Boston, MA: Birkhauser), pp. 547–566, March 1998. ISBN 0-8176-4078-9 `http://decision.csl.uiuc.edu/~piyush/com_chap.ps`.

[73] S. Narayanaswamy, V. Kawadia, R. S. Sreenivas, and P. R. Kumar, "Power control in ad-hoc networks: Theory, architecture, algorithm and implementation of the COMPOW protocol," in *Proc. of European Wireless 2002. Next Generation Wireless Networks: Technologies, Protocols. Services and Applications*, (Florence, Italy), pp. 156–162, February 25-28 2002.
`http://black1.csl.uiuc.edu/~prkumar/ps_files/compow_ewc_2002.pdf`.

[74] V. Kawadia, S. Narayanaswamy, R. Rozovsky, R. Sreenivas, and P. Kumar, "Protocols for media access control and power control in wireless networks," in *Proc. of the 40th IEEE Conference on Decision and Control*, (Orland, FL), pp. 1935–1940, December 4-7 2001. `http://citeseer.nj.nec.com/kawadia01protocols.html`.

[75] R. Wattenhofer, L. Li, P. Bahl, and Y.-M. Wang, "Distributed topology control for power efficient operation in multihop wireless ad hoc networks," in *Proc. IEEE INFOCOM 2001*, (Anchorage, Alaska), pp. 1388–1397, April 2001.
`http://citeseer.nj.com/article/wattenhofer01distributed.html`.

[76] P. H. Lehne and M. Pettersen, "An overview of smart antenna technology for mobile communications systems," *IEEE Communications Surveys*, vol. 2, no. 4, 1999. `http://www.comsoc.org/livepubs/surveys/public/4q99issue/pdf/Lehne.pdf`.

[77] T. J. Kwon and M. Gerla, "Clustering with power control," in *Proc. IEEE MILCOM'99*, vol. 2, (Atlantic City, NJ), pp. 1424–1428, November 1999.
`http://ww.cs.ucla.edu/NRL/wireless/PAPER/kwon-milcom.ps.gz`.

[78] V. Rodoplu and T. H. Meng, "Minimum energy mobile wireless networks," *IEEE J. Selected Areas in Communications*, vol. 17, pp. 1333–1999, August 1999. http://www.tik.ee.ethz.ch/~beutel/projects/picopositioning/minimum_energy_mobile_wireless_networks_rodoplu_meng1999.

[79] N. A. Lynch, *Distributed Algorithms*, pp. 51–80. Morgan Kaufmann, 1996.

[80] D. Mitra and J. Morrison, "A novel distributed power control algorithm for classes of service in cellular CDMA networks," in *Proc. of the Sixth WINLAB Workshop on Third Generation Wireless Information Systems*, (New Brunswick, NJ), pp. 141–157, 1997. http://citeseer.nj.nec.com/mitra97novel.html.

[81] G. J. Byers, "Concatenated space-time codes in rayleigh fading channels," Master's thesis, University of Natal, Durban, 2002.

[82] F. Berggren, "Distributed power control for throughput balancing in CDMA systems," in *Proc. IEEE PIMRC*, vol. 1, (San Diego, CA), pp. 24–28, 2001. http://citeseer.nj.nec.com/berggren01distributed.html.

[83] V. Erceg, L. J. Greenstein, S. Y. Tjandra, S. R. Parkoff, A. Gupta, B. Kulic, A. A. Julius, and R. Bianchi, "An empirically base path loss model for wireless channels in suburban environments," *IEEE J. Select. Areas Commun.*, vol. 17, pp. 1205–1211, July 1999.

[84] Y. Okumura, E. Ohmori, T. Kawano, and K. Fukua, "Field strength and its variability in UHF and VHF land-mobile radio service," *Rev. Elec. Commun. Lab.*, vol. 16, no. 9, 1968.

[85] M. Hata, "Empirical formula for propagation loss in land mobile radio services," *IEEE Trans. Veh. Technol.*, vol. 29, pp. 317–325, August 1980.

[86] R. Janaswamy, *Radiowave Propagation and Smart Antennas for Wireless Communications*. Kluwer Academic Publishers, 2001.

[87] M. Gudmundson, "Correlation model for shadow fading in mobile radio systems," *Electronic Letters*, vol. 27, pp. 2145–2146, November 1991.

[88] C. W. Sung and W. S. Wong, "Performance of a cooperative algorithm for power control in cellular systems with a time-varying link gain matrix," *Wireless Networks*, vol. 6, no. 6, pp. 429–439, 2000.

[89] H. Kim and Y. Han, "Enhanced correlated shadowing generation in channel simulation," *IEEE Commun. Letters*, vol. 6, pp. 279–281, July 2002.

[90] IMSL Statistical and Mathematical and functions, Version 2.0, Visual Numerics. `http://www.vni.com/products/imsl/`.

[91] A. B. McDonald and T. F. Znati, "A mobility-based framework for adaptive clustering in wireless ad hoc networks," *IEEE J. Select. Areas Commun.*, vol. 17, pp. 1466–1487, August 1999.